Ph. D. Thesis

Causes and dynamics of vegetation change in Mato Grosso State, Brazil.

Graduate School of Bioresources
Mie University

Sayaka YOSHIKAWA

March 2010

Abstract

Mato Grosso has emerged as the Brazilian state with the highest deforestation rate, and with the most dynamic changes in vegetation and land covers. In this paper, we focused on the fallowing two main objectives: (*i*) to quantitatively assess the extent of vegetation change over the past two decades for more accurate eco-climatic impact analysis, and (*ii*) to clarify the causes to these changes, with special focus to human factors, in Mato Grosso as our case study. 5-year Digital Vegetation Model (DVM) Maps between Phases I and IV were created for every five years during the 1981-2001 period using the first components of the principal components analysis (PCA) of NOAA/ AVHRR multi-spectral data (Channels 1, 2 and 4). Vegetation and land cover changes are characterized by destruction of primary forests in the north and large-scale human activity and savanna areas expanding from the south. Large-scale soybean production spreading over the central areas and vast herds of cattle in the north can be pointed to as the main causes to vegetation change in these areas. In Chapter 2, we suggest that 76.1 % (89.5 %) of the changes in land cover types occur within 30 km from paved and unpaved roads (roads and navigable rivers). This emphasizes not only the role of road building, but also that of navigable rivers, in accelerating deforestation, especially over the sparsely populated and road less north. In Chapter 3, we have the following three specific objectives to do more detailed analysis for cause of deforestation and savanization in particular these areas using agriculture and cattle ranching industry data at municipal districts levels. We clarified how there were the vegetation change 3 category of Degradation, Recovery and Transitional area with 5-year DVM vegetation change map I–II, II–III, III–IV and I–IV. About 46 % of MT area was deforestation degradation during 1981-2001 (Recovery areas are almost non-existant 0.9 %), and it developed that the cause depended on an advance of cattle

ranching and Corn production in northern part, Soybean and Sugarcane production in central and west MT and much agriculture and cattle business in southern part of MT using GIS and remote sensing data. We suggest clearly cause of deforestation and savannization in each municipal districts. Most of deforestation in tropical rainforests is caused by cattle ranchers or corn farm land in northwest MT and soybean or sugarcane farm land in central MT. And savannization by soybean and sugarcane farm land spread mainly in the west MT and by corn in the southwest. Corn productions have more savannization impacts than the soybean crop production. In Chapter 4, change rates are shown to be larger over non-inhabited areas (56 %) than over the populated zones in the south (42 %). All these findings denote the non-sustainable processes of resource development occurring in MT, mostly for needs of developed countries. For our stomachs and life of the developed country, most of treasured and valuable vegetation change and destroy. We pray that these and conventional studies will be with the decision making about the future of the Brazilian country when, in addition, our earth.

Contents

Acknowledgements

First and foremost my heartfelt gratitude goes to my Supervisor *Professor Dr. Sanga-Ngoie Kazadi* of dean International Cooperation and research division, Ritsumeikan Asia Pacific University, *Professor Dr. Yasuhisa Kuzuha*, *Professor Dr. Kaoru Fukuyama* and *Professor Dr. Yoshihiro Tachibana* of Mie University. Their advice, guidance and sacrifices in time contributed greatly to the success of this research. Their experience and expertise in world environmental issues was a great help during the many discussions we had in the course of the study period.

Secondly, we are very grateful to the members of the Eco-Climate Joint Seminar, Mie University, especially to *Professor Dr. Yoshihiko. Sekine*, *Professor Dr. Noto Matsumura*, *Associate professor Dr. Hideki Kiyosawa*, *Associate professor Ken Ono*, *Associate professor Dr. Noko Matsuo* and *Assistant professor Dr. Ryouei Ito* for their continuous remarks and suggestions during the elaboration of this work.

Tirdly, special thanks to *Associate professor Dr. Atuko Nonomura*, *Associate professor Dr. Musiega Douglas*, *Dr. Kobayashi*, *Dr. Aung Than Oo* and to *Ms. Yoshiko Yomogita*, *Ms. Yukiko Tokuda*, *Ms. Rika Doi*, *Ms. Haruka Suitou*, *Mr. Keigo Yanagita*, *Mr. Takaaki Osugi*, *Mr. Yuki Sugiura*, *Ms. Yuko Kondo*, *Mr. Yoshifumi Shibayama*, *Mr. Keisuke Sugimoto*, *Ms. Naomi Wakabayashi*, *Mr. Yusuke Araki*, *Mr. Masaki Munemoto*, *Mr. Tomoyuki Shida*, *Mr. Tomoya Nagasawa*, *Mr. Tadashi Takai* of the Laboratory of Climate and Ecosystems Dynamics (LCED) past members, in addition *Mr. Kensuke Komatsu*, *Ms. Diawara Alima*, *Mr. Masashi Ito*, *Ms. Koto Ogata* and *Ms. Hatsumi Nishikawa* of the new Laboratory of Climate and Ecosystems Dynamics member for

their kind collaboration.

And I sincerely thank to my friends *Ms. Miho Hada*, *Mr. Gensuke Kinoi*, *Mr. Wataru Sato*, *Mr. Yusuke Suzuki*, *Ms. Kayo Sakai*, *Mr. Keisuke Okada*, *Ms. Kaori Kawai*, *Ms. Haruka Sakata*, *Ms. Saori Okumura*, *Mr. Munetaka Kakei*, *Mr. Yoshitomo Miyazaki*, *Mr. Shinichi Fujio*, *Mr. Takuma Ikebo*, *Mr. Yoshiaki Kotake*, *Mr. Takayuki Sugihara*, *Mr. Masashi Ito*, *Ms. Emi Mizoguchi*, *Ms. Fuyumi Tujii*, *Ms. Ayako*, *Ms. Sayoko Muranishi*, *Mr. Tatuya Ogura*, *Mr. Hiroyuki Mizoguchi*, *Mr. Hiroshi Takakura*, *Mr. Takashi Ishihara*, *Ms. Chiaki Mizutani*, *Ms. Rie Yoshikawa*, *Ms. Mariko Fujiwara*, *Dr. Noriaki Satonaga*, *Dr. Hao Ren*, Dr. Chieri Ida who were alumnus in Mie University, *Ms. Yuka Inoue*, *Ms Ikuko Kashino*, *Ms. Takumi Ichikawa*, *Mr. Takayuki Yamada*, *Mr. Shingo Satake*, *Mr. Yu Kuniyasu*, *Ms. Arisa Nishiguchi*, *Ms. Kumiko Ogiwara*, *Ms. Yuki*, *Dr. Janya*, *Dr. Tsolmon*, *Dr. Keiko Mabuchi* who are my old friends, and *Dr. Masanori Katou*, *Ms. Miwa Katou* who are my acupuncturist, and *Ms. Tomoko Koide*, *Mr. Masanori Koide*, *Mr. Akihiko Suzuki*, *Mr. Sadanori Iwakiri*, *Mr. Shinichi Endo*, *Mr. Kazuma Yoshimoto*, *Mr. Hiroki Otake*, *Ms. Yukari Otake* who are family of my part time job for kindness and helps during all of my university life.

Fourthly, special thanks to the Ritsumeikan Asia Pacific University (APU) for making available its facilities during our long period of research at the Laboratory of Environmental Geoscience.

Fifthly I am deep grateful to professional Japanease folk dancers and stage designers of *Mr. Houshin Kachi*, *Ms. Houen Tanaka*, *Ms. Houyou Takeda*, *Ms. Houshukubun Ota*, *Ms. Houryujyou Kitou*, *Ms. Hougikuhori Horio*, *Ms. Houiku Okuda*, *Ms. Houei Nakagawa*, *Ms. Houkousuichi Inui*, *Ms. Houkouya Nomura*, *Ms. Hounoshiro Higuchi*, *the late Ms. Hounen Shimada*, *the late Ms. Houkin Kawamoto*, *the late Ms. Houtei Ishikawa*, *the late Ms. Houkyukou Fujiwara*, *the late Ms. Houteijyun Nakagawa*, *Ms. Houjine Sakakima*, *Mr. Yuuichi Ito*, *Ms. Houkyuyoshi Imaizumi*, *Mr. Yoshikazu Imaizumi*, *Ms. Housenyuumi*

Esaka and *Ms. Houdoujin Oosuka* and our disciple of *Ms. Tukino Mizuno*, *Ms. Fusako Takei*, *Ms. Harie Narita*, *Ms. Tamiko Mano*, *Ms. Shizuko Fujita*, *Ms. Akiko Yamada*, *Ms. Eiko Endou*, *Ms. Ichiko Itazu*, *Ms. Motoko Komori*, *Ms. Shizuko Teramachi*, *Ms. Kinuko Furumoto*, *Ms. Kikuko Sakamoto*, *Ms. Shizuko Tauchi* and *Ms. Toshiyo Hattori* given the opportunity to attract interest in Brazil and the cheered up always.

Sixthly, my parent *Ms. Akemi Yoshikawa* of Nagoya City, Aichi, provided the essential financial and emotional support that I needed during this eight-year research period. To them too, I am most indebted.

Lastly, to all others who may not have been mentioned in this acknowledgement, but assisted me in kind. To you all I say `THANK YOU, VERY MUCH`

List of Tables

List of Figures

Chapter 1

Introduction

Chapter 1

Introduction

1.1 Amazon

The Amazon River, which runs from Urubamba (Peru) through Amazon (Brazil), is 6500 km long from its source to the mouth, and is the second longest river in the world with 1000 tributaries. The Amazon Basin (Figure 1.1) covers an area of about 5.8×10^6 km^2 and drains about one-third of the land surface of South America. Its mean discharge is 17.5×10^4 m^2/sec and its total discharge of 5.5×10^{12} m^3/year is five times that of Congo, representing 15 to 20 % of the global freshwater supply (Salati and Vose 1984).

According to the investigation by The Brazilian National Water Agency (ANA 2002), annual average temperature for most of the basin ranges between 24 ℃ and 26 ℃. The hottest months of the year are September and October, and the coldest from June to August. Annual average rainfall is 2236 mm/year, oscillating between 1500 and 3300 mm/year throughout the basin (ANA 2002) and is marked by strong latitudinal change: the northern part represents tropical rainforests climate with weak dry season, and, from the central to the south Amazon, the savanna climate with less than 60 mm of precipitation within the period of four to about six months. In the areas close to the mouth of the Amazon River, on the coast of Para, and in the eastern section of the basin, total annual average rainfall exceeds 3000 mm, with no dry season. In the central-north and south-southeast sections, precipitation is lower; within the range of 1500 mm. In the Amazon, Salati and Vose (1984) show that only 25.9 % of its rainfall is brought by the equatorial Atlantic Ocean air mass and the Intertropical convergence zone (ITCZ) while the remaining 74.1 % is generated by evapotranspiration from Amazon forests. Additionally Annual average humidity is relatively uniform throughout the basin, at

around 80 %. March is the most humid month, with humidity tending to decrease in August, similar to the pattern of rainfall. Annual average evaporation is 1424 mm, varying between 800 and 1900 mm. During a year, evaporation rate rises for 3 months from August to October and lowers down from February to April (ANA 2002).

The Amazon Basin contains by far the largest area (56 %) of tropical rainforests in the world, covering 6×10^6 km^2 with 48 % in Brazil and the remainder in Peru, Ecuador, Colombia, Venezuela, Surinam, Guyana, Bolivia and French Guiana. Its physical features are floodplain of varzea and igapo and hard soil terra of terra firme. The Legal Amazon is the largest socio-geographic division of Brazil, which covers all of its territory in the Amazon Basin. It is officially designated to encompass all seven states of the North Region (Acre, Amapá, Amazonas, Pará, Rondônia, Roraima and Tocantins), as well as Mato Grosso state in the Centeral western Region and most of Maranhão state in the Northeast Region (Figure 1.1) until longitude 44 degrees.

Biologically, it is probably the richest and the diverse region in the world, Mark *et al.* (1990) estimates that there are 30,000 living species in the Amazon, which covers 50 to 70 % of the habitat in the world with about 20 % of all the highland plant species, perhaps the same proportion of bird species and around 10 % of the world's mammals. Each type of trees might be supporting more than 400 insect species. Much of the Amazon Basin remains unknown and each expedition there seems to discover something new.

Territories of indigenous people in the Brazilian Amazon occupy more than 1 million km^2, or approximately 21 % of the Brazilian Amazon area. The territories reside in 400 legally recognized "indigenous lands (Figure 1.2)" that are inhabited by some 200,000 people, or about 1 % of the regional population. State and federal protected areas comprise about 14 % of the Brazilian Amazon. Indigenous lands encompass much broader range of ecosystem types than all the other protected areas combined (Schwartzman and Zimmerman 2005).

Indigenous lands and other protected areas act as a principal barrier to forest cutting

and fires. The Kayapo indigenous territories of Para and Mato Grosso and the Xingu Indigenous Park (Figure 1.2), were created in 1961, providing a striking example of a barrier effect. It indicated that the presence of the Amerindian people halted an intense wave of deforestation for nearly two decades (Schwartzman and Zimmerman 2005).

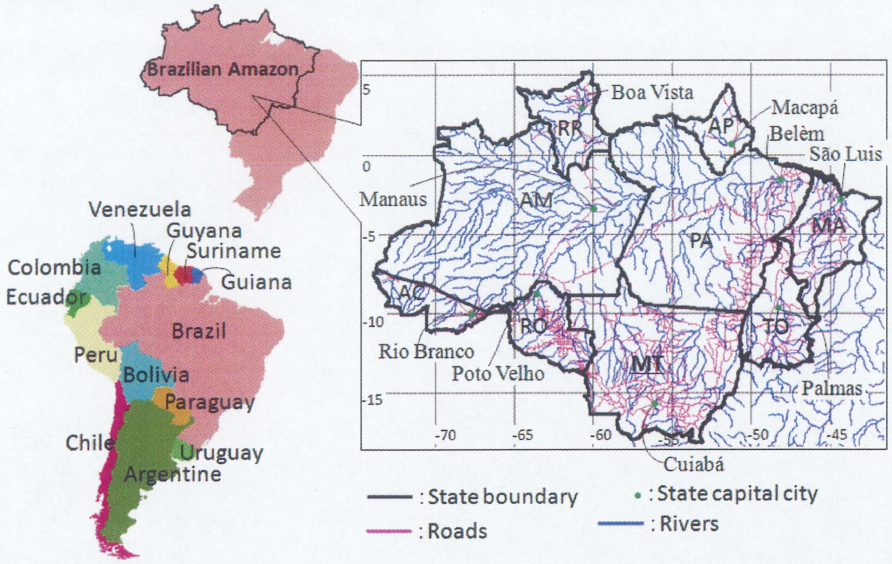

Figure 1.1. The Amazon River Basin consists of the following 9 states: Acre (AC), Amazonas (AM), Amapá (AP), Maranhão (MA), Pará (PA), Tocantins (TO), Rondônia (RO), Roraima (RR), and Mato Grosso (MT), within the Brazilian Amazon.

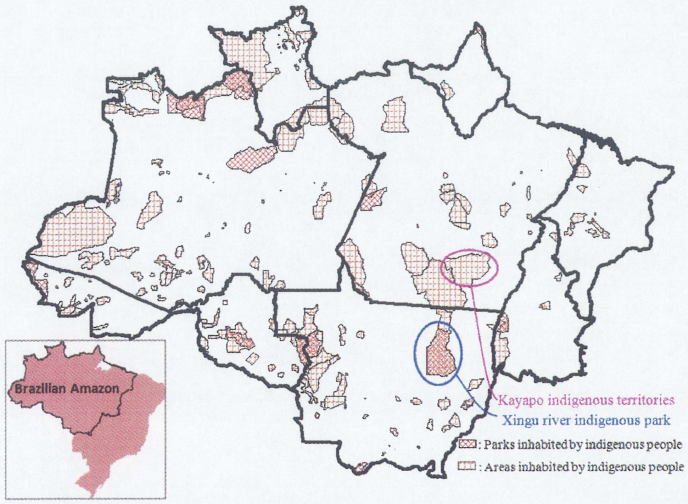

Figure 1.2. Protected parks and area inhabited by indigenous people in the Brazilian Amazon. Black bold lines denote state borders, red meshes are Parks inhabited by indigenous people and orange meshes are Areas inhabited by indigenous people.

1.2 Environmental problems in the Amazon

The environmental problems in the Amazon have two types; Human activities and Natural changes. Human activities comprise urban and land development. Natural changes comprise abnormal weathers such as drought, flood by heavy rain and so on.

Types of environment problems in the Amazon by Human activities were derived from two areas; urban and province. In the urban area, especially in each state capital city (Figure 1.1), air pollution and water contamination are caused by human activities. Especially Air pollution is worsened by exhaust gas from cars. The share of flex-fuel vehicles is 13.8 % of the total vehicles registered in the world (DENATRAN 2008). Flexible-fuel vehicles, compared with gasoline-powered ones, reduce CO_2 emission by 31 % but increase NO_x by 23 % (Faiz *et al.* 1996). As a result, air pollution in Brazilian urban areas (Figure 1.3) has a potential to become worst in the world.

However, deforestation in provincial areas away from big cities is one of the biggest environmental problems in the world. Deforestation due to commercial timber harvesting, slash-and-burn, large-scale mechanized agriculture and extensive cattle ranching (Figure 1.4) cause land degradation and decline of biodiversity. The followings indicate the flow of the cause of deforestation.

Firstly, non-indigenous population in the Brazilian Amazon have increased 10 times since the 1960s, from about 2 million to 20 million as a result of immigration from other areas of Brazil and the high rate of intrinsic growth (Park 1992). Secondly, industrial logging and mining are increasingly important, and road networks are expanding so sharply that increase access to forests for ranchers and colonists. Actually Brazilian Amazon forest remained largely intact until the modern era of deforestation began with the inauguration of Transamazon Highway in 1970. Although Amazonian forests are cut for various reasons, cattle ranching is predominant. Large and medium-sized ranches account for about 70 % of the total clearing activity (Fearnside 2005). Third, spatial patterns of forest losses are changing; in the past deforestation used to be concentrated

along densely populated eastern and southern margins of the basin, but nowadays new highways, roads, logging projects, and colonization are penetrating deep into the heart of the basin. Finally, human-ignited wildfires are becoming an increasingly important cause of forest loss, especially in logged or fragmented areas. Forest degradation results from logging, ground fires (facilitated by logging) and effects of fragmentation and edge formation. Degradation contributes to forest loss (Fearnside 2005). Moreover, in recent years possibility suggests that selective logging, which cuts the wood for high price value in the market, devastated the ground twice more than usual deforestation (Asner *et al.* 2005).

Figure 1.3. Traffic jams and air conditions in Brazilian urban area. This photograph was taken by Yoshikawa in ground observation from 20rd to 29th June 2008 at São Paulo.

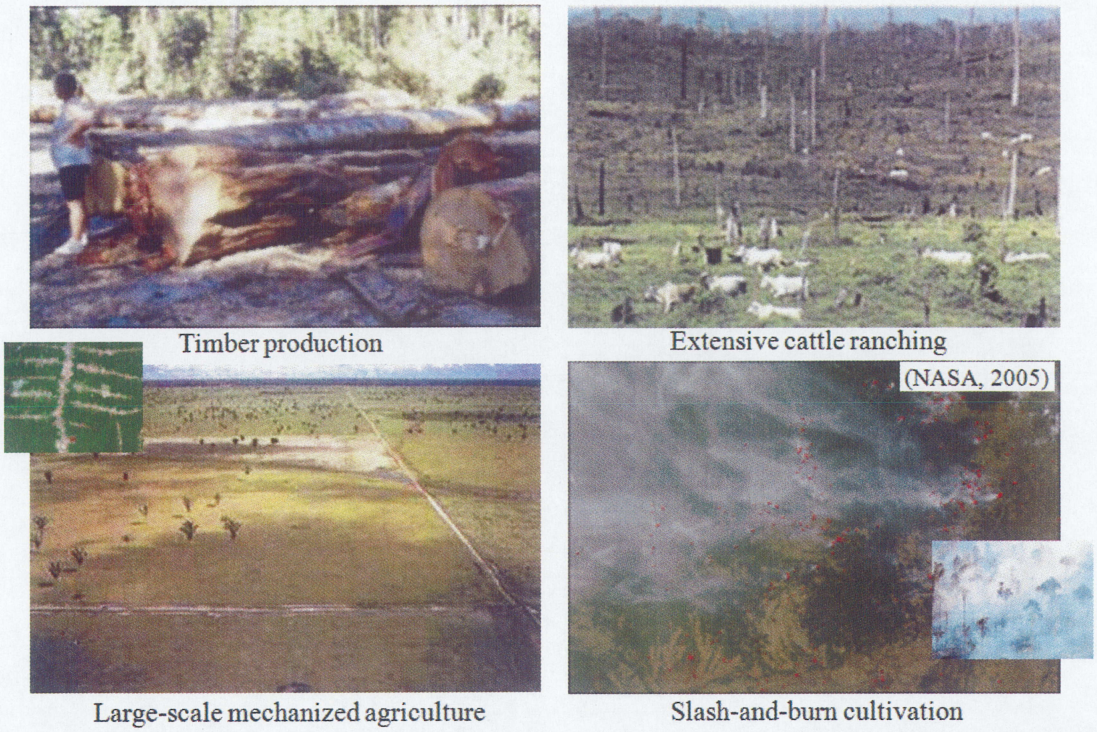

Figure 1.4. Human activities to deforestation in the province area as the environmental problem in the Amazon.

1.3 Prior Research

1.3.1 Effect on climate in regional scale by vegetation change

It has been reported that as a consequence of the influence by deforestation, there were steady decrease in annual precipitation in the past 50 years (Bruijnzeel 1996), notable change in the annual discharge of the Amazon River (Gentry 1980) and various water-related disasters (floods, drought, erosion, etc…).

As shown in Figure 1.5, long-term decrease in precipitation and increase in temperature are more likely to occur because increase in albedo and surface radiation following deforestation have been observed over the tropical area in central Africa (Sanga-Ngoie and Fukuyama 1996). Salati and Vose (1984) show that only 25.9 % of rainfall is brought by the climate system while remaining 74.1 % is generated by evapotranspiration from Amazon forests. Altogether, these facts underline the very

important role played by tropical rainforests in the regional and global water vapor or heat budget (Henderson-Sellers *et al.* 1996, Gash and Nobre 1997). It can therefore be argued that deforestation of in the tropics might bring forth deep impact on the climate system at various scales, and even contribute to enhancing global warming (Henderson-Sellers *et al.* 1996).

Therefore, deforestation may have greatly influenced the climate system on the earth scale, such as global warming. It is very important to clarify the relationship between the nature of vegetation and climate when we are to know more deeply about the climate change of the earth environment. It is of particular importance to know the vegetation change from the 1980s up to the present, while exploring the cause of such changes.

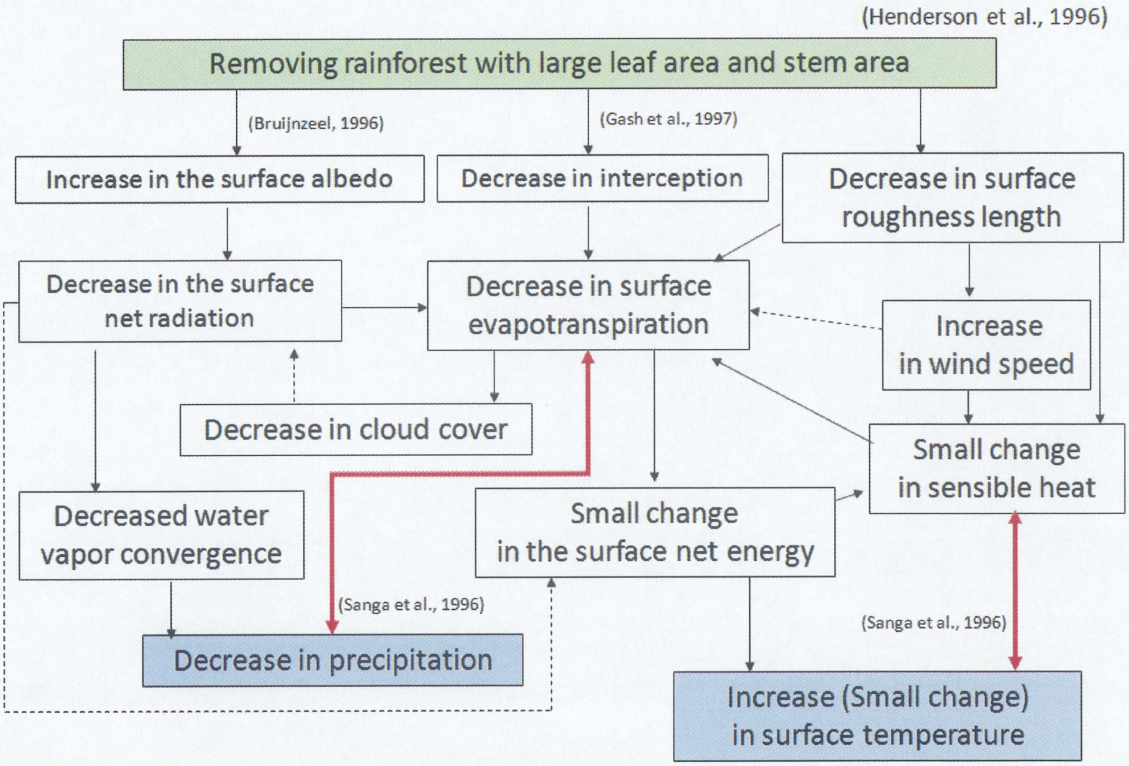

Figure 1.5. Schematic representation of the process by deforestation impacts on climate in the regional scale. Henderson *et al.* (1996) was reorganized by accompanying Bruijnzeel (1996), Gash *et al.* (1997) and Sanga and Fukuyama (1996).

1.3.2 Brazilian Government's research for protecting Amazon

The Brazilian Amazon contains about 48 % of the tropical rainforest remained in the world (Park 1992), playing vital roles such as maintaining biodiversity, regional hydrology and climate, and storing terrestrial carbon. It also suffers from the highest rate of deforestation in the world; currently nearly 2 million hectares per year on average (INPE 2002).

Brazilian Amazon forests had remained largely intact until the modern era. Deforestation began with the inauguration of Transamazon Highways in the 1970s (Fearnside 1986, 2005, 2006).

In order to prevent these destructive activities, the Brazilian government have put forth various policies. Since 1988, monitoring of annual gross deforestation of the Brazilian Amazon, known as Monitoring the Amazon Gross Deforestation Project (PRODES), has been conducted by INPE (INPE 1999, 2000, 2001, 2002). The forest evaluation is performed based on composite images (Channels 3, 4 and 5) of LANDSAT satellite data. Gross deforestation includes areas in the process of secondary succession or forest recovery: these are not subtracted in the calculation of the deforestation extent and rate. However, the above definition does not include areas of forest affected by selective logging activities or wild fires. According to PRODES, the largest areas of deforestation within the legal Amazon from 1988 to 2007 (INPE 2009) are found in the State of Mato Grosso (Figure 1.6), and its destruction is noted to increase exponentially (Fearnside 1986, INPE 2009). In a joint project by INPE and NASA called the Real Time Deforestation Monitoring System (DETER), real-time deforestation assessment system for controlling the deforestation in the Amazon using the data of MODIS satellite, was developed (Morton *et al.* 2005). However, this forest-resources evaluation research suffers from strong attenuation in satellite data accuracy due to the influence by abnormal weathers, and from the fact that they can only distinguish between forested and deforested areas. Moreover, Fearnside (1993)

suggests that much of controversy surrounding deforestation estimates is caused by whether or not cerrado (central Brazilian shrub savanna or savanna woodlands) is differentiated from forests in the estimates.

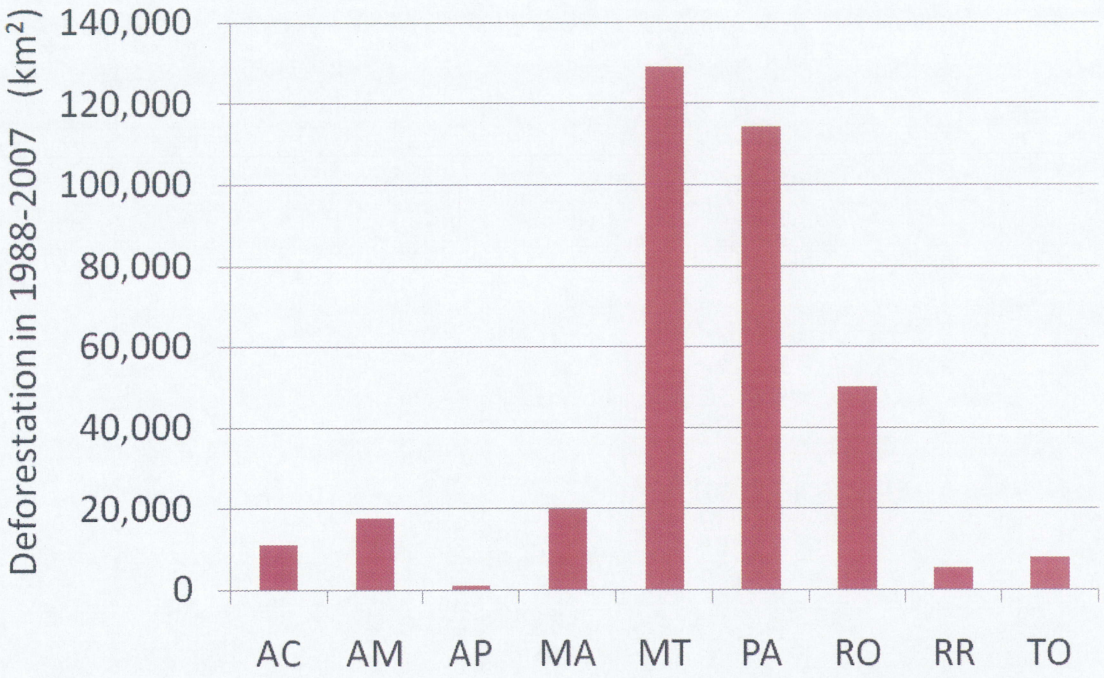

Figure 1.6. The total deforestation area is in Legal Amazon state from 1988 to 2007. Total deforestation is accumulated results of the analysis by INPE (2009). The first is Mato Grosso, second Pará and third Rondônia.

1.3.3 Deforestation control

With the purpose to maintain the Brazilian Amazon, the water utilization law, game law and forest law were enacted in 1934. The Legal Amazon was determined by Superintendência do Plano de Valorização Econômica da Amazônia (SPEVEA) in 1953 (Torres and Costa 1999). The Legal Amazon occupies 60 % of the total area of Brazil. The forest law was amended in 1965; it was decided to leave 50 % of the property as natural vegetation by the owner. The basic environmental law was enacted by the Brazilian government, and Conselho Nacional do Meio Ambiente (CONAMA) was established in 1981 (Lindenmayer and Franklin 2002). The CONAMA created

"Programa Nossa Natureza" to prohibit the export of logs and the use of mercury in rivers to obtain gold. By the Earth Summit held in Rio de Janeiro, Brazil in 1992, "Agenda 21" as a concrete action plan to achieve sustainable development, was formulated for the 21st century. The Lei de Crimes Ambientais 1998 was enacted to punish those who commit a crime against the law. The Forest Law was amended in 2000, whose major change is to keep the area of the property from 50 % to 80 % of the forest and 35 % of the cerrado in the Amazon and 20 % of the forest (and cerrado) outside the Amazon.

Notwithstanding the above policies, however, since the military coup in 1964, the development of private companies expanded in the Amazon. Programa de Integração Nacioal 1970, attracted them to the interior of the Amazon. The development of infrastructure such as road constructions advanced. In 1974, the Brazilian government created the Programa de Pólos Agropecuárias e Agrominerais da Amazônia (POLAMAZÔNIA), which set the base for agriculture and industry and enhanced cooperation with foreign companies for the development in Amazon (Sachs *et al.* 2009). As examples, there are the Projeto Grande Carajás in 1988 (Hall 1991) where pig iron production is recommended the construction of power plants, which makes 4800km^2 of the forest sink out of sight (Fearnside 2002). With the advent of "Pro-alcohol (1975)", the national programs were intended to replace part of gasoline consumption with ethanol, so that she can become a pioneering country of making use of alcohol in large scale as an automobile fuel (Faiz *et al.* 1996). Production of sugarcane increases its importance in Brazilian economy. As a result, the area for sugarcane production has increasingly expanded. Furthermore, the Brazilian government in 1976 admitted 50 % deduction of the income tax for companies to invest in developing Amazon. Thus, development is further advanced.

Meanwhile, the Mato Grosso's State Foundation for the Environment (FEMA) implemented a program to license and control deforestation from 1999 to 2001. Because of such a program, there was an encouraging reduction of about 32 % in the scale of

deforestation of MT in the two-year period (2000–2001) as compared to 1998–1999, possibly due to aggressive monitoring, licensing and enforcement policies (Fearnside 2003). On the other hand, INPE data suggest that deforestation in MT state decreased by only 9 % in 1999–2000, while a marginal increase was recorded in the surrounding Pará (PA) and Rondônia (RO) states. In other states, this policy came to be adopted in 2002 or later.

1.4 Overall objectives and scope of the study

Although vegetation has been investigated with various techniques various to date, we also investigate the vegetation change for the past 20 years using Geographic Information System (GIS) and remote sensing technology in this paper. GIS and remote sensing are techniques used for speeding up broader-based inquiry or analysis where the conventional system based on an on-site inspection is unsuitable in order to get hold of vegetable change, which changes all the time.

Moreover, searching for many forest-resources evaluations or vegetation maps which have been published by the Brazilian government and other researchers, we have found they include attenuation of data accuracy because of the influence of abnormal weathers, and define only the distinction with forests and non-forests. For a future research such as its adaptation in the climate system evaluation of an albedo, and the amount of evapotranspiration, we suggest that more accurate vegetation evaluation is necessary to evaluate correctly what, where, and how vegetation can serve as an important parameter.

Despite an increasing number of studies on vegetation changes in the Brazilian Amazon, several questions still remain to be answered: What kind of vegetation is changing? What is the cause of deforestation by human activities? The present research is motivated by these questions and its main objectives are: to quantitatively assess the extent of vegetation change with more accurate eco-climatic impact analysis over the past two decades (1981-2001); and clarify the relations among vegetation changes,

highway road construction and population pressure in MT.

Hereafter, the vegetation change dynamics and role of access networks are given in Chapter 2, concernment between pastoral-agricultural frontier and vegetation change dynamics in Chapter 3, population dynamics in Chapter 4, and our final product followed by general conclusion in Chapter 5.

Chapter 2

Vegetation change Dynamics and Role of access networks

This chapter is based on
Yoshikawa, S. and Sanga-Ngoie, K., (2009) Deforestation Dynamics in Mato Grosso in the Southern Brazilian Amazon using GIS and NOAA/AVHRR data, *International Journal of Remote Sensing*, accepted on 03 November 2009

Chapter 2

Vegetation change Dynamics and Role of roads and access networks

2.1 Introduction

The Brazilian Amazon River Basin encompasses about 48 % of the world's remaining tropical rainforests (Park 1992). It also plays a vital role in maintaining biodiversity (Mark 1990), in regulating regional hydrology and climate, as well as the terrestrial carbon storage (Dale 1994). Brazil holds the largest continuous tropical forest, but also at the same time, it is the country that loses the highest amount of forest covers in the world. Estimates of the total forest cover of the Brazilian Legal Amazon or the original forest cover show remarkably wide discrepancies: 3,562,800 km^2 according to FAO (1981), 4,195,660 km^2 by Fearnside (1990), and 4,090,831 km^2 by Skole and Tucker (1993). As for the actual annual deforestation, Skole and Tucker (1993) put it at 15,200 km^2 per year, while the National Institute For Space Research (INPE) estimated it at 11,968 km^2 per year in 2008 (INPE 2009).

As a result this deforestation, a steady reduction in annual precipitation over the past 50 years (Bruijnzeel 1996), notable changes in the annual discharge of the Amazon River (Gentry and Lopez-parodo 1980) and increased water-related disasters (floods, drought, erosion, etc...) have been reported. Salati and Vose (1984) show that only 25.9 % of the Amazonian rainfall is brought in by the equatorial Atlantic Ocean air mass and the Intertropical convergence zone (ITCZ) while the remaining 74.1 % is generated by evapotranspiration from Amazon forests. In a coupled numerical model of global atmosphere and biosphere, Nobre *et al.* (1991) suggest that there would be an increase in mean surface temperature and a decrease in the annual evapotranspiration

and precipitation in Amazon if tropical rainforests were changed into pasture. Altogether, these facts underline the very important role that the tropical rainforests play in the regional and global water vapor or heat budget (Henderson-Sellers *et al.* 1996, Gash and Nobre 1997). It can therefore be argued that deforestation of in the tropics, especially in the Amazon, might bring forth deep impacts on the climate system at various scales, and even contribute to enhancing the global warming (Henderson-Sellers *et al.* 1996).

INPE has been conducting assessment research on deforestation rate in the Amazonia using LANDSAT since 1978 (INPE 2009). Recently, the Real-time Deforestation Monitoring System (DETER) was jointly developed with NASA using MODIS data (Morton *et al.*, 2005). INPE (2009), made it clear that the highest deforestation rates (Figure 2.1 and 2.2) are found in Mato Grosso State (abbreviated as MT hereinafter). However, INPE assessed deforestation rates only, with no reference to changes in other vegetation covers. Errors due to climatic effects were not considered. Moreover, Fearnside (1993) suggests that much of controversy surrounding deforestation estimates is caused by whether or not the cerrado (central Brazilian shrub savanna or savanna woodlands) is differentiated from forests in the estimates.

Despite the increasing number of studies on vegetation change in the Brazilian Amazon, several fundamental questions still remain to be answered: "What kinds of vegetation covers are changing?", "What is the rate of the changes?", "What are the causes, and factors, of deforestation?". This chapter is motivated by these questions and its main objectives are: (*i*) to quantitatively assess the extent and the rates of vegetation change over the 1981-2001 period, aiming at more accurate eco-climatic impact analysis than INPE`s assessments; and (*ii*) to reinforce the causes, and factors, of the deforestation, especially about the relationships between vegetation change and agro-pastoral activities and/or access networks (paved and unpaved roads). Mato Grosso (Figure 2.1) will be our study area for the reasons mentioned above. Geographic Information System (GIS) and remote sensing technology will be used for fast,

comprehensive, multi-criteria and broad-based inquiry and analysis.

Hereafter, the study site is presented in section 2.2, the data sets and analysis method in section 2.3 and 2.4, respectively. Our analysis results (5-year vegetation maps, causes to vegetation and land cover changes, etc) are given in section 2.5. Discussion and concluding remarks are highlighted in section 2.6.

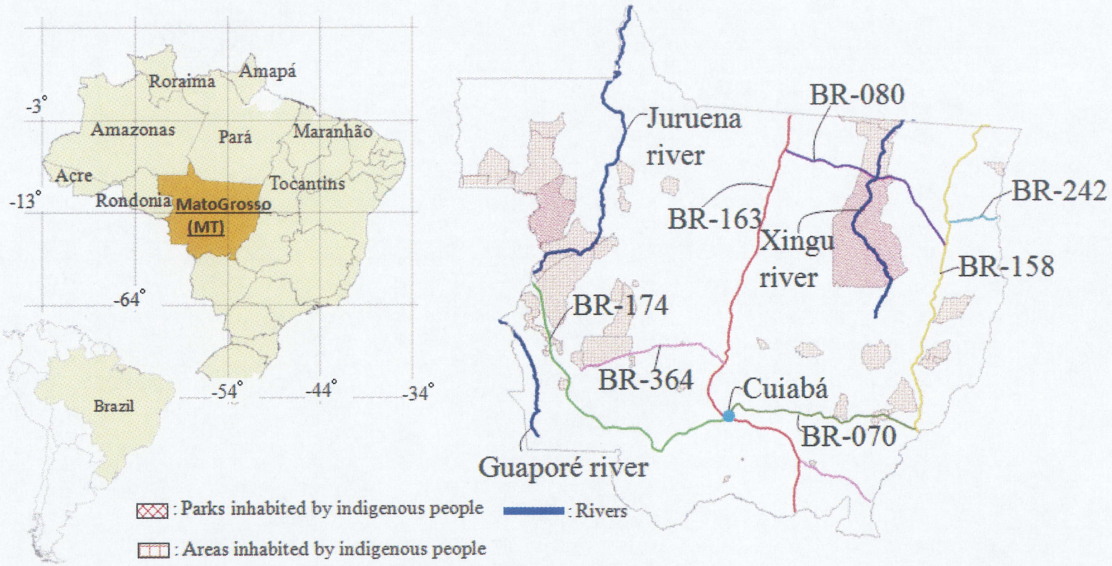

Figure 2.1. Our study area, Mato Grosso state, is located in the Southern Brazilian Amazon. Cuiabá is capital city of the south Mato Grosso. Guaporé, Juruena and Xingu river are three representative rivers which drew bold blue lines. And federal main roads of BR-174 (light green line), BR-163 (red line) and BR-158 (dark yellow line) are extending from the north to the south. BR-070 (dark green line), BR-080 (purple line), BR-364 (pink line) and BR-242 (light blue line) are undergoing elongation to the east and west in Mato Grosso. Red meshes are Parks inhabited by indigenous people and orange meshes are the Areas inhabited by indigenous people.

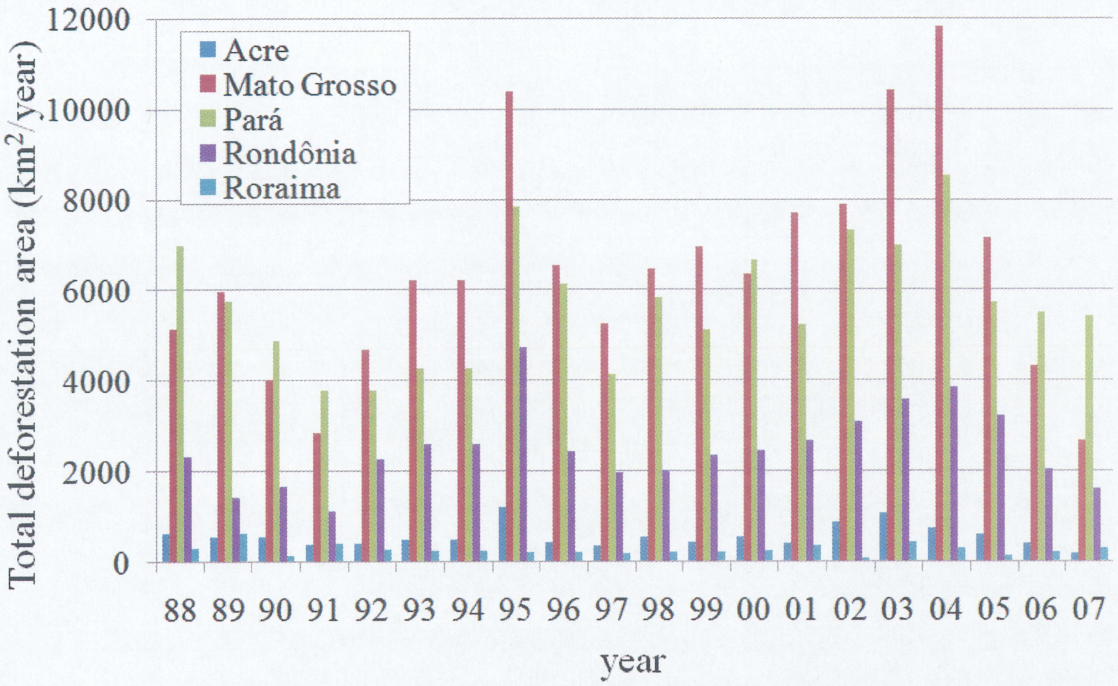

Figure 2.2. Total deforestation area for the top 5 states in the Legal Amazon, located in Figure 2.1, as estimated by INPE (2009). Mato Grosso shows, by far, the largest annual deforestation rates since the early 1990s.

2.2 Study site description

Our research area, Mato Grosso State (MT) is located in the central-west Brazil (Figure 2.1), between 7° 21' S and 18° 02' S of latitude, and 50° 14' W and 61° 38' W of longitude. MT total area is 903 386 km^2, nearly 2.4 times as large as Japan. This state spreads over the southern part of the Amazon River basin: 67.8 % of its area is part of the Amazon basin (ANA 2002).

Vegetation in Mato Grosso is characterized by latitudinal variation: forests in the north, mixed ecotones in the middle, and cerrado in the south (Fearnside 2003), along the climatic divides. The climate in this region is also marked by a latitudinal change: the northern part is the realm of the tropical rainforests climate with a short dry season, while the central and the southern parts witness four to about six months a year with less than 60 mm of monthly mean precipitation (dry season).

The intensive program of highway building in the Amazon has been pointed to be going along with the deforestation in this area (Fearnside 1986, Park 1992).The main highways in Figure 2.1, such as the BR-070 (Brasília–Bolivian Border, MT), the BR-163 (Tenente Portela–Suriname Border, PA), the BR-174 (Caceres, MT–Venezuela Border, RO), and the BR-364 (Limeira–Peru Border, AC), built across MT since the 1980s, are known to have drawn waves of developers within this area (Fearnside 2005). The state's total population has jumped to 2 502 260 inhabitants and its population density to 2.77 inhabitants/km^2 in 2002. Its capital city, Cuiabá (Figure 2.1), boasts 542 861 inhabitants and a population density of 153.4 inhabitants/km^2 in 2000 (ANA 2002).

Recently, large-scale mechanized plantations and pasture lands have increased in the mixed zone and the cerrado. In particular, these are the places where the largest quantity of soybean is produced in Brazil (Morton *et al.* 2006). Further lands are therefore needed for large-scale infrastructures such as roads and dams. This is done by cutting down forests.

2.3 Data sets

The data sets and other important materials utilized in this chapter are summarized in Table 2.1, and described hereafter.

We adopt here the Land 8km AVHRR (Advanced Very High Resolution Radiometer sensor) Data Set provided by the International Water Management Institute (IWMI, 2004). This data set is made from the 0.1° resolution global equal area projection NOAA/NASA Pathfinder AVHRR Land Data Sets, as changed into equal angular projection 10-day composites per month for each year. Data from July 1981 to June 2001 are used, except for the data from September to December in 1994, missing because of satellite trouble. The National Atlas of Brazil, 4th edition, published by Brazilian Institute of Geography and Statistics (IBGE), gives the dominant vegetation types maps based on ground survey (IBGE 2005). These maps have been updated every five years since 1970, and the newest one was produced in 2002. In this chapter, the

newest IBGE vegetation map is used as source of ground truth data for vegetation classification and comparison, and for accuracy assessment of our classified results.

The Variability Analyses of Surface Climate Observations (VASClimO) 50-year precipitation climatology dataset was downloaded from the Global Precipitation Climatology Centre (GPCC) website (GPCC 2005). Weather station observation temperature data from the Center for Weather Prediction and Climate Studies (CPTEC/INPE) website (CPTEC/INPE 2009) in Brazil, and Digital Elevation Model (DEM) from the United States Geological Survey (USGS) website (USGS 1997) are utilized as ancillary data during vegetation map creation.

Various statistical data on Brazil are available from the Sistema IBGE de Recuperação Automática (SIDRA) within IBGE. These are, among others, annual data of cattle heads from 1974 to 2006 and soybean planted areas from 1990 to 2006 in each municipal district of MT (SIDRA 2008).

Topographic maps, and other ancillary data such as rivers, main roads, local roads (including highways and all paved and unpaved roads), parks and areas inhabited by indigenous people in MT were downloaded from the Mapas Interativos IBGE website (IBGE 2005), and were used as reference for land covers identification and analysis.

Table 2.1. List of data sources.

	Data Set	*Periods*	*Remarks*
1	NOAA/AVHRR Ch1, Ch2, Ch4 data - Land 8km AVHRR Data Set, IWMI	1981.07–2001.06	0.1° resolution
2	Vegetation map - National Atlas of Brazil, 4th edition, IBGE (polygon)	2002	1:3000000
3	Climatology data - VASClimO 50-year precipitation climatology, GPCC (text)	1951–2000	1.0° resolution
4	Observation Climatology data - Weather Station Observation data, CPTEC/INPE	1996–2005	
5	Digital Elevation Model (DEM) data - Hydro 1K Elevation Derivative Database, USGS	1997	1 km resolution
6	Cattle heads data - Sistem IBGE de Recuperação Automática (table)	1981–2001	Municipal districts (144)
7	Soybean planted areas data - Sistem IBGE de Recuperação Automática (table)	1990–2001	Municipal districts (144)
8	State line map - Malha Municipal Digital , IBGE (line)	1997	1:5000000
9	Rivers and roads map - Mapa da Série Brasil Geográfico, IBGE (line)	2002	1:5000000

2.4 Analysis methods

2.4.1 Reviews

Most of the studies related to the identification and mapping of vegetation are based on the premise of spectral difference between the reflectance by vegetated and other land cover types, especially in the red and near-infrared bands. Most of these works are carried out using the Normalized Difference Vegetation Index (NDVI) calculated as the normalized ratio of the difference of surface reflectance in the near-infrared (Ch2) and the visible (Ch1) wavelengths (equation (1)).

$$NDVI = \frac{Ch2 - Ch1}{Ch2 + Ch1} \qquad (1)$$

The NDVI definition takes advantage of the differential absorption spectrum of vegetation chlorophyll: a strong absorption of the red light in the visible (Ch1) proportionally to leaf chlorophyll density, and a high reflectance in the infrared (Ch2) as a function of leaf density. Healthy vegetation thus tends to be characterized by high NDVI values because of its high reflectance in the Ch2 and low reflectance in the Ch1 (Rouse *et al.* 1973). Several studies have shown that NDVI is correlated with climate variables under a wide range of environmental conditions (Anyamba and Eastman 1996, Batista *et al.* 1997, Richard and Poccard 1998, Nonomura *et al.* 2003, Gurgel and Ferreira 2003).

Using NDVI values calculated from NOAA AVHRR data spanning from April 1982 to February 1983, Tucker *et al.* (1985) showed that there was a high correlation between the integrated NDVI image and the major land cover types over Africa. They performed supervised classification to create an African vegetation map using training sites selected form known available vegetation maps. By compressing the data using principal component analysis (PCA), which undertakes a linear transformation of a set

of image bands in terms of the maximum variance explained in the original data, and by calculating the transformation coefficients from the principal eigenvectors of the variances, they could ensure that bands with higher variability contribute more to the development of the component images.

Eastman and Fulk (1993) performed PCA on a 36-month NDVI dataset (1986–1988) over African continent. They showed that the first component clearly represents the characteristic NDVI integrated over all seasons. As for the second principal component of NDVI, Tucker *et al.* (1985) showed that it characterizes the asynchronous rainy seasons in the two hemispheres of Africa over the known vegetation. Notwithstanding the performance of the PCA in their analysis, it can be argued that Tucker *et al.* (1985) findings can hardly be generalized to represent African vegetation due to the fact that, on one hand, they had used only a 1 year period of NDVI data, which might contain strong year-to year variability bias and that, on the other hand, they based their analysis on training sites covering only 5% of African area.

Murai and Honda (1991) developed a World Vegetation Map using the monthly mean NDVI data from 1985 to 1987. Geographical adjustment was introduced to avoid seasonal differences between the northern and southern hemispheres by adjusting the peak month of the southern hemisphere to that of the northern hemisphere. Dividing, and then sticking, the global vegetation along equational line is not natural: the geographical equator can hardly be considered as the vegetation equator.

Loveland *et al.* (2000) produced a 1km resolution global land cover database developed through a continent-by-continent unsupervised classification of monthly NDVI composites from NOAA/AVHRR covering the 1992-1993 periods. We have to note here that 1992 was plagued with abnormal weathers as related to the 1992-1993 El Niño that influenced the state of vegetation cover all over the world.

Gurgel and Ferreira (2003) analyzed the connections between the changes in vegetation cover and the annual and interannual climate variability in Brazil. Their analyses were based on the NDVI derived from the AVHRR sensor and the monthly

mean outgoing longwave radiation (OLR) data for the January 1982–December 1993 period. The PCA first component reveals that NDVI data have potential for characterizing the main patterns of vegetation types in Brazil. It was also possible to characterize the annual and interannual climate-related variability of the vegetation cover types in the same way as in Tucker *et al.* (1985), Townshend (1987), and Eastman and Fulk (1993).

As an improvement to previous vegetation classifications that use short term NDVI satellite databases (Tucker *et al.* 1985, Murai and Honda 1991, Eastman and Fulk 1993, Loveland *et al.* 2000), Tsurumi and Sanga-Ngoie (2000) use a 5-year (1985-1991) monthly mean NDVI database for global land cover mapping using PCA on a GIS analytical platform.

However Nonomura *et al.* (2003) stress that using NDVI alone does not allow for detailed classification, especially over arid lands or sparsely vegetated areas, where NDVI values hardly indicate the difference of vegetation conditions. Consequently, they designed a Digital Vegetation Model (DVM) using 1985–1991 NOAA AVHRR data in an attempt to get an accurate and upgradeable digital image of African land cover types. Their PCA fusion analysis combined the visible band (Ch1), the near-infrared band (Ch2), and the thermal infrared band (Ch4) of the 5 year monthly mean NOAA AVHRR GVI climatology spanning the entire African continent with 0.15° spatial resolution. Then they performed unsupervised classification using only the so-obtained PCA first components of the NOAA/AVHRR multi-spectral data on GIS platform. Their analysis produced a macro-scale seven-category African DVM, consistent with Köppen's climatic classification. Including Ch4 data in their scheme was pivotal for allowing full-scale classification from dense forests to sparsely or non-vegetated areas, on the continental level. By so doing, they managed to retain each spectral information for differentiating surface features (vegetation and geomorphology) while at the same time avoiding the year to year variability bias embedded in the short term (1-year) datasets as in most of the previous studies.

2.4.2 Our analytical methodology

First of all, the NOAA/AVHRR data were corrected. In general NOAA/AVHRR dataare not corrected for the influence of the Mie scattering by aerosols, water vapor, etc (Agbu and James 1994). Noise or outliers due to presence of clouds or smoke from slash-and-burn cultivation are dominant from September to December in low latitudes areas. Outliers due to clouds are characterized by high reflection and low temperature. Accordingly, corresponding values in Channel 1 (Ch1) and Channel 2 (Ch2) are high, while those in Channel 4 (Ch4) are low (Nishida *et al.* 2005). Data quality control and outliers correction are made as follows, taking advantage of these characteristics.

We consider hereafter that values falling within either one of the following categories were erroneous. They were thus removed and/or subsequently corrected.

(1) For each scene: digital numbers (DN) larger than 0.3 in Channel 1, or larger than 0.5 in Channel 2, or calibrated temperatures values in Channel 4 smaller than 253 K (10℃) were considered as erroneous.

(2) For each channel:

- $\mathrm{Ch1}_i$ is erroneous if

$$Ch1_{i-1} < Ch1_i > Ch1_{i+1} \text{ and } Ch1_i > Ch1_{i+1} + Ch1_{sdi} \text{ or } Ch1_i > Ch1_{i-1} + Ch1_{sdi} \quad (2)$$

where i denotes months (i=1, 2, …, 12) and sdi the i-th month standard deviation of the pixel DN.

- $\mathrm{Ch2}_i$ is erroneous if

$$Ch2_{i-1} < Ch2_i > Ch2_{i+1} \text{ and } Ch2_i > Ch2_{i+1} + Ch2_{sdi} \text{ or } Ch2_i > Ch2_{i-1} + Ch2_{sdi} \quad (3)$$

- $\mathrm{Ch4}_i$ is erroneous if

$$Ch4_{i-1} > Ch4_i < Ch4_{i+1} \text{ and } Ch4_i < Ch4_{i+1} - Ch4_{sdi} \text{ or } Ch4_i < Ch4_{i-1} - Ch4_{sdi} \quad (4)$$

(3) For each channel: the i-th month data is considered erroneous if

$$Ch1_i - (Ch1_{mi} + Ch1_{sdi}) > 0 \text{ and}$$
$$Ch2_i - (Ch2_{mi} + Ch2_{sdi}) > 0 \text{ and} \quad (5)$$
$$Ch4_i - (Ch4_{mi} - Ch4_{sdi}) < 0$$

(where mi is the i-th month average.)

Erroneous data were corrected by using the average value of the previous and the nextmonth data. In this research, we made our analysis using the monthly-corrected data, since time resolution is one month.

The analytical methodology in this work for making vegetation maps is made along the procedure developed by Nonomura *et al.* (2003), especially for the creation of the 5-year mean DVM over Brazil. The overall methodology is given in Figure 2.3, and can be summarized in 4 main steps described as here after. Clark Lab's IDRISI 32 Release 2.2 GIS platform (Eastman 2001) was used for all the analyses, together with CARTALINX, the digital database builder software.

Firstly, following Tucker *et al.* (1985), Eastman and Fulk (1993) and Nonomura *et al.* (2003), we perform Principal Component Analysis (PCA) so as to extract the first components of each 5-year mean data of each one of the selected NOAA/AVHRR channels (Ch1, Ch2 and Ch4), respectively. These are shown to carry more than 69 % of each channel's variability and to represent the seasonally independent features of the underlying surface cover.

Secondly, Land use/land cover classification was then made by unsupervised classification of the composite image of the obtained first PCA components of Ch1, Ch2 and Ch4 into 30 land cover clusters using the IDRISI module CLUSTER (Sanga-Ngoie and Yoshikawa 2007). The following step by step procedure helped us reclass the unsupervised 30 clusters into 7 land use/land cover types that we think are the best fit to the present study, keeping in mind that accurate DVMs of MT are important inputs for eco-climatic analysis over this region.

Using climatological GPCC rainfall data and temperature data from CPTEC/INPE (2009), we defined the dominant Köppen climatic zones over MT and digitized them into Boolean polygons. Then 5-years mean monthly NDVI were calculated for each one of the 30 clusters. The combined use of the Köppen climatic zones and the specific characteristics of the annual variation of the NDVI made it possible to differentiate between the forests types clusters on one side, and between the different types of

grassland biomes and non-vegetated areas clusters, on the other side. Using DEM data, further differentiation among grassland biomes were obtained by delineating waterlogged parts of river watersheds especially over the southwestern and the southern parts of MT. All this procedure lead us to a total of 7 new reclassified land use/land cover types that we identified by comparison to the IBGE vegetation map, used as ground truth.

Our DVM maps (Figure 2.4) are created for the following 5-year terms: July 1981–June 1986 (Phase I), July 1986–June 1991 (Phase II), July 1991–June 1996 (Phase III), except for September to December in 1994, and July 1996–June 2001 (Phase IV).

Thirdly, accuracy assessment of the created 5-year DVM maps (Phases I–IV) is performed by comparison with the IBGE vegetation map as ground truth.

Finally, using the obtained 5-year DVM maps (Phases I–IV), causes to deforestation are investigated by analysis of the relationship between the changes in the DVM maps and the related pastoral activities and access networks (paved and unpaved roads) for each region. Eco-climatic impacts of these changes are also discussed.

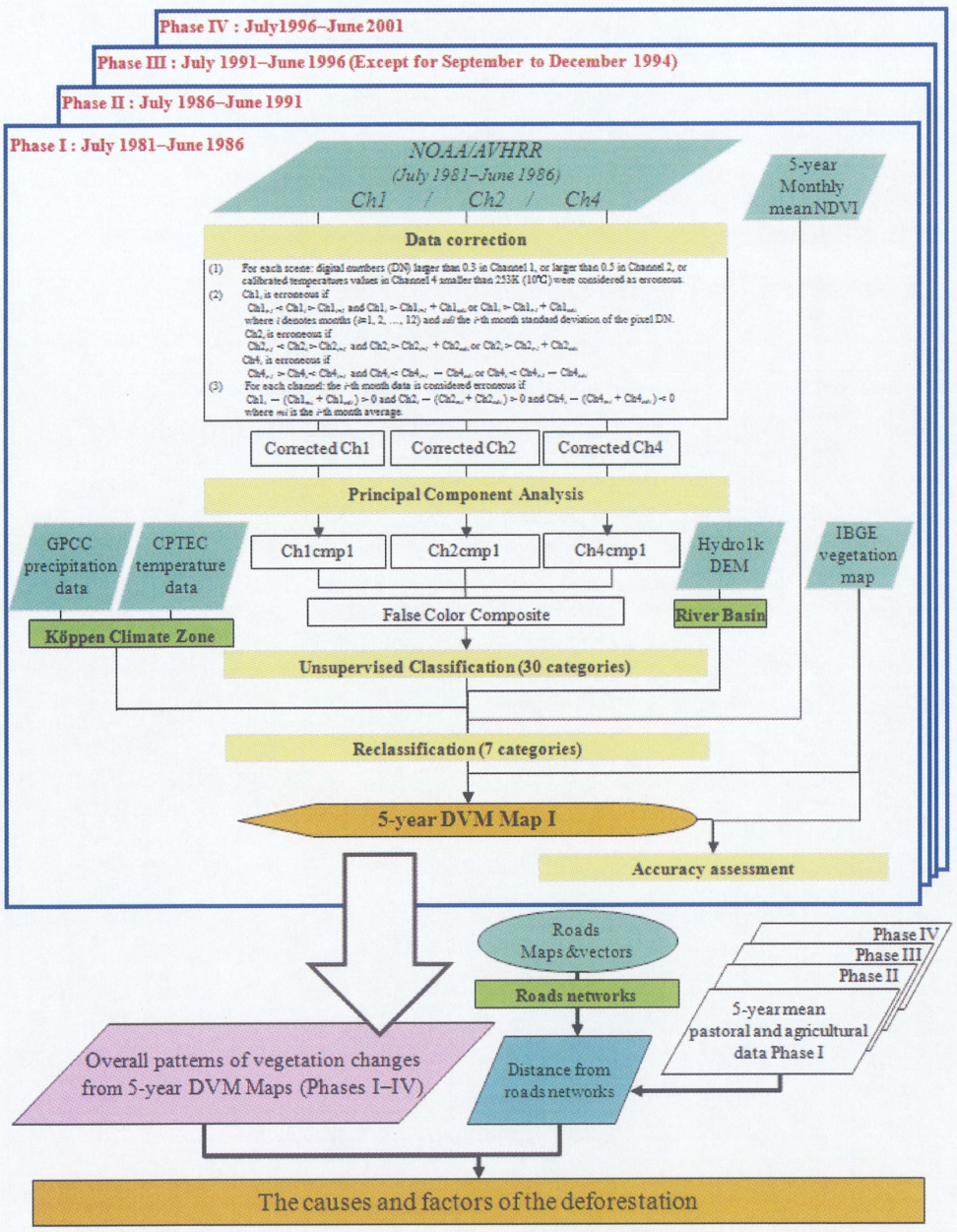

Figure 2.3. Flowchart for our analysis method.

2.5 Results

2.5.1 5-year vegetation maps

Based on the analysis flowchart in Figure 2.3, and referring to IBGE vegetation map (IBGE 2005) as ground truth, we successfully classified MT vegetation and land covers for every 5 years periods between 1981 and 2001 (Figures 2.4) into the following 7

main land cover types: the Evergreen Broadleaf Forests (abbreviated as EBF hereinafter), the Semi-deciduous Seasonal Forests (SdF), the Broadleaf and Seasonal Forests (BSF), the Savanna Woodlands (SW), the Savanna Grasslands (SG), the Savanna (S) and the Deeply Altered Areas (DA). Both EBF and BSF are dense forests, while SW are sparse forests. EBF are found in wet climates, with more than 9 months of rains. BSF prevail in areas with 3–5 months of dry season. SW and other savanna biomes are found in drier regions with 4–5 months of dry season. SG are grasslands prevailing over areas flooded during wet seasons while S are tropical grasslands covering drier places, including abandoned croplands (WWF 2001). No clear distinction has been made among these various ecosystems in previous works (Lovelands *et al.* 2000, Tsurumi and Sanga-Ngoie 2000, Morton *et al.* 2005 and INPE 2009). DA that we also call the Human activity areas, include such human activity as ranches, croplands, slash-and-burn agriculture and urban areas.

Figure 2.4a shows the 5-year DVM Map I obtained for the July 1981 to June 1986 period. From this, and the respective area coverage given in Table 2.2, EBF are shown to cover 38.1 % of the total area, spreading over the northwestern and the central north areas. BSF (15.1 %) cover the area near the Xingu River upper stream in the northeast. SW (24.0 %) and the DA (15.3 %) are distributed over most of the southern areas. The DA seems to spread especially around Cuiabá city and along the southern main roads. The S, almost not found, covers only 2.9 % of the total area. SdF (3.6 %) and SG (1.0 %) areas are dominant in the southwest, in the upper area of the Guaporé River basin, and in the upper stream of the Juruena River.

Figure 2.4b (areas statistics are given in Table 2.2) shows the 5-year DVM Map II for the July 1986 to June 1991 period. Most of the EBF (18.5 % of total area) are found in the northwestern MT, while BSF (24.8 %) expend over the northeast. Increased SW (30.4 %), DA (18.3 %) and S (4.1 %) spread over the southern part. We have to note here the sharp decrease in the EBF and the remarkable invasion of SW over the central area, especially in the upper reaches of the Xingu River and the Paraguay River, where

no roads are found. Significant increase in DA land cover types can be noted along the BR-158 road in the southeast region.

Figure 2.4c shows the 5-year DVM Map III for the July 1991 to June 1996 period. The EBF shrink to 16.5 % in coverage mostly confined to the northwest. The BSF cover 24% of the state, especially in the northeast. SW covers (26.4 %) spread mostly over the formerly EBF areas. DA types increase to 16.9 % and the S to 10.8 % in the southern part, the SdF to 4.1 % and the SG grow up to 1.2 % in the southwest. Invasion by the SW in the northern areas, which were initially covered by EBF, is quite remarkable. Vegetation covers become very fragmented. Human activity openings spread along BR-158 from the southeastern to northeastern areas.

The 5-year DVM Map IV (Figure 2.4d) covers the period from July 1996 to June 2001. Here, the EBF shrink furthermore to 13.8 %, mostly in the northwest, while the BSF drop to 23.4 % in the northeast. We have to note here that the following land cover types become dominant: the SW (17.3 %), DA (20.7 %) and S (21.6 %) in the southern part. S slightly exceeds DA types in coverage. Moreover, DA spread throughout up to the northern MT along all the main roads from southern regions. In the western reaches, parks and areas inhabited by indigenous people witness a dramatic change from EBF to BSF, with strong EBF decrease into northwest. SdF (2.4 %) and SG (0.8 %) are found in the southwest. Continuity for each vegetation type is no more a dominant feature: dramatically enhanced fragmentation is omnipresent. It is worth noting that, while only minor changes have occurred over the Xingu Indigenous Park during the last two decades, our results show remarkable changes from EBF to BSF between Phase III and Phase IV over the western park.

These results show that the most dramatic changes have occurred in the following 4 categories: EBF, SW, S and DA. We therefore focus on these 4 categories for further investigation in the following subsections.

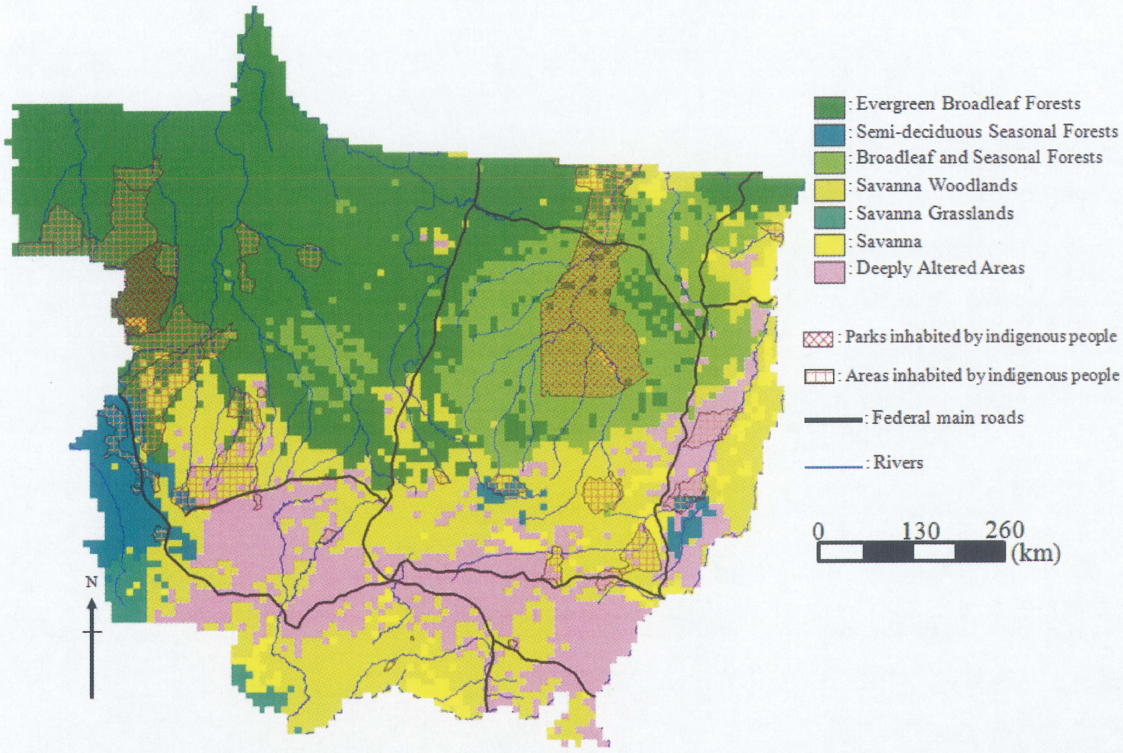

Figure 2.4a. 5-year DVM Maps I for the July 1981 to June 1986 (Phase I) in MT. Blue lines denote rivers, black bold lines are federal main roads, red meshes are Parks inhabited by indigenous people and orange meshes are Areas inhabited by indigenous people.

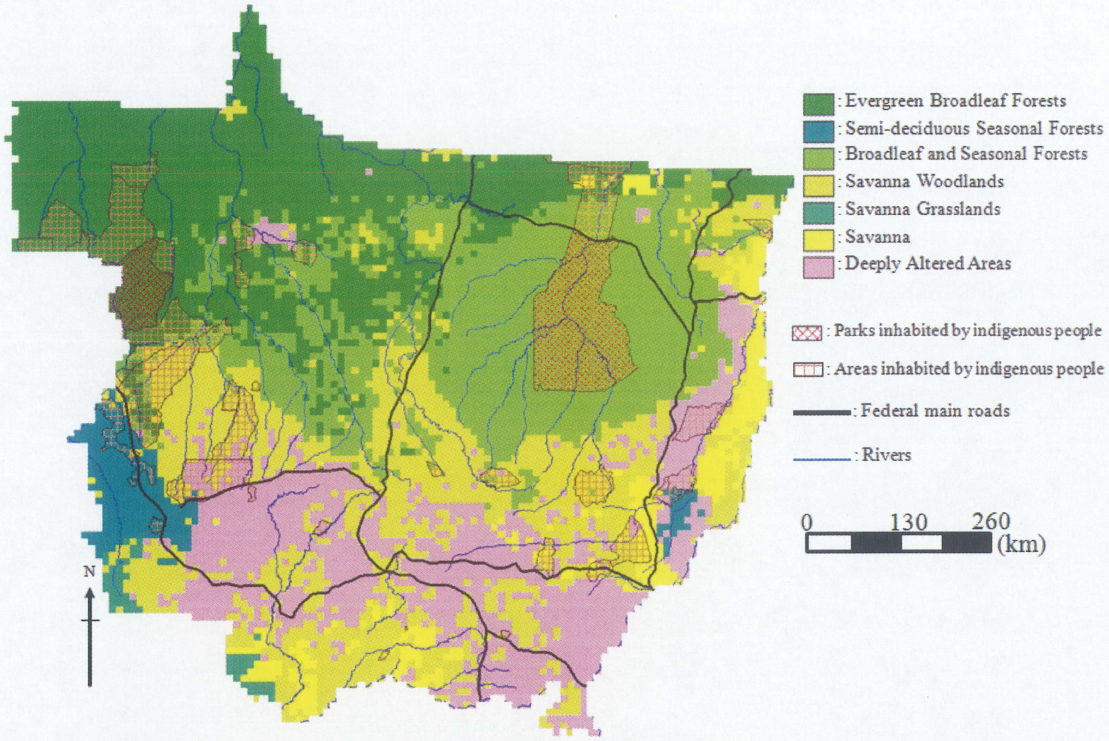

Figure 2.4b. Same as in Figure 2.4a, but for the 5-year DVM Map Phase II.

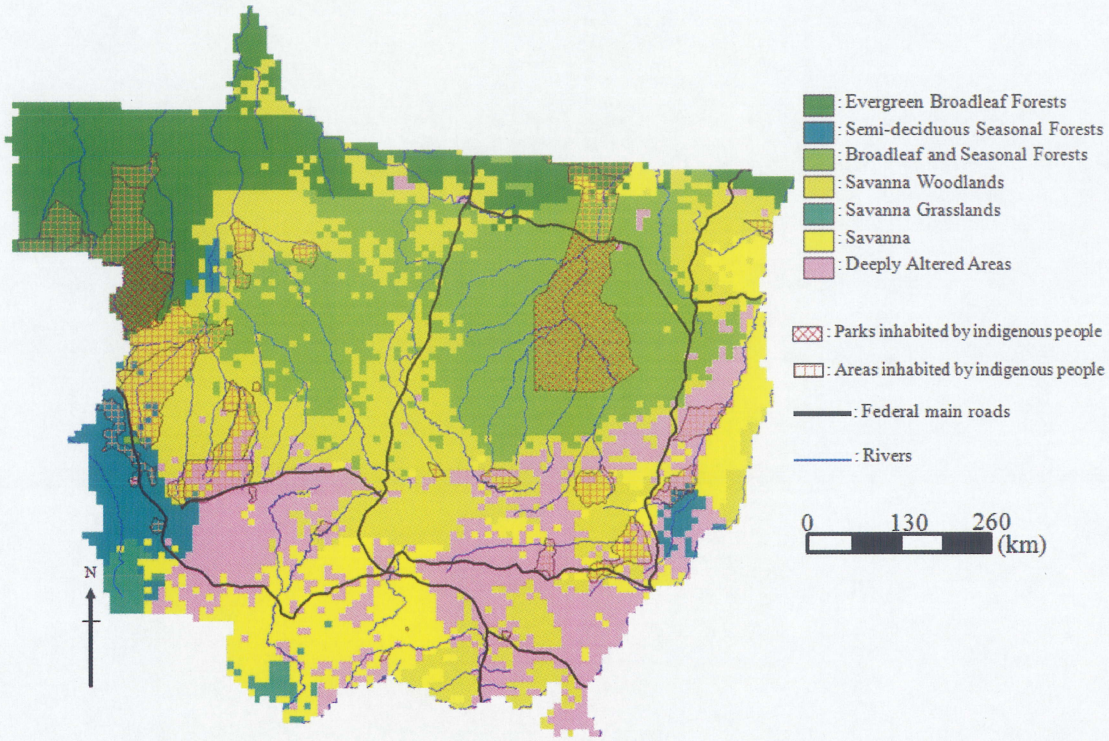

Figure 2.4c. Same as in Figure 2.4a, but for 5-year DVM Map Phase III.

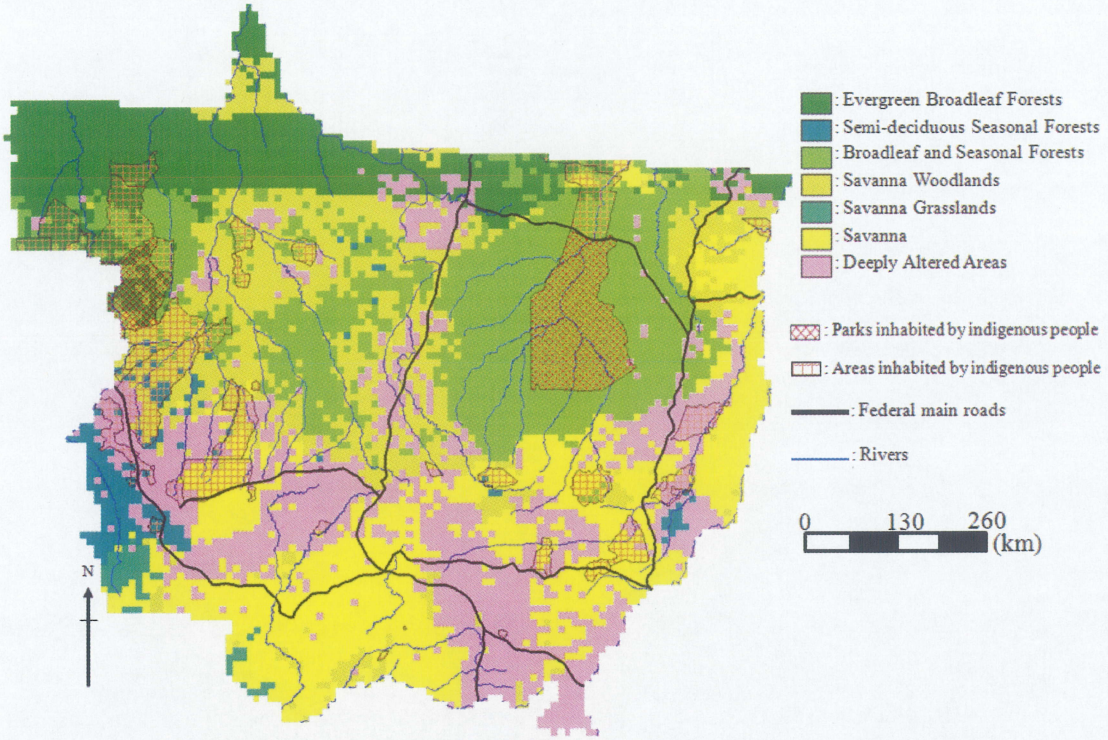

Figure 2.4d. Same as in Figure 2.4a, but for 5-year DVM Map Phase IV.

Table 2.2. 5-year DVM maps (Phases I–IV), their area ($\times 10^6$ ha) and their relative coverage within the whole state area (%).

	Area (%)			
	Phase I	Phase II	Phase III	Phase IV
Evergreen Broadleaf Forests	34.5 (38.1)	16.7 (18.5)	14.9 (16.5)	12.5 (13.8)
Semi-deciduous Seasonal Forests	3.3 (3.6)	2.9 (3.2)	3.8 (4.1)	2.2 (2.4)
Broadleaf and Seasonal Forests	13.7 (15.1)	22.5 (24.8)	21.8 (24.0)	21.2 (23.4)
Savanna Woodlands	21.7 (24.0)	27.5 (30.4)	23.9 (26.4)	15.7 (17.3)
Savanna Grasslands	0.9 (1.0)	0.7 (0.7)	1.1 (1.2)	0.7 (0.8)
Savanna	2.6 (2.9)	3.7 (4.1)	9.8 (10.8)	19.6 (21.6)
Deeply Altered Areas	13.6 (15.3)	16.6 (18.3)	15.3 (16.9)	18.7 (20.7)
Total	90.6 (100)	90.6 (100)	90.6 (100)	90.6 (100)

2.5.2 Accuracy assessments

Accuracy assessment was made for each one of the four 5-year DVM Maps (Phases I–IV) using the technique developed by Congalton (1991). An error matrix, or confusion matrix (Congalton 1991), was generated for a total of randomly selected points in order to determine the accuracies of the classified land cover types in each Phase. We extracted only the no changed vegetation from Phase I to Phase IV, because the IBGE vegetation map was different from 5-year DVM maps of Phase I, Phase II and Phase III. So the points extracted at random were decreased by comparison with 5-year DVM map Phase IV. Measures of accuracy were calculated for each category, especially the producer's accuracy (a measure of the omission error: it indicates the probability that a classified sample of a category actually represents the training site sample), the user's accuracy (a measure of the commission error indicating the probability that a classified sample of a category actually represents that category of reference on the ground), and the overall accuracy (the total number of correctly classified samples divided by the total number of reference samples, expressed in percent) using the IDRISI software module ERRMAT (Eastman 2001), respectively. All these measures are given in Tables 2.3a-d for each period, respectively.

Firstly, we compared IBGE vegetation maps to the contemporaneous 5-year DVM map Phase IV. An overall accuracy of 70.2 % was obtained using 3140 randomly selected points for this DVM map (Tables 2.3d).

Then, we extracted only those areas with no vegetation change between each one of the early DVM maps (Phase I, Phase II and Phase III) and Phase IV, respectively, to create vegetation control maps. We have to recall that the IBGE vegetation map was made in 2002, in the same period as Phase IV. Ground truth control points were selected from each one of these vegetation control maps and accuracy assessed accordingly. Overall accuracies of 70.3 % (using 3096 points) for Phase III (Tables 2.3c), 72.8 % (using 3086 points) for Phase II (Tables 2.3b) and 75.6 % (using 3069 points) for Phase

I (Tables 2.3a), were obtained.

Table 2.3a. Error matrix and accuracy assessment for the 5-year DVM Map Phase I.

	IBGE vegetation map								
5-year DVM Map I (number of pixels)	Evergreen Broadleaf Forests	Semi-deciduous Seasonal Forests	Broadleaf and Seasonal Forests	Savanna Woodlands	Savanna Grasslands	Savanna	Deeply Altered Areas	Total	Errors of Commission (%)
EBF	766	0	76	74	0	5	51	972	20
SdF	0	68	0	8	4	16	26	122	44
BSF	12	9	665	69	0	50	62	867	22
SW	1	8	5	117	0	99	49	279	58
SG	0	0	0	1	28	11	2	42	33
S	0	0	0	1	1	201	6	185	4
DA	0	0	1	7	0	93	477	602	20
Total	779	85	747	277	33	475	673	3069	
Errors of Omission (%)	2	20	11	58	15	58	29		24

Overall accuracy = 75.6%

Table 2.3b. Same as in Table a, but for the 5-year DVM Map Phase II.

	IBGE vegetation map								
5-year DVM Map II (number of pixels)	Evergreen Broadleaf Forests	Semi-deciduous Seasonal Forests	Broadleaf and Seasonal Forests	Savanna Woodlands	Savanna Grasslands	Savanna	Deeply Altered Areas	Total	Errors of Commission (%)
EBF	606	0	44	60	0	4	39	753	20
SdF	0	51	0	6	2	11	21	91	44
BSF	36	9	635	98	0	48	67	893	29
SW	18	9	60	252	0	68	75	482	48
SG	0	0	0	0	15	5	1	21	29
S	0	0	1	9	1	255	10	276	8
DA	2	3	2	11	0	117	435	570	24
Total	662	72	742	436	18	508	648	3086	
Errors of Omission (%)	8	29	14	42	17	50	33		27

Overall accuracy = 72.8%

Table 2.3c. Same as in Table a, but for the 5-year DVM Map Phase III.

	IBGE vegetation map								
5-year DVM Map III (number of pixels)	Evergreen Broadleaf Forests	Semi-deciduous Seasonal Forests	Broadleaf and Seasonal Forests	Savanna Woodlands	Savanna Grasslands	Savanna	Deeply Altered Areas	Total	Errors of Commission (%)
EBF	503	0	44	50	0	3	21	621	19
SdF	0	46	0	5	3	11	19	84	45
BSF	20	9	618	109	0	45	56	857	28
SW	61	7	66	220	0	96	82	532	59
SG	0	0	0	1	16	8	2	27	41
S	0	1	1	48	2	382	46	480	20
DA	1	0	1	8	0	95	390	495	21
Total	585	63	730	441	21	640	616	3096	
Errors of Omission (%)	14	27	15	50	23	40	37		30

Overall accuracy = 70.3%

Table 2.3d. Same as in Table a, but for the 5-year DVM Map Phase IV.

	IBGE vegetation map								
5-year DVM Map IV (number of pixels)	Evergreen Broadleaf Forests	Semi-deciduous Seasonal Forests	Broadleaf and Seasonal Forests	Savanna Woodlands	Savanna Grasslands	Savanna	Deeply Altered Areas	Total	Errors of Commission (%)
EBF	396	0	36	36	0	4	24	496	20
SdF	1	41	1	10	3	15	17	88	53
BSF	63	6	518	25	0	41	51	704	26
SW	34	9	50	158	0	92	43	386	59
SG	0	0	0	2	14	8	2	26	46
S	0	6	3	37	5	517	67	635	19
DA	20	7	24	50	0	144	560	805	30
Total	514	69	632	318	22	821	764	3140	
Errors of Omission (%)	23	41	18	50	36	37	27		30

Overall accuracy = 70.2%

2.5.3 Overall patterns of changes

The overall statistics of each one of the vegetation types (Table 2.2) show the sustained decrease in EBF and SW, as opposed to strong increase in S and DA land cover types during all the four periods. The total decrease in EBF coverage from Phase I to Phase IV was 22.0×10^6 ha and that in SW was 6.0×10^6 ha from the initial 34.5×10^6 ha and 21.7×10^6 ha, respectively. These are equivalent to 63.8 % and 27.6 % decrease as compared to the total initial coverage for each category, respectively, each one being replaced by other herbaceous or denuded land cover types. In opposite, S cover types have increased by 17.0×10^6 ha and the DA types by 5.1×10^6 ha in the same period from their initial 2.6×10^6 ha and 13.6×10^6 ha, respectively. This means that each one of these cover types increased 7.5 and 1.4 times, respectively, during this period of intense land cover alterations in Mato Grosso. Especially in the park over the Xingu river basin, there are few changes of the vegetation during two decades. But in the northern park EBF changed BSF dramatically from Phase III to Phase IV.

Using cross-tabulation analysis, overall vegetation changes were calculated from the changes in DVM maps between Phase I and Phase IV (figures not shown). The following dominant 10 change patterns were obtained. Of the total change area, 0.3 % was involved with changes from BSF, SW and S into EBF (Recovery Type 1), 0.7 % with the changes from SW, SG and DA into SdF (Recovery Type 2), 0.1 % with changes from S and DA into BSF (Recovery Type 3), and 1.1 % with changes from SG, S and DA into SW (Recovery Type 4). Moreover, changes from EBF and BSF into SdF (Degradation Type 1) covered 0.5 % of the total change area, changes from EBF and SW into BSF (Degradation Type 2) 18.5 %, changes from EBF, SdF and BSF into SW (Degradation Type 3) 22.6 %, and changes from SdF, SW and S into SG (Degradation Type 4) covering 0.3 % of the area, especially over the northwest and the central parts. Two types of Transitional areas were found: the Type 1 (22.2 % of the total change area), involving changes from EBF, SdF, BSF, SW and S into DA along roads all over

MT, and the Type 2 (33.7 % of the total change area) for changes from EBF, SdF, BSF, SW, SG and DA into S, spreading along roads over the southern Mato Grosso.

2.5.4 Causes of changes

In the early 1980s, Myers (1981) coined the phrase "Hamburger connection" to stigmatize the relationship between the export of beef from Central and South America to American fast food chains and the rampant deforestation of the Amazonian rainforests. Data available from SIDRA (2008) show that cattle herd size within the Legal Amazon did rapidly increase between 1990 and 2002, and the increase rate of MT is known to be the biggest in Brazil. Cattle ranching are noted to expand northward, especially together with roads construction and the conversion of forests into pasture lands (Moran 1993, Margulis 2004).

Figure 2.5 show the 5-year mean cattle counts distribution maps (Phases I–IV) for every municipal district of MT at same periods as for the 5-year DVM maps (Phases I–IV) in Figure 2.4. The following general patterns of the spatial and temporal changes in heads of cattle distribution were pinpointed. Large herds were initially concentrated in the south of MT (Phase I: on the upper left of Figure 2.5). Ranching activities started to spread northward from Phase II (upper right of Figure 2.5) along BR-158 and BR-163. These findings support and confirm the results by Moran (1993) who suggested that road construction lead to forests to pasture conversions. However, spatial distribution of large herds in the 1990's (Phase III and IV) shows that they tend to be located everywhere, not only in the south and east of MT, but also in the northern municipal districts where major roads are non-existent. Their presence in the Juruena and Xingu rivers basins, and the existence of riverine ports along many other navigable streams over upper reaches of the Xingu and Juruena river basins, suggests the important role of rivers and water ways as access networks especially from the north over the road less central and northern MT (Barreto *et al.* 2006, Calmon *et al.* 2008, Multimapas 2008).

Figure 2.6 show the 5-year mean soybean planted areas (Phases II–IV) for each municipal district at same periods as for the 5-year DVM maps (Phases II–IV) in Figure 4. The general spatial distribution (Figure 2.6) shows the dominance of soybean plantations in the southeast (East of Cuiabá) and the central western parts, mostly along the BR-163. Later changes between Phase III and Phase IV (Figure 2.6) are marked by the intensification of Soybean planted areas on the both zones, and their northward and westward spread over the central-western areas, to occupy most of the planted areas not only in MT but also all of the Brazil.

In fact, in terms of planted areas, Soybean always comes in the first place, occupying about 50% of the total of cultivated area in MT throughout our investigation period. The spectacular increase in Soybean production in MT is the results of combined action by major multinational companies in grain business from all over the world, and that of the MT governor since 2002 (Fearnside 2003). The impacts onto infrastructure building in order to support this intensified production can be easily figured out. Consequently, MT has turned out recently as the single world's largest soybean production area, and the major causes to deforestation after 2000 mostly involve farmland expansion for soybean production (Morton *et al.* 2006).

We therefore can point out that the main causes to deforestation in MT, as summarized in Figure 2.7, are: (1) urban development in the southern parts, (2) soybean production spreading and intensifying over the southeast, and mostly over the central-western parts, and (3) cattle ranching in the north along access networks (roads and water ways). These findings support and update previous works such as those by Moran (1981), Fearnside (2006) and Morton *et al.* (2006).

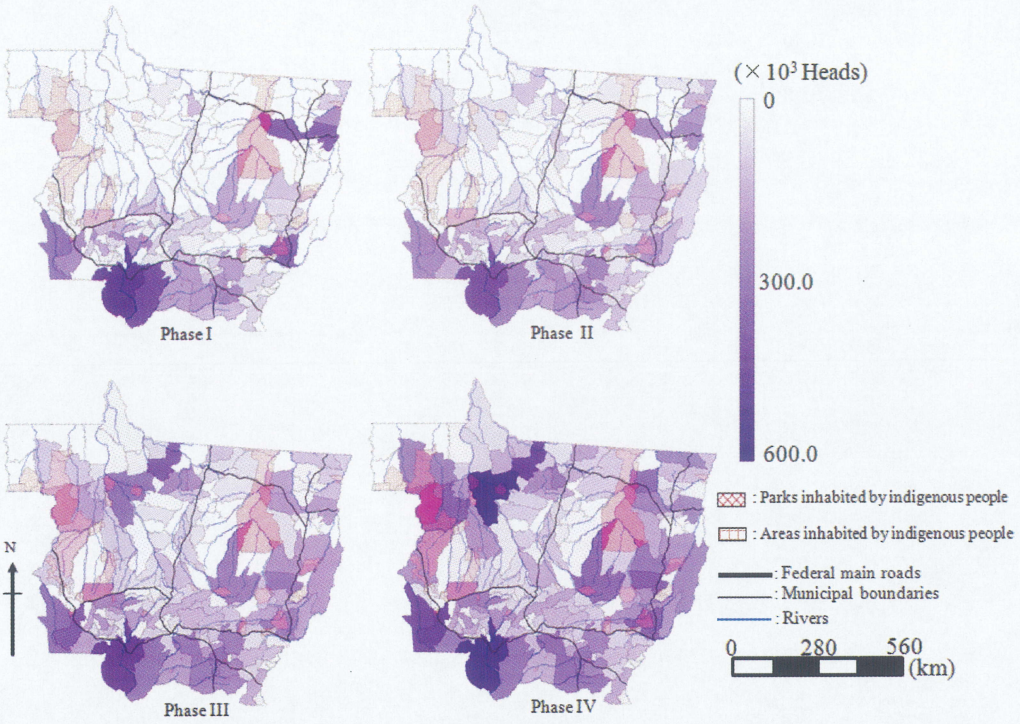

Figure 2.5. The distribution map in 5-year mean cattle counts of every municipal district in Mato Grosso.

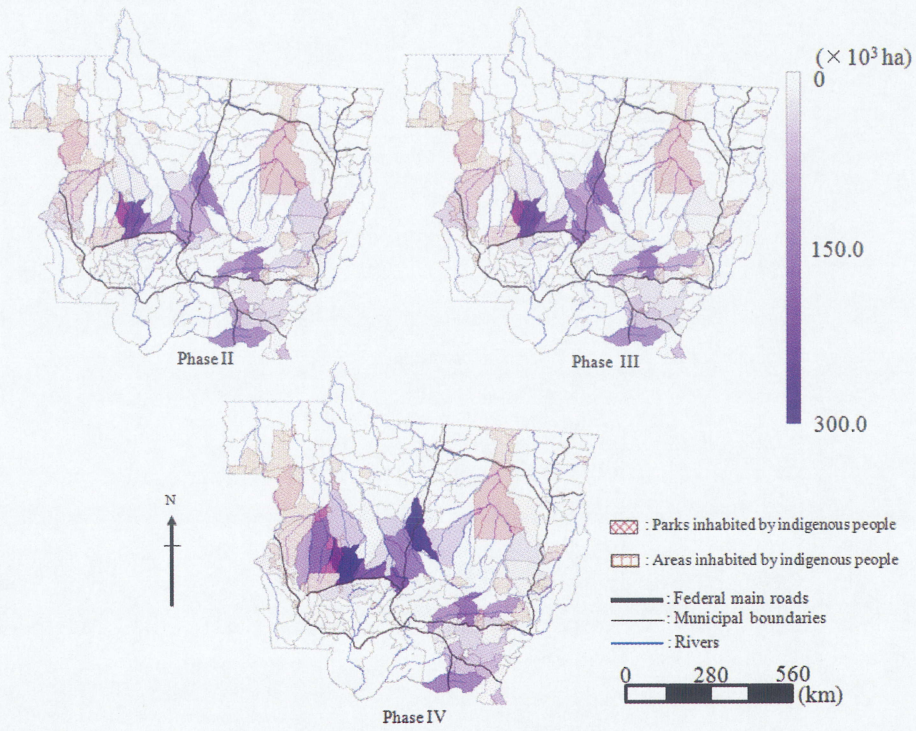

Figure 2.6. The distribution map in 5-year mean soybean planted areas of every municipal district in Mato Grosso.

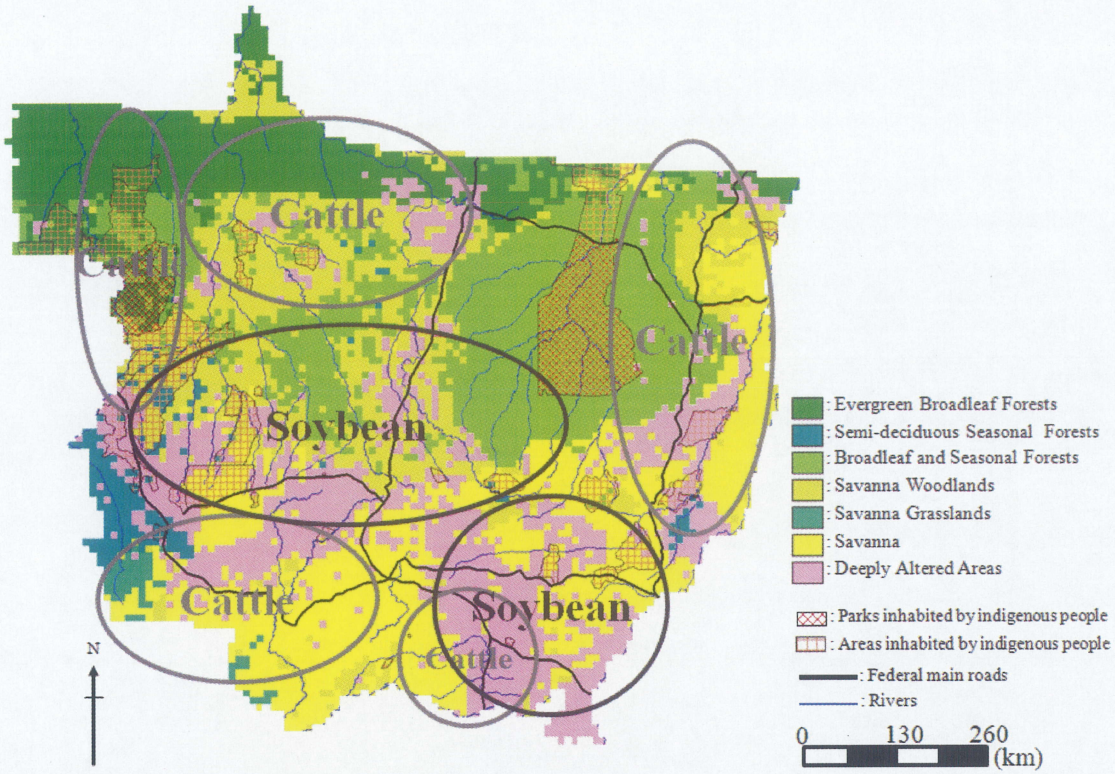

Figure 2.7. Summary of cause of vegetation change on 5-year DVM Map Phase IV. Grey ellipses denote cattle ranching areas and black ellipses soybean planted areas.

2.5.5 Role of roads networks as factors to deforestation

The findings in previous subsections have hinted at roads and water ways as possible factors related to the intensifications of deforestation in MT. This has also been pointed to by Fearnside (1986, 1993, 2005, 2006) and in many other works on the Amazon. We therefore focus on this issue in this subsection. As for the buffer zones, Nepstad *et al.* (2001) note that more than 2/3 of deforestation in legal Amazon occurred within 50 km of major paved highways. Alves (2002), using field investigation data alone, suggested that a large fraction (86 %) of total deforestation between 1991-1996 was found within 25 km from roads, while Barreto *et al.* (2006) recently show that about 80 % of the total deforested area is located within 30 km from official roads in the Amazon. In this work, we update and confirm these previous findings, using GIS and satellite data, for each

5-year period between 1981 and 2001. We consider 10 km-wide buffer zones centered on the communication network up to 50 km, to investigate more in detail the relative impacts of human activities to the Amazonian ecosystems, with the paved and unpaved roads communication network as centers of propagation.

Distance from roads networks, including paved and unpaved roads, (w: km) was calculated and classified into six categories ((1) $0<w\leqq10$; (2) $10<w\leqq20$; (3) $20<w\leqq30$; (4) $30<w\leqq40$; (5) $40<w\leqq50$ and (6) $50<w$), and covers for each vegetation type in each distance category during each analysis period were estimated (Table 2.4).

In the first category ($0<w\leqq10$ km) (Table 2.4), EBF and SW are shown to decrease from 10.9×10^6 ha and 8.2×10^6 ha to 3.0×10^6 ha and 5.7×10^6 ha, respectively, between Phases I and IV. However DA and S do increase from 7.8×10^6 ha and 0.7×10^6 ha to 10.6×10^6 ha and 7.6×10^6 ha, respectively. In other terms, during these phases, EBF decreased to a one-third, while S increased about 9 times within 10 km along roads. Spatially, changes from EBF into BSF and DA are remarkable along BR-080 and in the area along the upper reach of Xingu river between Phases I (Figure 2.8, upper left) and II (Figure 2.8, upper right), while more intense changes from EBF to SW, from SW to DA or S, and from DA to S tend to occur along BR-174, BR-163 and BR-158, spreading from the south between Phases II and IV (Figure 2.8, lower right). An overall change of 7.0×10^6 ha (13.6 %) of Transitional area Type 2 (Table 2.5) is strongly remarkable. The same is true for Transitional area Type 1 and Degradation Type 3. These alteration patterns suggest that waves of developers initiate vegetation changes along paved roads from the southern part, progressing northward and westward.

In the $10<w\leqq20$ km category (Table 2.4), EBF decrease from 7.3×10^6 ha to 2.3×10^6 ha, while BSF and S increase from 3.6×10^6 ha and 0.5×10^6 ha to 5.2×10^6 ha and 4.6×10^6 ha, respectively. Other vegetation types do not change so much. Changes from EBF into BSF and SW occur mostly by an invasion from the Juruena River in the upper reaches of the Amazon River through all phases. Similar change patterns are observed for the $20<w\leqq30$ and $30<w\leqq40$ category (Table 2.4).

Table 2.5 shows an overall change of 4.1×10^6 ha (8.0 %) for Transitional area Type 2 and 2.8×10^6 ha (5.4 %) for Degradation Type 3. In fact, the savannization becomes an issue from the late 1990's, likely consequently to vegetation degradation and abandonment of unproductive farms. In general, from the late 1990's, SW are on the rise, replacing EBF along roads networks, while in the southern parts, areas in the upper reaches of Xingu and Paraguay rivers are also changed into full scale savannas. This denotes the eventual progressive deforestation through selective or illegal logging in remote areas.

The four following points emerge from our findings as consolidated in Table 2.5. (1) the $0<w\leqq30$ categories altogether involve a total of 0.8×10^6 ha (amounting to 1.5 % of the total change) of recovering areas, 15.7×10^6 ha (30.5 %) of degradation areas, and 23.4×10^6 ha (45.7 %) of transitional land cover types. This implies that 76.1 % of the total negative change (degradation and transitional areas) in MT occur within 30 km along the access networks (roads and rivers). (2) For $30<w$ categories, the changes are 0.4×10^6 ha (0.3 % of total changes) for recovery, 6.2×10^6 ha (12%) for Degradation and 5.0×10^6 ha (9.8 %) for Transitional areas. (3) Coverage for Transitional areas is larger than Degradation in $0<w\leqq30$, while the opposite is true in $30<w$. This suggests that deforestation comes first, before introduction of agro-pastoral developments. (4) As a whole, recovering land covers types are very scarce: less than1.8 % of the change.

Table 2.4. Coverage ($\times 10^6$ ha) of 7-vegetation types of the classified 5-year DVM Maps (Phase I—Phase IV) as related to distance from roads networks (w: km) categories.

5-year DVM Maps (Phase I – Phase IV)	Area ($\times 10^6$ ha) per category of distance from access networks (w: km)					
	0<w≦10	10<w≦20	20<w≦30	30<w≦40	40<w≦50	50<w
Evergreen Broadleaf Forests Phase I	10.89	7.30	4.75	3.15	2.54	5.49
EBF Phase II	6.01	4.56	3.38	2.50	2.07	4.57
EBF Phase III	2.87	2.57	2.06	1.62	1.47	4.01
EBF Phase IV	3.03	2.31	1.69	1.23	1.17	2.74
Semi-deciduous seasonal Forests Phase I	1.78	0.94	0.36	0.10	0.06	0.01
SdF Phase II	1.63	0.77	0.31	0.10	0.06	0.01
SdF Phase III	2.03	0.95	0.42	0.16	0.10	0.01
SdF Phase IV	0.89	0.56	0.26	0.11	0.11	0.21
Broadleaf and Seasonal Forests Phase I	5.00	3.60	1.95	1.02	0.73	1.41
BSF Phase II	8.95	5.77	3.16	1.66	1.11	1.73
BSF Phase III	8.20	5.75	3.22	1.79	1.20	1.63
BSF Phase IV	6.66	5.20	3.22	2.02	1.51	2.58
Savanna Woodlands Phase I	8.21	4.63	2.85	1.88	1.25	2.64
SW Phase II	8.13	4.65	2.40	1.53	1.03	2.35
SW Phase III	9.90	5.46	2.78	1.62	1.23	2.83
SW Phase IV	5.73	3.62	2.18	1.20	0.71	2.13
Savanna Grasslands Phase I	0.35	0.22	0.06	0.01	0.00	0.27
SG Phase II	0.21	0.13	0.04	0.01	0.01	0.26
SG Phase III	0.34	0.24	0.07	0.03	0.01	0.38
SG Phase IV	0.24	0.22	0.07	0.02	0.02	0.13
Savanna Phase I	0.73	0.48	0.25	0.21	0.19	0.67
S Phase II	0.97	0.75	0.57	0.46	0.37	1.22
S Phase III	3.05	2.08	1.47	1.00	0.60	1.47
S Phase IV	7.60	4.55	2.52	1.48	0.93	2.34
Deeply Altered Areas Phase I	7.81	3.57	1.55	0.58	0.23	0.11
DA Phase II	8.86	4.12	1.93	0.71	0.35	0.45
DA Phase III	8.38	3.70	1.75	0.75	0.39	0.25
DA Phase IV	10.61	4.28	1.82	0.91	0.54	0.45

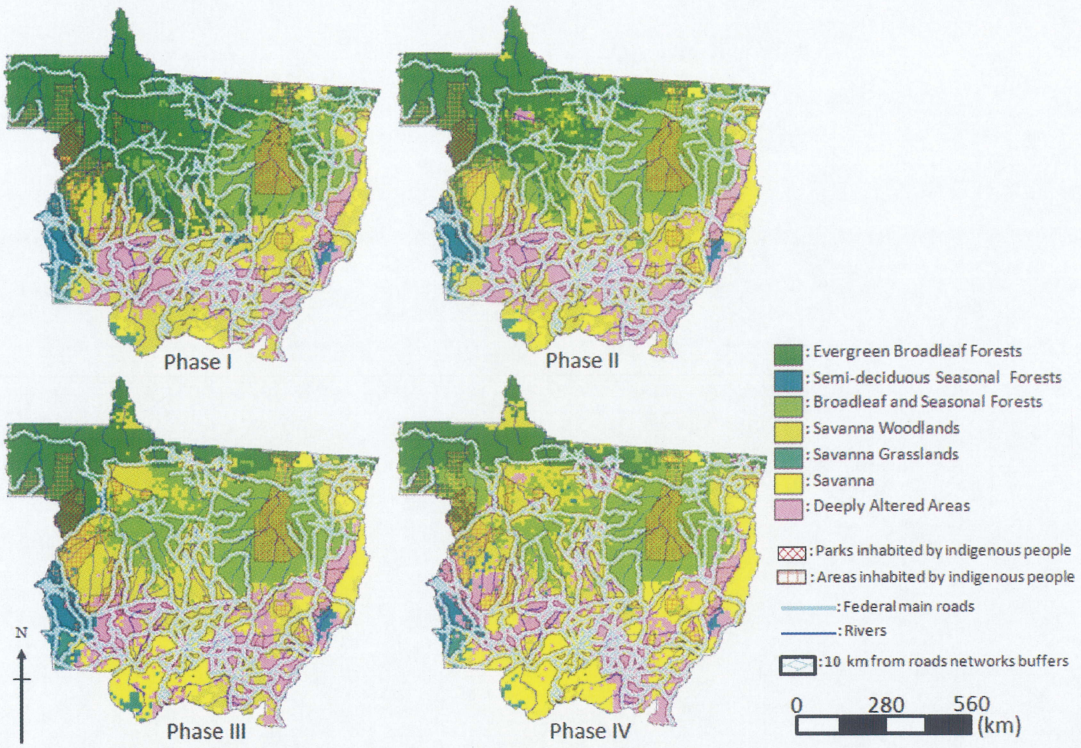

Figure 2.8. The 5-year DVM maps Phase I—Phase IV and 10 km buffers around roads networks.

Table 2.5. Coverage changes area ($\times 10^6$ ha) and rates of changes (%) as related to categories of distances from roads networks (w: km) between Phases I and IV.

5-year DVM maps (Phases I–IV)		Area ($\times 10^6$ ha) and relative coverage (%)					
		0<w≦10	10<w≦20	20<w≦30	30<w≦40	40<w≦50	50<w
Recovery Type 1	BSF・SW・S → EBF	0.06 (0.11)	0.04 (0.08)	0.02 (0.05)	0.00 (0.01)	0.01 (0.01)	0.01 (0.02)
Recovery Type 2	SW・SG・DA → SdF	0.04 (0.08)	0.04 (0.08)	0.03 (0.06)	0.04 (0.08)	0.05 (0.10)	0.28 (0.00)
Recovery Type 3	S・DA → BSF	0.04 (0.08)	0.03 (0.05)	0.00 (0.01)	0.00 (0.00)	0.00 (0.00)	0.00 (0.00)
Recovery Type 4	SG・S・DA → SW	0.26 (0.50)	0.14 (0.27)	0.07 (0.13)	0.03 (0.06)	0.00 (0.00)	0.02 (0.05)
Degradation Type 1	EBF・BSF → SdF	0.04 (0.09)	0.06 (0.11)	0.05 (0.09)	0.02 (0.05)	0.03 (0.06)	0.06 (0.12)
Degradation Type 2	EBF・SW → BSF	2.80 (5.45)	2.28 (4.43)	1.60 (3.12)	1.04 (2.02)	0.79 (1.53)	1.18 (2.30)
Degradation Types 3	EBF・SdF・BSF → SW	4.31 (8.39)	2.77 (5.39)	1.62 (3.15)	0.91 (1.78)	0.57 (1.10)	1.49 (2.90)
Degradation Types 4	SdF・SW・S → SG	0.06 (0.11)	0.05 (0.10)	0.02 (0.03)	0.02 (0.03)	0.02 (0.04)	0.02 (0.03)
Transitional area Types 1	EBF・SdF・BSF・SW・S → DA	6.36 (12.40)	2.59 (5.04)	1.08 (2.10)	0.53 (1.03)	0.35 (0.69)	0.36 (0.70)
Transitional area Types 2	EBF・SdF・BSF・SW・SG・DA → S	6.96 (13.57)	4.13 (8.05)	2.31 (4.50)	1.30 (2.54)	0.76 (1.48)	1.72 (3.35)

2.5.6 Role of access networks as factors

The findings in previous subsections have hinted at roads and water ways as possible factors related to the intensifications of deforestation in MT. This has also been pointed to by Fearnside (1986, 1993, 2005, 2006) and in many other works on the Amazon. We therefore focus on this issue in this subsection.

Distance from roads (paved and unpaved) and navigable rivers (r: km) as access networks was calculated and classified into six categories ((1) $0<r\leqq10$; (2) $10<r\leqq20$; (3) $20<r\leqq30$; (4) $30<r\leqq40$; (5) $40<r\leqq50$ and (6) $50<r$), and covers for each vegetation type in each distance category during each analysis period were estimated (Table 2.6).

In the first category ($0<r\leqq10$ km) (Tables 2.6a), EBF and SW are shown to decrease from 15.3×10^6 ha and 11.4×10^6 ha to 4.2×10^6 ha and 8.3×10^6 ha, respectively, between Phases I and IV. However DA and S do increase from 8.9×10^6 ha and 1.2×10^6 ha to 12.5×10^6 ha and 10.1×10^6 ha, respectively. In other terms, during these phases, EBF decreased to a one-fourth, while S increased about 8 times within 10 km along roads and water ways. Spatially, changes from EBF into BSF and DA are remarkable along BR-080 and the upper reaches of Xingu river between Phases I (Figure 2.9, upper left) and II (Figure 2.9, upper right), while more intense changes from EBF to SW, from SW to DA or S, and from DA to S tend to occur along BR-174, BR-163, BR-158, and the Juruena river, spreading from the south between Phases II (Figure 2.9, upper right) and IV (Figure 2.9, lower right). An overall change of 9.0×10^6 ha (17.6 %) of Transitional area Type 2 (Table 2.7) is strongly remarkable. The same is true for Transitional area Type 1 and Degradation Type 3. These alteration patterns suggest that waves of developers initiate vegetation changes along paved roads and water ways from the southern part, progressing northward and westward.

In the $10<r\leqq20$ km category (Tables 2.6), EBF decrease from 8.2×10^6 ha to 2.7×10^6 ha, while BSF and S increase from 4.0×10^6 ha and 0.7×10^6 ha to 6.0×10^6 ha and 5.4×10^6 ha, respectively. Other vegetation types do not change so much. Changes from EBF into

BSF and SW occur mostly by an invasion from the Juruena River in the upper reaches of the Amazon River through all phases. Similar change patterns are observed for the $20<r\leqq30$ and $30<r\leqq40$ category (Tables 2.6).

Table 2.7 shows an overall change of 4.8×10^6 ha (9.4 %) for Transitional area Type 2 and 3.0×10^6 ha (5.9 %) for Degradation Type 3. In fact, the savannization becomes an issue from the late 1990's, likely consequently to vegetation degradation and abandonment of unproductive farms. In general, from the late 1990's, SW are on the rise, replacing EBF along access networks. This denotes the eventual progressive deforestation through selective or illegal logging in remote areas. In the southern part, areas in the road less upper reaches of Xingu and Paraguay river are changed into full scale savannas. All this shows that not only roads, but also water ways are important factors to the sustained intensification of deforestation in the Brazilian Amazon.

The four following points emerge from our findings as consolidated in Table 2.7. (1) the $0<r\leqq30$ categories altogether involve a total of 1.0×10^6 ha (amounting to 2.0 % of the total change) of recovering areas, 19.1×10^6 ha (37.2 %) of degradation areas, and 26.9×10^6 ha (52.4 %) of transitional land cover types. This implies that 89.5 % of the total negative change (degradation and transitional areas) in MT occur within 30 km along the access networks (roads and rivers). (2) For $30<r$ categories, the changes are 0.09×10^6 ha (0.29 % of total changes) for recovery, 2.7×10^6 ha (5.3 %) for Degradation and 1.6×10^6 ha (3.1 %) for Transitional areas. (3) Coverage for Transitional areas is larger than Degradation in $0<r\leqq30$, while the opposite is true in $30<r$. This suggests that deforestation comes first, before introduction of agro-pastoral developments. (4) As a whole, recovering land covers types are very scarce: less than 2.26 % of the change.

Table 2.6. Coverage ($\times 10^6$ ha) of 7-vegetation types of the 5-year DVM Maps (Phase I – Phase IV) as related to distance from navigable rivers and roads (r: km) categories.

5-year DVM Maps (Phase I – Phase IV)	Area ($\times 10^6$ ha) per category of distance from navigable rivers and roads (r: km)					
	0<r≦10	10<r≦20	20<r≦30	30<r≦40	40<r≦50	50<r
Evergreen Broadleaf Forests Phase I	15.33	8.20	4.60	2.83	1.54	1.62
EBF Phase II	8.91	5.50	3.46	2.21	1.35	1.64
EBF Phase III	4.61	3.25	2.33	1.58	1.21	1.62
EBF Phase IV	4.23	2.69	1.86	1.29	0.98	1.13
Semi-deciduous seasonal Forests Phase I	2.13	0.88	0.22	0.00	0.00	0.00
SdF Phase II	1.92	0.74	0.21	0.00	0.00	0.00
SdF Phase III	2.43	0.95	0.28	0.00	0.00	0.00
SdF Phase IV	1.21	0.59	0.23	0.09	0.03	0.00
Broadleaf and Seasonal Forests Phase I	6.52	4.01	1.69	0.67	0.36	0.46
BSF Phase II	11.58	6.16	2.57	1.06	0.52	0.48
BSF Phase III	10.76	6.25	2.64	1.12	0.52	0.50
BSF Phase IV	9.26	5.97	2.83	1.39	0.77	0.98
Savanna Woodlands Phase I	11.37	5.80	2.65	1.09	0.36	0.19
SW Phase II	10.72	5.34	2.32	1.25	0.35	0.11
SW Phase III	13.10	6.17	2.66	1.39	0.39	0.12
SW Phase IV	8.28	4.22	1.93	0.91	0.20	0.03
Savanna Grasslands Phase I	0.42	0.20	0.06	0.04	0.05	0.13
SG Phase II	0.26	0.12	0.04	0.04	0.06	0.14
SG Phase III	0.46	0.31	0.11	0.07	0.04	0.05
SG Phase IV	0.31	0.20	0.04	0.03	0.05	0.07
Savanna Phase I	1.23	0.71	0.31	0.11	0.10	0.07
S Phase II	2.03	1.26	0.72	0.17	0.09	0.07
S Phase III	4.78	2.65	1.44	0.52	0.14	0.15
S Phase IV	10.12	5.44	2.48	0.83	0.30	0.25
Deeply Altered Areas Phase I	8.87	3.59	1.12	0.25	0.03	0.00
DA Phase II	10.46	4.26	1.35	0.26	0.06	0.02
DA Phase III	9.74	3.81	1.20	0.31	0.13	0.03
DA Phase IV	12.48	4.27	1.30	0.45	0.11	0.01

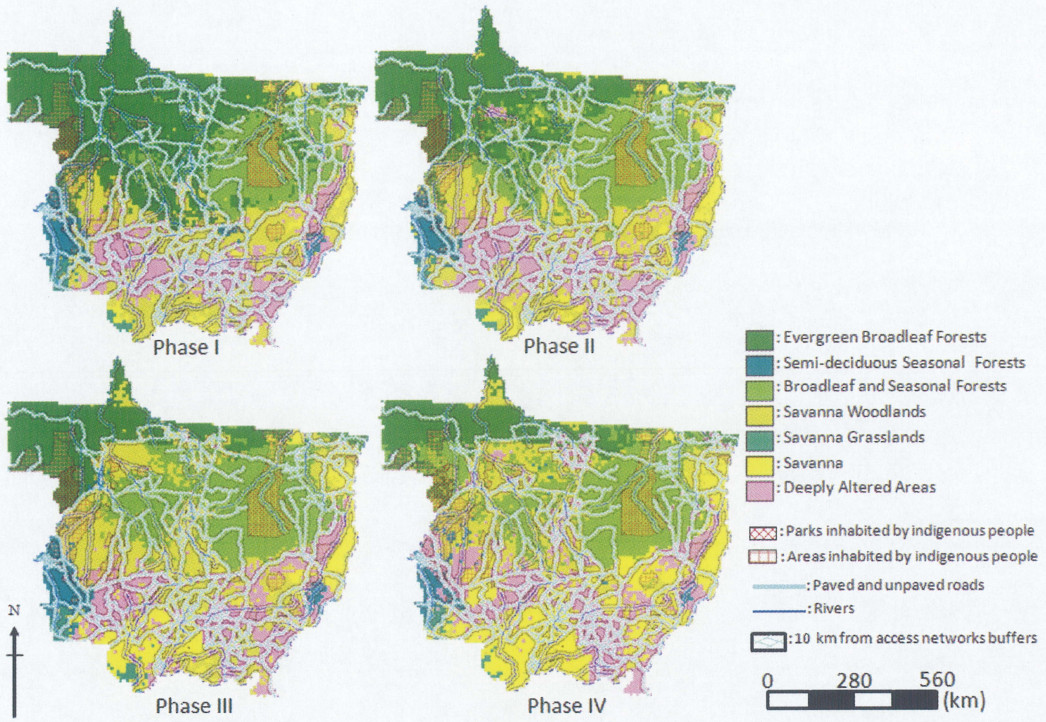

Figure 2.9. The 5-year DVM maps Phase I—Phase IV and 10 km buffers around access networks.

Table 2.7. Coverage changes area ($\times 10^6$ ha) and rates of changes (%) as related to categories of distances from navigable rivers and roads (r: km) between Phases I and IV

5-year DVM maps (Phases I–IV)		Area ($\times 10^6$ ha) and relative coverage (%)					
		0<r≦10	10<r≦20	20<r≦30	30<r≦40	40<r≦50	50<r
Recovery Type 1	BSF・SW・S → EBF	0.07 (0.14)	0.05 (0.10)	0.02 (0.04)	0.01 (0.01)	0.00 (0.00)	0.00 (0.00)
Recovery Type 2	SW・SG・DA → SdF	0.14 (0.28)	0.09 (0.17)	0.08 (0.15)	0.03 (0.06)	0.01 (0.02)	0.00 (0.02)
Recovery Type 3	S・DA → BSF	0.07 (0.13)	0.01 (0.01)	0.00 (0.00)	0.00 (0.00)	0.00 (0.00)	0.00 (0.00)
Recovery Type 4	SG・S・DA → SW	0.27 (0.53)	0.17 (0.33)	0.05 (0.09)	0.02 (0.04)	0.01 (0.01)	0.01 (0.13)
Degradation Type 1	EBF・BSF → SdF	0.08 (0.16)	0.07 (0.14)	0.04 (0.08)	0.06 (0.11)	0.01 (0.03)	0.00 (0.00)
Degradation Type 2	EBF・SW → BSF	3.99 (7.78)	2.65 (5.17)	1.37 (2.66)	0.73 (1.42)	0.41 (0.79)	0.52 (1.04)
Degradation Types 3	EBF・SdF・BSF → SW	6.28 (12.25)	3.01 (5.88)	1.42 (2.77)	0.75 (1.47)	0.18 (0.35)	0.00 (0.00)
Degradation Types 4	SdF・SW・S → SG	0.06 (0.11)	0.06 (0.12)	0.02 (0.04)	0.01 (0.02)	0.03 (0.05)	0.00 (0.00)
Transitional area Types 1	EBF・SdF・BSF・SW・S → DA	7.48 (14.58)	2.51 (4.89)	0.85 (1.66)	0.33 (0.64)	0.09 (0.17)	0.01 (0.03)
Transitional area Types 2	EBF・SdF・BSF・SW・SG・DA → S	9.01 (17.55)	4.82 (9.38)	2.21 (4.30)	0.74 (1.45)	0.22 (0.44)	0.19 (0.36)

2.6 Discussion and concluding remarks

In this chapter, using the data fusion technique initially proposed by Tsurumi and Sanga-Ngoie (2000), later on modified by Nonomura *et al.* (2003), we obtained seven-category and high quality 5-year DVM maps (Phases I–IV: Figures 2.4) for four 5-year periods over the 1981-2001 period. These high accuracy classification land use/land cover maps show an overall good agreement with the most recent IBGE (2005) vegetation map. Long-term NOAA/AVHRR remote sensing data were used on a GIS platform for low-cost but highly performing mapping in an analytical methodology that allowed us to avoid the main weaknesses of previous studies, such as: (i) vegetation classification based on short-term satellite databases, using NDVI only (Tucker *et al.* 1985, Townshend *et al.* 1987, Murai and Honda 1991, Eastman and Fulk 1993), (ii) oversimplification by 2-category classifications specifying only forested and non-forested areas (Skole and Tucker 1993, Morton *et al.* 2005, INPE 2009 on Figure 2.2) and (iii) successful distinction between various Amazonian land cover types, especially between BSF and EBF, contrarily to results by DeFries *et al.* (1998), Lovelands *et al.* (2000) and Tsurumi and Sanga-Ngoie (2000).

Our analysis results (Figure 2.4) show that, by mid-1980's, MT was covered by 7 main land cover and vegetation types that can be aggregated into the following 4 main groups: (1) EBF (38.1 % of MT), especially over the northwestern and north-central areas; (2) BSF (15.1 %) in the upper stream of Xingu river in the northeastern part, together with SdF (3.6 %) in the southwest; (3) the S complex (27.9 %) in the southern part, dominated by SW (24.0 %) with patches of S (2.9 %) and SG (1.0 %) in the upper part of the Guapore and Juruena river basins in the southwestern part of the State; and (4) DA (15.3 %), spreading especially around Cuiabà City and along the main roads in the south. Dramatic changes in vegetation covers from EBF to BSF are remarkable in the western parks and the areas inhabited by indigenous people. However, only little changes could be detected in the northern park spanning over the Xingu river basin.

Figure 2.8 summarizes the temporal vegetation change patterns in MT, with the strength and the dynamics of the changes (recovery, degradation and transitional process) indicated by solid arrows of different widths. The change patterns throughout the analysis period are characterized by a sharp decrease in EBF from the initial 38.1 % of MT total lands to 18.5 % (Phase II), to 16.5 % (Phase III) and finally to 13.8 % (Phase IV) on one side, and by the remarkable increase of thinner forest cover types (SdF and BSF), of herbaceous vegetation types (the savanna complex grows from 27.9 % in Phase I to 35.2 %, then to 38.4 %, and finally to 39.7 % in Phase IV), and of the DA (from 15.3 % in Phase I to 20.7 % in Phase IV) on the other side. The sharp decrease by 19.6 % in EBF between Phase I and II is quite remarkable. These findings confirm, and update, those by Fearnside (1993) who notes a decrease of about 16.3 % in forests covers by 1991 in MT.

The main trends in the changes (Figure 2.10) show the dominance of deforestation of natural forests between Phase I and Phase II, and of deforestation plus savannization between Phase II and Phase III. Savannization, quite remarkable from Phase II, becomes dominant later on. It seems to result either from deforested lands changing into pastures or farm lands, or from those abandoned DA. S covers spread from 2.9 % in Phase I to 4.1 % (Phase II), and then to 10.8 % (Phase III), and finally to 21.6 % in Phase IV. In general, huge areas of soybean production spreading over the southeastern and the central-western parts (Figure 2.6), together with vast cattle rearing ranches along access networks in the northern parts (Figure 2.5), are shown to be the leading causes to vegetation change in MT.

Park (1992) noted a 10-time increase of non-indigenous population in the Brazilian Amazon since the 1960s, from about 2 million to 20 million people, as the result of transmigration from other areas in Brazil, especially from the highly populated southern megalopolises. He postulated this to be the biggest impetus to deforestation in this region. Moreover, Margulis (2004) and Fearnside (2006) suggest that expanding road networks strongly increase the access to remote forests by the ranchers and colonists,

bringing in tremendous industrial logging, mining, large-scale mechanized agriculture, and cattle ranching, as well as negative ecological impacts, non-accounted for so far.

Taking distance from access networks into consideration, we could shed new light on their important role as multiplicand factors to the deforestation rates: in total, 76.1 % and 89.5 % of land cover degradations do occur within 30 km from ***roads*** (including paved and unpaved roads) and ***access networks*** (Table 2.5 and 2.7). These findings update those by Nepstad *et al.* (2001) who noted that more than two-thirds of deforestation in Legal Amazon occurred within 50 km of major paved highways, and the results by Alves (2002) who found that 86 % of the total deforested areas were within 25 km from federal highways and Barreto *et al.* (2006) who suggest that 80% were within 30 km of official roads. And our analysis results show that recovery rate within the 30 km from the roads and access networks amounts only to 0.9 % and 1.2 % for the total state lands.

Expansion of croplands or pastures over the southern part, and deforested areas in the northern part from the late 1980's is remarkable within 30 km along access networks. From the late 1990's, these altered lands cover types change either into savannas in the southern lands, or into croplands and pastures in the northern parts of MT. No new roads construction is noted in these northern areas, but pockets of human settlements and deep vegetation changes are remarkable along main rivers. In the upper reaches of the Juruena river, logging prevails from the late 1980's, followed by invasion by DA as early as the late 1990's. The same is true in the upper reaches of the Xingu river and the Paraguay river, where logging prevailed in the early 1980's, followed by wide-spread savannization in the late 1990's. All this emphasizes the fact that, not only roads construction, but also access by waterways access, played an important role as multiplicand factors to deforestation in MT between 1981 and 2001. On Figure 2.2, deforestation rate of the Pará state increases as a recent tendency. The rainforest of MT may be destroyed exhaustively by about 2000, and this shows invasion advances to Pará state in the northern state of MT after 2000.

By accurately specifying the cover types and by quantitatively assessing their spatial and temporal changes, our methodology seems to lay more quantitative grounds for more accurate eco-climatic impact analyses involving land cover discrimination and changes not only for the Amazon, but also for the tropical rainforests in general, or for such ecological applications as CO_2 emission/sequestration estimations along the Kyoto Protocol framework, as noted by Santilli *et al.* (2005) and DeFries *et al.* (2007). Analytical outputs by using this methodology can also provide initial data for prediction of later states of the Amazonian forests, instead of using model-based simulated data (Laurance *et al.* 2001). We also foresee its use for sound decision-making aimed at sustainable use or management of biosphere resources not only for Mato Grosso or Brazil, but also for many other tropical rainforests areas.

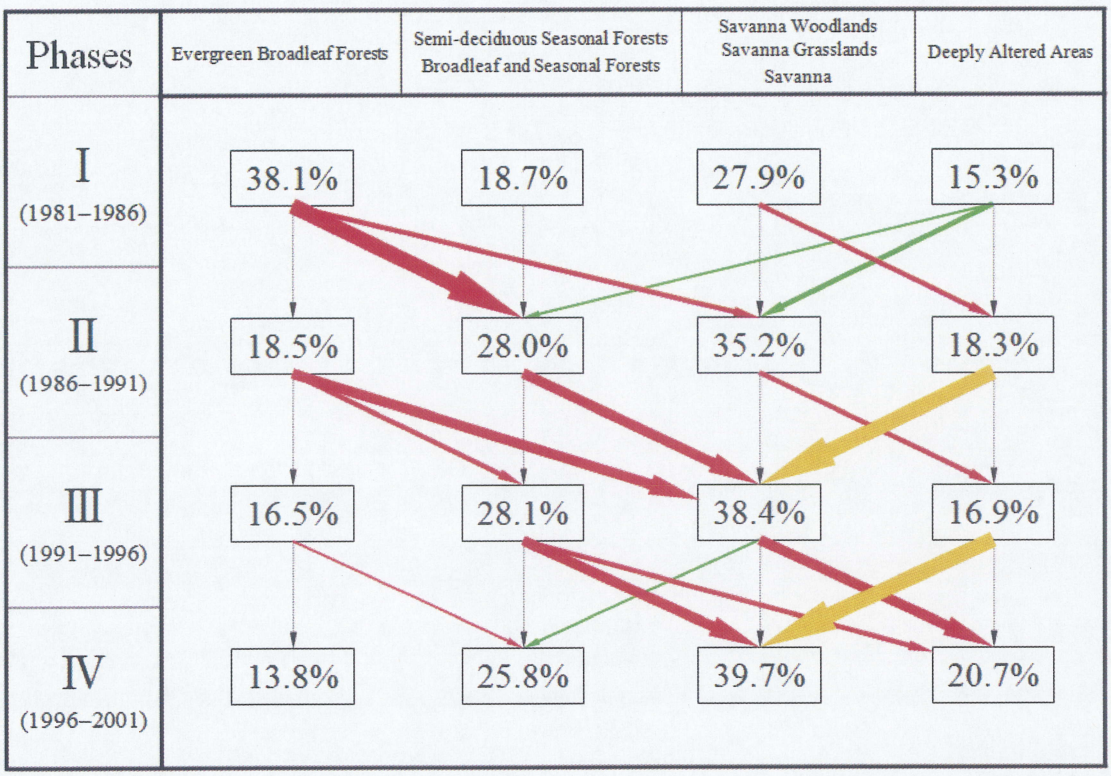

Figure 2.10. Trend of Vegetation changes from Phases I to Phase IV. Solid arrows denote recovery (green), degradation (red) and transitional process (yellow), respectively. The solid arrows thickness denotes the change rates, in decreasing order: 7–10 %, 5–7 %, 3–5 % and 1.5–3 %.

Chapter 3

Concernment between agro-pastoral frontier and vegetation change dynamics

This chapter is based on
Yoshikawa, S. and Sanga-Ngoie, K., 2009, Vegetation change and cause of changes in Mato Grosso, central-western Brazil, using NOAA/AVHRR and GIS during the 1981-2001, Theory and Application of GIS, Vol.17, No.2 p.11-20

Chapter 3

Concernment between agro-pastoral frontier and vegetation change dynamics

3.1 Introduction

Deforestation in the southern and eastern Brazilian Amazon continues to spread in relations with, among others, the exploding population growth (Park 1992), expanding road network, uncontrolled slash-and-burn cultivation, large scale mechanized agriculture and cattle ranching (Fearnside 1986; 2005; 2006; Morton *et al.* 2006), commercial timber harvest, mining and selective logging (Asner *et al.* 2005). Nowadays, soybean, bio-fuel which made from corn and sugarcane produced by large scale mechanized agriculture and cattle ranching have become major contributors to the Brazilian economy. However, Soares-Filho *et al.* (2006) stress that the current tendency in agricultural expansion might eliminate a total of 40 % of the Amazon forests by 2050.

Amazon deforestation is noted to be Brazil's largest source of CO_2 emission (Santilli *et al.* 2005). It has been reported that deforestation increases temperature while decreasing evapotranspiration and precipitation (Sanga-Ngoie and Fukuyama 1996, Gash *et al.* 1997). This is particularly remarkable over the Amazon during dry seasons from June to November in model experiments (Sampaio *et al.* 2007). Therefore, deforestation in the tropics might bring profound impacts on the climate system at various scales, and even contribute to enhancing global warming (Henderson-Sellers *et al.* 1996).

Various techniques are being used for environmental monitoring and impact assessment at the regional and global level, consequent on deforestation in the tropics.

The Brazilian government has entrusted the monitoring of annual gross deforestation of the Brazilian Amazon since 1988 to the Instituto Nacional de Pesquisas Espaciais (INPE) using remote sensing data (INPE 1999, 2000, 2001, 2002, 2006). In addition, the Real Time Deforestation Monitoring System (DETER), which is a real-time deforestation assessment system for controlling deforestation in the Amazon, was set up by INPE and NASA (Morton *et al.* 2005). However these researches on forest-resources evaluation suffer from strong attenuation in satellite data accuracy due to the influence of abnormal weathers, and from the fact that they only distinguish between forests and deforestation areas.

In our previous work (Yoshikawa and Sanga-Ngoie 2010) in Chapter 2, we analyzed the state and change in the tropical rainforest cover types in the Brazilian Amazon for the past 2 decades (1981-2001) taking MT as a case study. We developed a set of 5-year Digital Vegetation Model (DVM) maps (Phase I, II, III and IV) for every five years between 1981-2001 using the Nonomura *et al.* (2003) method. This procedure was done by using 5-year mean NOAA/AVHRR monthly data in 1985-1991 in an attempt to acquire accurate and upgradeable digital images of land cover types based on fusion analysis of the visible red band (Channel 1: 0.58~0.68μm), the near-infrared band (Channel 2: 0.73~1.10μm), and the thermal infrared band (Channel 4: 10.3~11.3μm) of the 5-year monthly mean NOAA/AVHRR GVI (Green Vegetation Index) climatology throughout the entire African continent.

Our analysis results (Yoshikawa and Sanga-Ngoie 2010) show that, among 7 main land cover types found in MT, four vegetations types (EBF, SW, S and DA) did undergo most of the changes in this region. Moreover Vegetation and land cover changes are characterized by destruction of rain forests in the north and large-scale savannization expanding from the south. Large-scale soybean production spreading over the central area and vast herds of cattle in the north and south can be pointed out as the main causes of vegetation change in these areas. It is shown that 76.1 % and 89.5 % of the changes in land cover types occur within 30 km from (paved and unpaved) roads (Sanga-Ngoie

and Yoshikawa 2008 (a), 2008 (c), 2009 (a)) and access (roads and navigable rivers) networks (Sanga-Ngoie and Yoshikawa 2009 (b), 2009 (c)). This emphasizes not only the role of road building, but also that of navigable rivers, in accelerating deforestation, especially over the north without roads.

MT is nowadays known to be the largest soybean and beef production area in the Brazil. Soybean production greatly contributes to cerrado development. The production volume increases year by year, fueled by world markets demands and is accelerated by the emergence of foreign-financed companies. The increase of cattle ranches in MT is shown to account for the bulk of deforestation expansion towards the north (Margulis 2004). On the other side, this increase of cattle herd in the Brazilian Amazon is shown to be largely responsible for the recent world-wide beef prices dropping in fact (Kaimowitz *et al.* 2004).

Morton *et al.* (2006) showed that the amount of deforestation for cropland in MT was strongly and positively correlated with the mean annual soybean price during 2000-2004. At the same time they showed that deforestation averaged twice the size of clearings for pasture. In recent years, Brazilian croplands are shifting to corn or sugarcane for bio-fuel production, and quite a number of factories are being built for that purpose. MT is not an exception: changes in *agro-industry* are tremendous (cf. Figure 3.1).

However, so far only few quantitative analyses between the vegetation change and these agro-industrial data are available. In this chapter, the specific research objective is to deal more in detail with following issue; analyzing the causes of deforestation and savannization by using agro-industry data at municipal levels in MT as a case study.

This present work consists of 6 sections. Hereafter, the study site description is presented in section 3.2, the data sources and materials and analysis methods in section 3.3 and 3.4, respectively. Our analysis results (vegetation change, dynamics of the vegetation changes, Cause of changes and Statistical analysis of the change) are given in section 3.5. The discussion and concluding remarks are given in section 3.6.

Figure 3.1. Agro-industry areas have cultivated soybean (above) and corn (below). These photographs were taken by Yoshikawa in ground observation on 27th June 2008.

3.2 Study site description

The research area (Figure 3.2) is the MT in the central-west Brazil, located between 7° 21' S and 18° 02' S of latitude, and 50° 14' W and 61° 38' W of longitude. MT is divided into 141 municipal districts.

Fearnside (2003) suggested that federal requirements specify that the "legal reserve" of native vegetation to be maintained in each property (or in registered lands elsewhere) must be equal to 80 % of the property in forested area and 35 % in the cerrado in 2000. The MT government specifies that 50 % of the whole MT area should be in the "transition" area, the ecotone between the forest and the cerrado. Forests are located in the north part of the state, the transition in the center and, the cerrado in the south (Fearnside 2005).

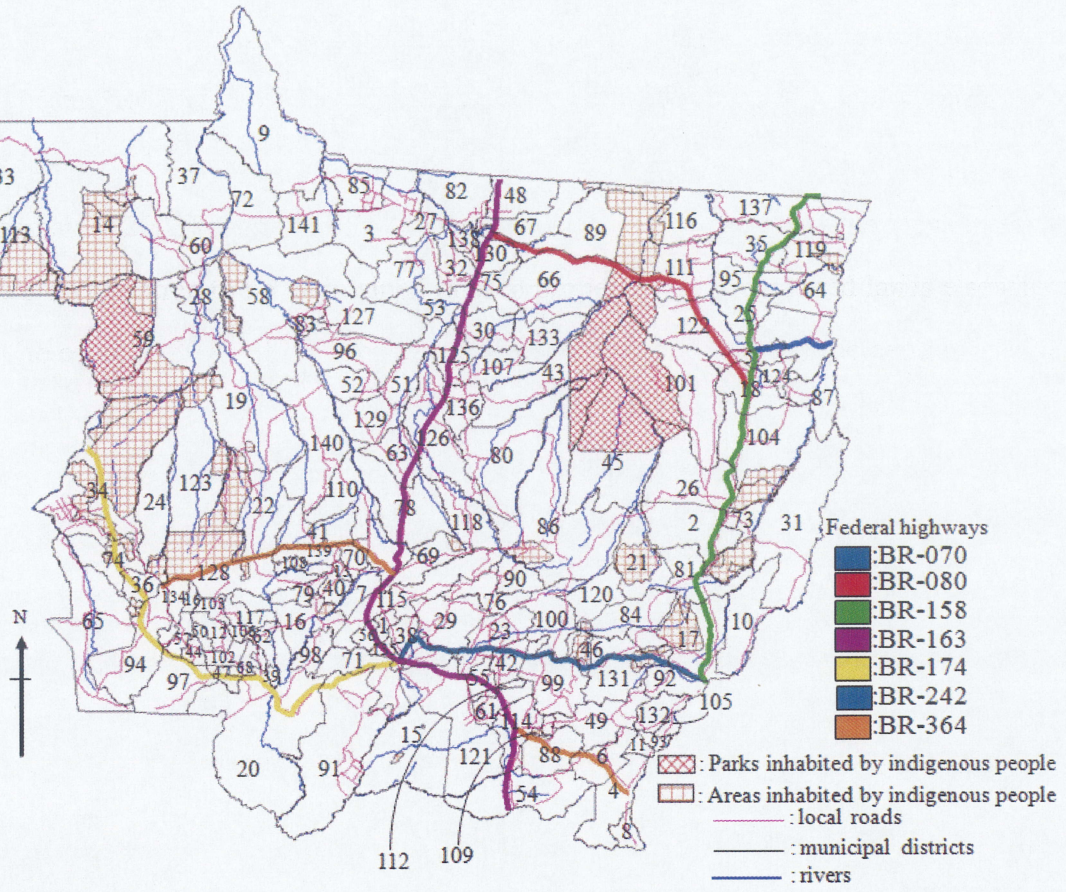

Figure 3.2. The 141 municipal districts in Mato Grosso, our study site, located in the

Southern Brazilian Amazon. Bold lines denote federal main highways: BR-070, BR-080, BR-158, BR-163, BR-174, BR-242 and BR-364, while pink lines are local roads, red diagonal grids are Parks inhabited by indigenous people and orange normal grids are Areas inhabited by indigenous people and black lines are municipal districts:

1-Acoriza (1,876.17km^2), 2-Água Boa (7,610.05 km^2), 3-Alta Floresta (8,963.19 km^2), 4-Alto Araguaia (5,509.19 km^2), 5-Alto Boa Vista (2,394.21 km^2), 6-Alto Garças (3,740.03 km^2), 7-Alto Paraguai (2,048.55 km^2), 8-Alto Taquari1 (392.47 km^2), 9-Apiacás (20,535.07 km^2), 10-Araguaiana (6,475.39 km^2), 11-Araguainha (676.12 km^2), 12-Araputanga (1,605.71 km^2), 13-Arenápolis (439.43 km^2), 14-Aripuanã (25,215.07 km^2), 15-Barão de Melgaço (11,151.86 km^2), 16-Barra do Bugres (609.39 km^2), 17-Barra do Garças (9,118.49 km^2), 18-Bom Jesus do Araguaia (4,239.00 km^2), 19-Brasnorte (15,982.05 km^2), 20-Cáceres (24,416.24 km^2), 21-Campinápolis (5,984.68 km^2), 22-Campo Novo do Parecis (9,555.36 km^2), 23-Campo Verde (4,839.31 km^2), 24-Campos de Júlio (6,863.09 km^2), 25-Canabrava do Norte (3,487.75 km^2), 26-Canarana (10,894.37 km^2), 27-Carlinda (2,457.69 km^2), 28-Castanheira (3,911.60 km^2), 29-Chapada dos Guimarães (5,623.02 km^2), 30-Cláudia (3,855.69 km^2), 31-Cocalinho (16,597.66 km^2), 32-Colíer (3,048.51 km^2), 33-Colniza (27,596.82 km^2), 34-Comodoro (21,727.36 km^2), 35-Confresa (5,704.32 km^2), 36-Conquista D'Oeste (2,708.31 km^2), 37-Cotriguaçu (9,424.35 km^2), 38-Cuiabá (3,500.05 km^2), 39-Curvelândia (776.83 km^2), 40-Denise (1,292.60 km^2), 41-Diamantino (7,581.80 km^2), 42-Dom Aquino (2,160.98 km^2), 43-Feliz Natal11 (472.43 km^2), 44-Figueirópolis D'Oeste (923.31 km^2), 45-Gaúcha do Norte (16,904.14 km^2), 46-General Carneiro (3,765.47 km^2), 47-Glória D'Oeste (873.38 km^2), 48-Guarantã do Norte (4,671.89 km^2), 49-Guiratinga (5,419.50 km^2), 50-Indiavaí (632.33 km^2), 51-Ipiranga do Norte (4,169.80 km^2), 52-Itanhang (2,958.31 km^2), 53-Itaúba (4,676.69 km^2), 54-Itiquira (8,593.61 km^2), 55-Jaciara (1,673.42 km^2), 56-Jangada (1,045.78 km^2), 57-Jauru (1,216.12 km^2), 58-Juara (21,480.54 km^2), 59-Juína (26,263.24 km^2), 60-Juruena (2,778.18 km^2), 61-Juscimeira (2,252.27 km^2), 62-Lambari D'Oeste (1,337.27 km^2), 63-Lucas do Rio Verde (3,660.52 km^2), 64-Luciára (4,207.91 km^2), 65-Vila Bela da Santíssima Trindade (13,652.13 km^2), 66-Marcelândia (12,356.49 km^2), 67-Matupá (5,289.26 km^2), 68-Mirassol d'Oeste (1,044.10 km^2), 69-Nobres (3,859.66 km^2), 70-Nortelândia (1,392.58 km^2), 71-Nossa Senhora do Livramento (5,361.53 km^2), 72-Nova Bandeirantes (9,616.92 km^2), 73-Nova Nazaré (3,936.70 km^2), 74-Nova Lacerda (4,716.13 km^2), 75-Nova Santa Helena (2,327.41 km^2), 76-Nova Brasilândia (3,413.52 km^2), 77-Nova Canãdo Norte (5,971.43 km^2), 78-Nova Mutum (9,606.51 km^2), 79-Nova Olímpia (1,438.54 km^2), 80-Nova Ubiratã (12,727.59 km^2), 81-Nova Xavantina (5,539.54 km^2), 82-Novo Mundo (5,765.63 km^2), 83-Novo Horizonte do Norte (939.36 km^2), 84-Novo São Joaquim (5,064.60 km^2), 85-Paranaíta (4,848.37 km^2), 86-Paranatinga (24,182.32 km^2) 87-Novo Santo Antnio (4,360.53 km^2), 88-Pedra Preta (4,272.68 km^2), 89-Peixoto de Azevedo (14,421.24 km^2), 90-Planalto da Serra (2,415.98 km^2), 91-Poconé (17,165.21 km^2), 92-Pontal do Araguaia (2,788.57 km^2), 93-Ponte Branca (724.78 km^2), 94-Pontes e Lacerda (8,504.11 km^2), 95-Porto Alegre do Norte (3,987.61 km^2), 96-Porto dos Gaúc-hos (6,962.44 km^2), 97-Porto Esperidião (5,867.40 km^2), 98-Porto Estrela (2,040.95 km^2), 99-Poxoréo (6,840.80 km^2) 100-Primavera do Leste (5,453.57 km^2), 101-Querência (17,871.37 km^2), 102-São José dos Qu-atro Marcos (1,238.91 km^2), 103-Reserva do Cabaçal (1,096.26 km^2), 104-Ribeirão Cascalheira (11,406.30 km^2), 105-Ribeirãozinho (556.14 km^2), 106-Rio Branco (559.51 km^2), 107-Santa Carmem (3,898.19 km^2), 108-Santo Afonso (1,269.79 km^2), 109-São José do Povo (459.50 km^2), 110-São José do Rio Claro (5,147.20 km^2), 111-São José do Xingu (7,408.57 km^2), 112-São Pedro da Cipa (339.44 km^2), 113-Rondolândia (12,522.52 km^2), 114-Rondonópolis (4,134.14 km^2), 115-Rosário Oeste (7,973.45 km^2), 116-Santa Cruz do Xingu (5,660.67 km^2), 117-Salto do Céu (1,728.97 km^2), 118-Santa Rita do Trivelato (4,627.75 km^2), 119-Santa Terezinha (6,573.85 km^2), 120-Santo Antônio do Leste (3,607.89 km^2), 121-Santo Antônio do Leverger (12,261.35 km^2), 122-São Félix do Araguaia (16,929.26 km^2), 123-Sapezal (13,823.70 km^2), 124-Serra Nova Dourada (1,455.06 km^2), 125-Sinop (3,233.83 km^2), 126-Sorriso (9,370.25 km^2), 127-Tabaporã (8,236.74 km^2), 128-Tangará da Serra (11,477.71 km^2), 129-Tapurah (4,479.43 km^2), 130-Terra Nova do Norte (2,479.34 km^2), 131-Tesouro (4,074.59 km^2), 132-Torixoréu (2,396.20 km^2), 133-União do Sul (4,620.25 km^2), 134-Vale de São Domingos (1,875.85 km^2), 135-Várzea Grande (898.85 km^2), 136-Vera (3,004.40 km^2), 137-Vila Rica (7,500.07 km^2), 138-Nova Guarita (1,091.68 km^2), 139-Nova Marilândia (1,857.21 km^2), 140-Nova Maringá (11,434.75 km^2) and 141-Nova Monte Verde (6,505.43 km^2)

3.3 Data sources and materials

The data sets and other important materials utilized in this chapter are summarized in Table 3.1, and described hereafter.

3.3.1 5-year DVM Maps

In our previous work (Yoshikawa and Sanga-Ngoie 2010) on Chapter 2, a set of 4

vegetation maps, the 5-year DVM Maps Phase I from July 1981 to June 1986, Phase II from July 1986 to June 1991, Phase III from July 1991 to June 1996 and Phase IV from July 1996 to June 2001, were created for every five-year period between 1981-2001, using the first component of the PCA of NOAA/AVHRR multi-spectral data and GIS as analytical platform (Figure 2.4a-d). These data were classified into the following seven land use/land cover types: EBF, SdF, BSF, SW, SG, S and DA. Vegetation change statistics were computed from these digital vegetation maps for every five years.

3.3.2 SIDRA/IBGE Data

Various statistical data on Brazil are available from the SIDRA (Sistem IBGE de Recuperação Automática) within IBGE. For our analysis, we did download tables of yearly data for cattle and agriculture, describing heads count of cattle per year in each municipal district of MT from 1974 to 2006 and planted areas (unit: ha) of each products per year in each municipal district of MT from 1990 to 2006 (SIDRA 2008) without charge. We selected the data of the 3 most important products (Soybean, Sugarcane, Corn) of MT.

3.3.3 IBGE Vector data

Topographic maps, and other ancillary data such as rivers, main federal highways, local roads (including paved and unpaved roads), parks and areas inhabited by indigenous people in MT were downloaded from the Mapas Interativos IBGE website (IBGE 2005) without charge, and were used as reference for land cover identification and analysis. Municipal district boundary lines and polygons are downloaded from the same site and added to the database. See details in section 2.3 on Chapter 2.

Table 3.1 List of data sources and materials.

	Data Set	*Periods*	*Remarks*
1	5-year DVM Maps (Phase I, II, III and IV) - Yoshikawa and Sanga-Ngoie (2010)	1981-2001	0.1degree
2	Cattle heads data - Sistem IBGE de Recuperação Automática (table)	1974-2006	Municipal districts (144)
3	Agricultural (soybean and corn) products data - Sistem IBGE de Recuperação Automática (table)	1990-2006	Municipal districts (144)
4	State line map - Malha Municipal Digital, IBGE (line)	1997	1:5,000,000
5	River, main road, park and area inhabited by indigenous people maps - Mapa da Série Brasil Geográfico, IBGE (line)	2002	1:5,000,000

3.4 Analysis Methods

The overall analysis methodology is given in Figure 3.3, and can be summarized in the following 4 main steps described hear after. Clark Lab's IDRISI32 Release 2.2 (Eastman 2001) was used as GIS platform for all the analyses, together with CARTALINX, database builder software.

First, using the municipal districts data provided by IBGE, the area of each district polygon was calculated and stored. We have to note here that average values obtained by using IDRISI 32 were within 0.2 % of accuracy deviation as compared to area values provided by ANA (2002).

Second, based on the 5-year DVM Maps (Figure 2.4a-d), patterns of vegetation change over the past 20 years were devised, focusing on four land cover types with the most dramatic changes: the EBF, the SW, the S and the DA. For this purpose, a set of four 5-year DVM Maps (Phase I, II, III and IV) were reclassified from their initial 7 land cover types into the following 4 types (as named Reclass 5-year DVM Map Phase I, II, III and IV): (1) the *f1* category equivalent to the EBF, (2) the *f2* category made of the other forest types (SdF, BSF and SW), (3) the *Savanna* (hereafter *Sv*)

category consisting of SG and S, and (4) the *Deeply Altered Areas* (hereafter *DAA*) (DA). In the following *f1* and *f2* are sometimes put together into a single category (*Forests*) when needed.

Then, vegetation change maps were calculated from 4-category Reclassified 5-year DVM Maps Phase I, II, III and IV (Figure 3.4), between consecutive phases through the analysis period, using cross tabulation methods. By keeping only significant patterns of changes among the possible ones, we could identify types of changes that were dominant when passing from one phase to another. And we clarify the vegetation change from Phase I to Phase II as being named 5-year DVM vegetation change Map Phase I–II, from Phase II to Phase III as Phase II–III, from Phase III to Phase IV as Phase III–IV on Figure 3.5a-c and from Phase I to Phase IV as Phase I–IV which is overall of change during 2 decades on Figure 3.6.

Third, in order to elucidate the causes of these changes, correlation coefficients between vegetation changes and data of head count of cattle or agricultural planted areas (the 3 most important products: Soybean, Sugarcane and Corn) for each municipal district, were analyzed for each one of four phases between 1981 and 2001. Test of significance using the correlation coefficients were obtained by t-test. The correlation coefficients of P-value below 0.05 from the test results were adopted as significant correlation coefficients. Using the area data for each district, cattle density were also calculated for each phase and each district with spatial distribution. The planted areas are available only from 1990. Therefore we assumed the 1990 data for planted areas could represent the Phase II of analysis.

With these vegetation and agro-pastoral statistics in both time and space, the relationship between vegetation changes and each change in agro-pastoral data were obtained both by comparison and through statistical analysis correlations. This shed new light on our understanding of causes for changes in land cover types and dynamics of changes in both spatial and temporal characteristics.

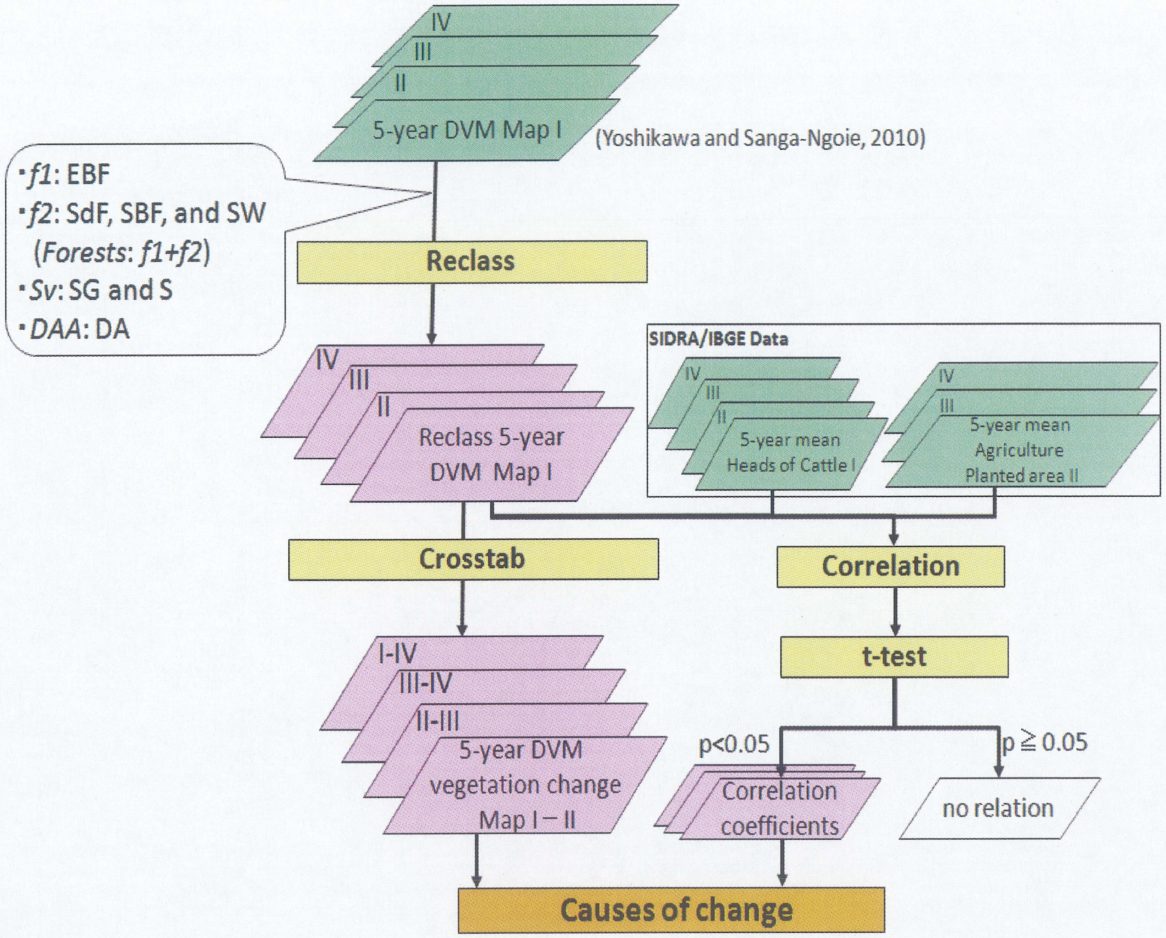

Figure 3.3. Flowchart for our analysis methods

3.5 Analysis Results

3.5.1 Vegetation changes

The following main features are obtained from the reclassified 5-year DVM Maps Phase I, II, III and IV (Figure not shown): (1) dominance of *f1* type covers from MT central part to the northern areas throughout the period, (2) *f2* types spread over the northeastern, central and southwest parts, and (3) *Sv* and *DAA* are found over southern areas, especially in the east and center (cf. Figure 2.4a-d).

Statistics from these reclassified 5-year DVM Maps (according to Figure 3.3) are characterized by a sharp decrease in *f1* areas from 34.5×10^6 ha in Phase I to 12.5×10^6 ha in Phase IV. *f2* covers witness a remarkable decrease from 49.5×10^6 ha in Phase III to 39.1×10^6 ha in Phase IV, after sustained expansion in the previous phase, which is more likely to be related to the decrease in *f1*. The *Sv* covers do not change much from 13.9×10^6 ha in Phase I to 18.7×10^6 ha in Phase IV. *DAA* in particular, however, sharply increased from 5.1×10^6 ha in Phase II to 20.3×10^6 ha in Phase IV.

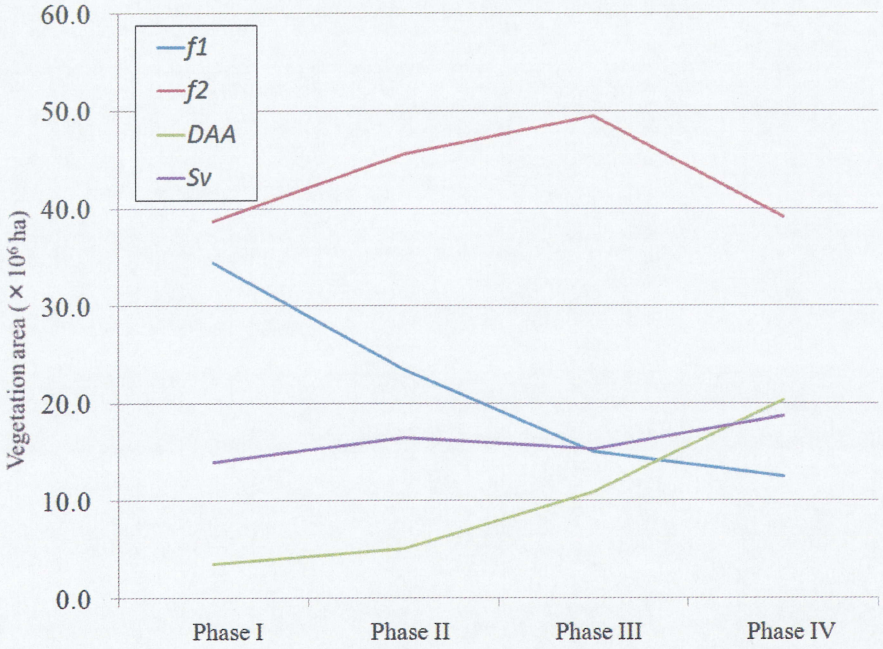

Figure 3.4. Area ($\times10^6$ ha) of Reclassified 5-year DVM Map Phase I, II, III and IV.

3.5.2 Dynamics of the vegetation changes

Figure 3.5a-d show 5-year DVM vegetation change Map Phase I–II, Phase II–III and Phase III–IV and Phase I–IV with overall results on Figure 3.5. Our CROSSTAB analysis emphasizes the following 8 dominant types of changes which simple arrows (→) indicate the flow of change from the previous phase to the next one (and the arrows (⇔) indicate the flow of inter-change) : *f1*→*f2*, *Forests* (*f1, f2*)→*DAA*, *Forests*→*Sv*, *f2* →*f1*, *DAA*→*Forests*, *Sv*→*Forests*,*Sv*→*DAA* and *DAA*→*Sv* on Figure 3.5a-d and Figure 3.6.

These can be effectively grouped into the following 3 patterns.

(a) Degradation: *f1*→*f2*, *Forests*→*DAA*, *Forests*→*Sv*

(b) Recovery: *f2*→*f1*, *DAA*→*Forests*, *Sv*→*Forests*

(c) Transitional area: *DAA*⇔*Sv*

We calculated the ratio of each category held from an area of the whole vegetation change.

In the 5-year DVM vegetation change Map Phase I–II (Figure 3.5a), the change from *f1* to *f2* (47.7 %) is showing to be spreading over north and central areas. Most of the changes from *Forests* to *DAA* (21.1 %) are found in the southern part of MT and changes from *Forests* to *Sv* (9.9 %) in southwestern areas include the Pantanal area. The change from *DAA* to *Forests* (10.7 %) is spreading towards the middle southern area. Changes from *DAA* to *Sv* or *Sv* to *DAA* (Put it together 3.3 %) are rare.

In the 5-year DVM vegetation change Map Phase II–III (Figure 3.5b), change from *f1* to *f2* (35.3 %) is showing to spread over the northern area, especially over the Juruena River basin. Areas of changes from *Forests* to *DAA* (17.3 %) or *Sv* (17.7 %) are found in all of the southern area. And changes from *DAA* to *Forests* (13.9 %) spread over the roadside of the southern part. These areas are showing recovery. The change from *DAA* to *Sv* (10.5 %) is spreading over the south-west around Cuiabá city, which is the provincial capital of MT

In the 5-year DVM vegetation change Map Phase III–IV (Figure 3.5c), the change from *f1* to *f2* (12.6 %) shows to be spreading along the northern border of the state, and over parks and areas inhabited by indigenous people in the northwest area. Most of changes from *Forests* to *DAA* (35.9 %) are found along BR-163, BR-174 and BR-158 extending from the north to south and changes from *DAA* to *Sv* (21.2 %) are in the southern area. The changes from *f2* to *f1* (4.3 %) spread to the northern area.

In the 5-year DVM vegetation change Map Phase I–IV (Figure 3.6) as an overall result, most of the change from *f1* to *f2* (40.4 %) are distributed over the northwest and the central part. Area of changes from *Forests* to *DAA* (22.8 %) spread along the roadside of the whole MT region. Additionally the change area from *Forests* to *Sv* (22.6 %) intruded from the road of the south and the east MT. And changes from *DAA* to *Sv* (12.3 %) spread over the roadside of the southern part.

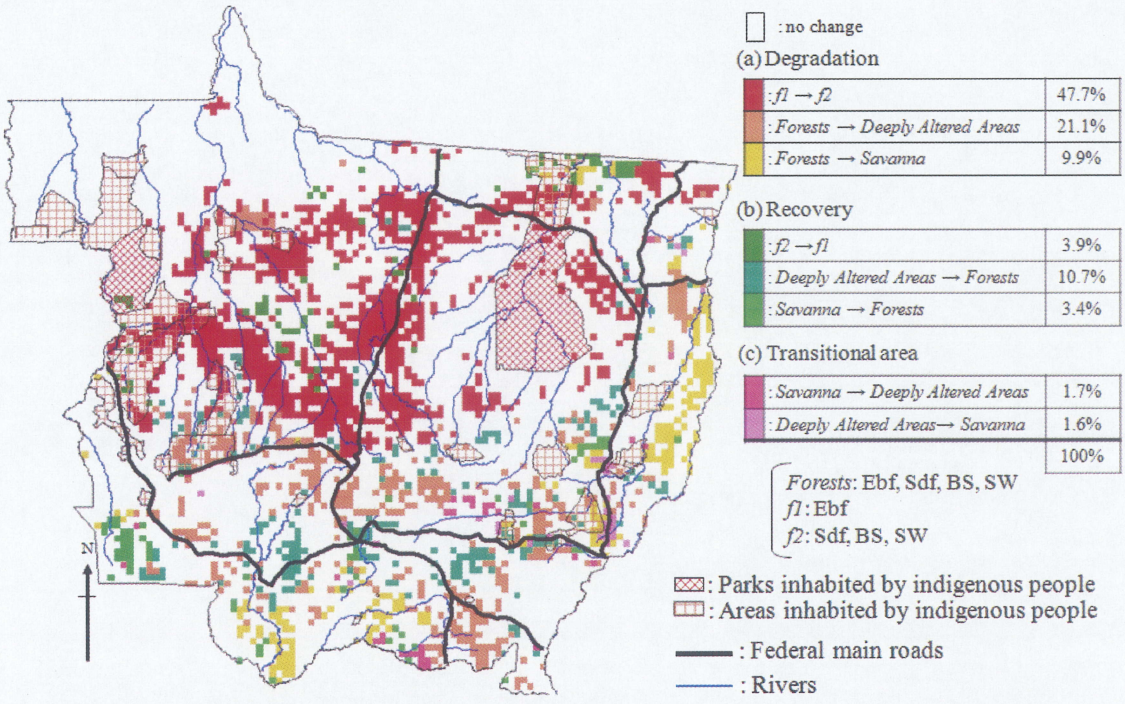

Figure 3.5a. The 5-year DVM vegetation change Map Phase I–II in MT. Blue lines denote rivers, black bold lines paved roads, pink lines local roads, black lines municipal districts, red meshes Parks inhabited by Indians and, orange meshes Areas inhabited by Indians.

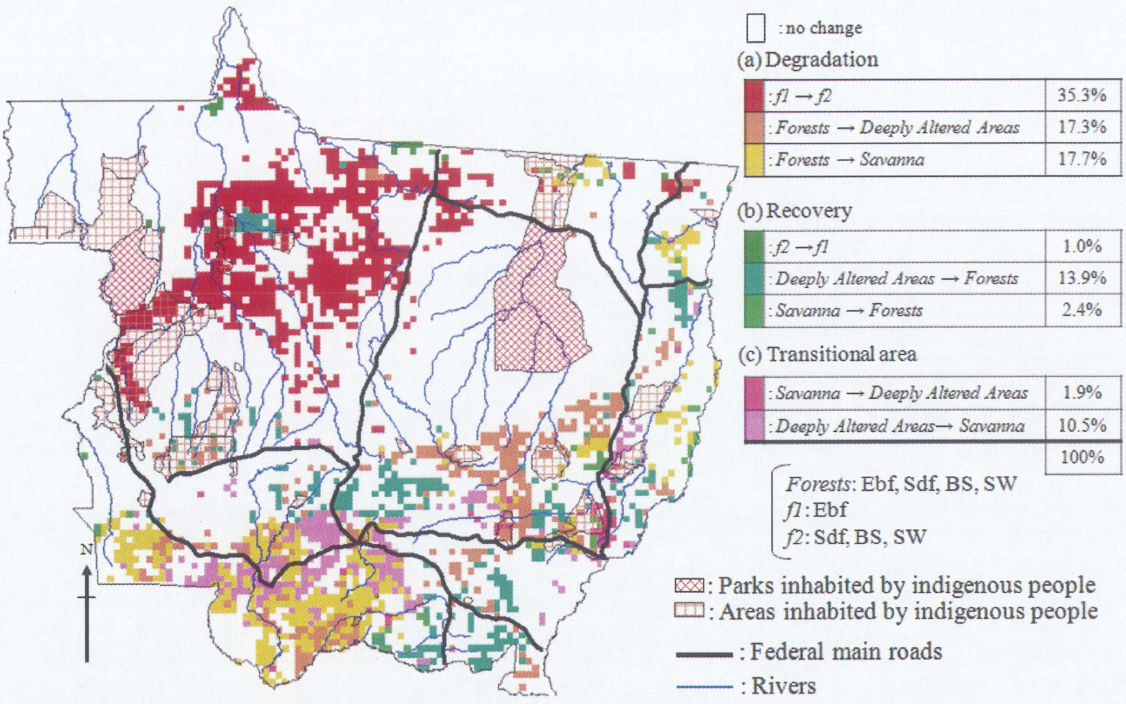

Figure 3.5b. Same as in Figure 3.5a, but for the 5-year DVM vegetation change Map Phase II–III.

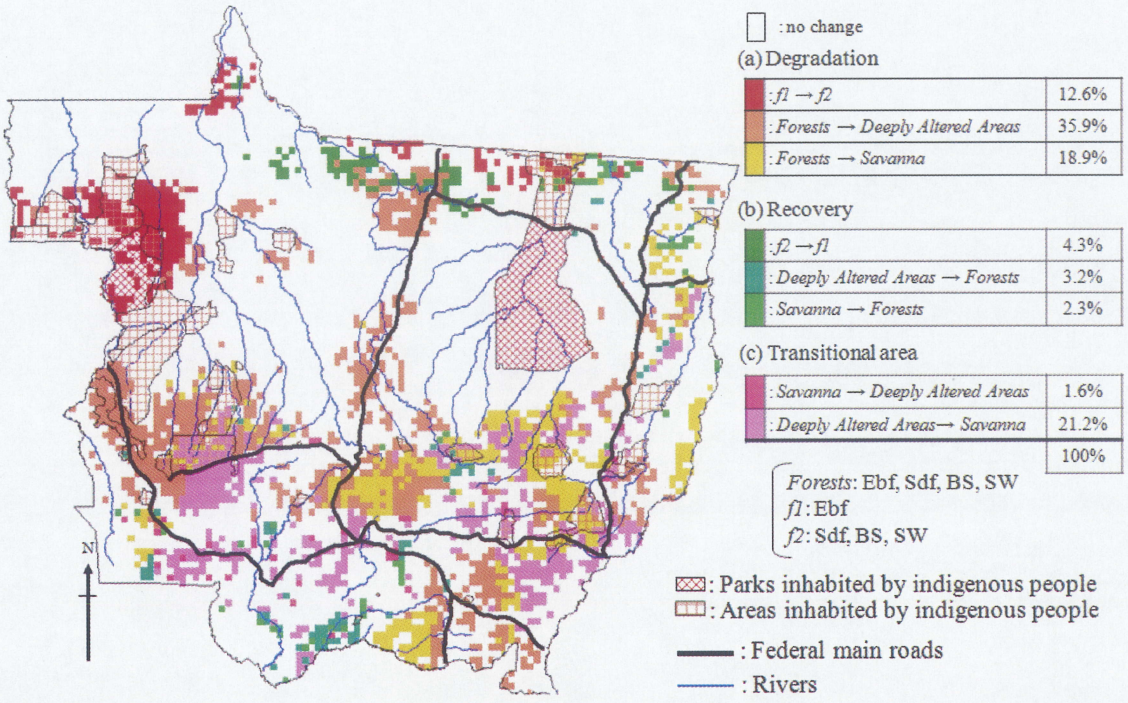

Figure 3.5c. Same as in Figure 3.5a, but for the 5-year DVM vegetation change Map Phase III–IV.

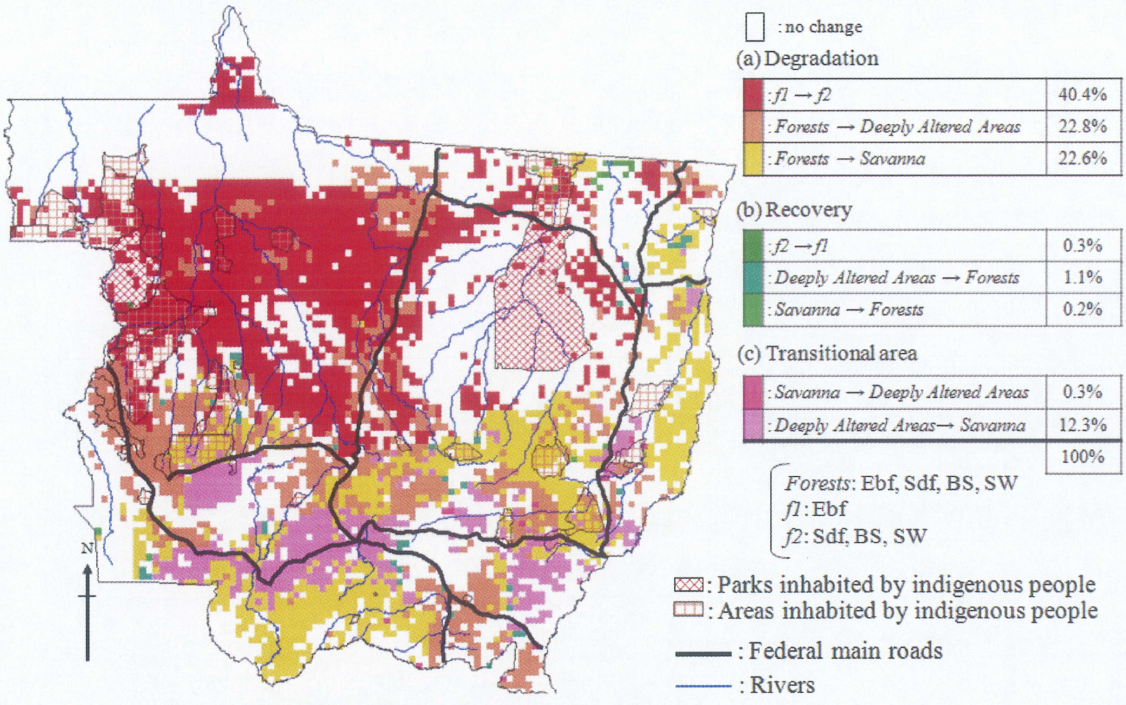

Figure 3.6. The 5-year DVM vegetation change Map Phase I–IV (overall change).

(a) **Degradation**

Degradation has changed greatly. The quantity of change from *f1* to *f2* decreased by 35.1 % from the 5-year DVM vegetation change Map Phase I–II to Phase III–IV. There is very much land and degradation is advancing little by little toward the northern MT. We can suggest that commercial timber harvest is accompanied with these changes.

However, the change from *Forests* to *DAA* or *Sv* has increased 14.7 % or 9.0 % from the 5-year DVM vegetation change Map Phase I–II (Figure 3.5a) to Phase III–IV (Figure 3.5c). These distributions are penetrated from the south to the north along main paved roads of BR–163, BR–174 and BR–364 through large-scale cattle ranching and farm development.

Degraded areas occupy 85.8 % of the total in the 5-year DVM vegetation change Map Phase I–IV (Figure 3.6). The degraded areas (42.0×10^6 ha: 1.14 times as large as Japan) occupy 46.4 % of the entire MT area (90.6×10^6 ha) as seen in Figure 3.6. It is suggested that the area nearly half the size of MT was degraded. At the same time, in

terms of the quantity of vegetation change, the degradation decreases from 78.7 % in the 5-year DVM vegetation change Map Phase I–II to 67.4 % in the Phase III–IV. This is because the ratio of the quantity of vegetation change is displaced from Degradation to some others.

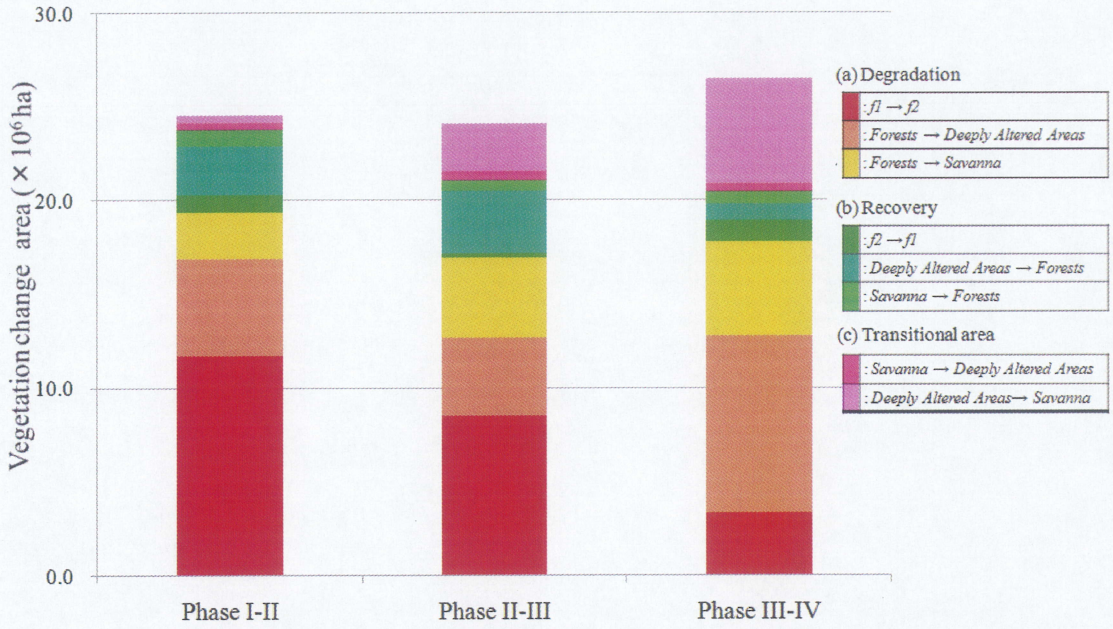

Figure 3.7. The vegetation change area ($\times 10^6$ ha) each type in 5-year DVM vegetation change Map Phase I–II, Phase II–III and Phase III–IV.

(b) **Recovery**

Recovery is also seen slightly. These areas are considered to be an abandoned ground after cultivation or deforestation. Especially in the area of change from *DAA* to *Forests*, quantity of recovery decreases 7.5 % from the 5-year DVM vegetation change Map Phase I–II (Figure 3.5a) to Phase III–IV (Figure 3.5c). This suggests that, a big wave of urbanization and development in rather than waiting for recovery after agriculture or cattle ranching is approached. In addition, these Recovery areas are 1.6 % of the total in the 5-year DVM vegetation change Map Phase I–IV and decrease from 18.0 % in Phase I–II to 9.8 % in Phase III–IV (Figure 3.5a and c). The ratio of Recovery areas (0.77×10^6 ha) against the whole MT area is 0.85 % in Phase I-IV and it is hardly recovery. These

results was clarified that vegetation recovery was became difficult since 1990s.

(c) Transitional areas

The change from *DAA* to *Sv* shows a dramatic increase by 19.6 % from the 5-year DVM vegetation change Map Phase I–II (Figure 3.5a) to Phase III–IV (Figure 3.5c). In the area of overall change from *Sv* to *DAA* is very little or 0.3 % in the 5-year DVM vegetation change Map Phase I–IV (Figure 3.6). A value has hardly changed throughout the period. In addition, these Transitional areas are 12.6 % of the total in the 5-year DVM vegetation change Map Phase I–IV. The ratio of Transitional areas (6.18×10^6 ha) occupy 6.82 % of the whole MT area (Figure 3.6). These areas are neither degraded nor recovered. These have the possibility to shift the land use from cattle ranching to farming or from farming to cattle ranching. We will argue the cause of these changes in the next section.

3.5.3 Cause of changes

3.5.3.1 Head count of cattle

In the early 1980s, Myers (1981) coined the new phrase "Hamburger connection" to stigmatize the relationship between the export of beef from Central and South America to fast food chains in the United States of America, and rampant deforestation of the rainforests in Amazon. The head count of cattle in the Legal Amazon rapidly increased between 1990 and 2002, and its increase rate in MT is known to be the biggest in the state of Brazil. After 2002, the head count of cattle, and the quantity of export sharply increased because of the drastic drop in prices and the problem of *Bovine Spongiform Encephalopathy* (BSE) in the United States of America, which occurred around the same time (Kaimowitz *et al.* 2004).

The head count of cattle in Brazil reached 92.5×10^6 heads in 1974. A sustained increase in the number of cattle brings the statistics to 205.9×10^6 heads in 2006. In MT

by Figure 3.8, the total head count of cattle was 5.5×10^6 heads in 1981 and 26.7×10^6 in 2005. This means that cattle ranchers increase 4.8 times.

Figures 2.5a-d show the 5-year mean of the number of cattle for each municipal districts at the same periods as in the 5-year DVM maps Phases I, II, III and IV. The following general patterns of the spatial and temporal change in the number of cattle distribution and density can be pinpointed. With large herds initially concentrated in the south MT in Phase I (Figures 2.5a), ranching activities spread northward, while intensified head density reaches to be distributed all over the state land, passing from an average heads density of 6.9 heads/km^2 in Phases I to an outstanding value of 19.0 heads/km^2 in Phases IV (Figures 2.5d). In Phases IV (Figures 2.5d), municipal districts with more than 200.0×10^3 heads are not only in the south, but everywhere in the state. This can be illustrated by considering 2 districts with characteristic changes: Cáceres (Figure 3.1, no.20) in the southern MT, Nova Canãdo Norte (Figure 3.1, no.77) and Juara (Figure 3.1 no.58) located in the far-north.

In the Cáceres municipal district, the number of cattle tripled in only 20 years: 453.6×10^3 heads (1.9 heads/km^2) in Phase I and 549.0×10^3 heads (22.5 heads/km^2) in Phase IV. The Nova Canãdo Norte municipal district had no cows in Phase I. Its number increased from 35.9×10^3 heads (6.0 heads/km^2) in Phase II to 216.6×10^3 heads (36.3 heads/km^2) in Phase IV. The head count of cattle and its density increased 6.0 times in two decades. This suggests that pastoral areas generally spread toward the northern part. However, the spatial distribution of recent pastures tends to locate them within the inland area between the northern and the southern parts of MT, far away from major paved roads.

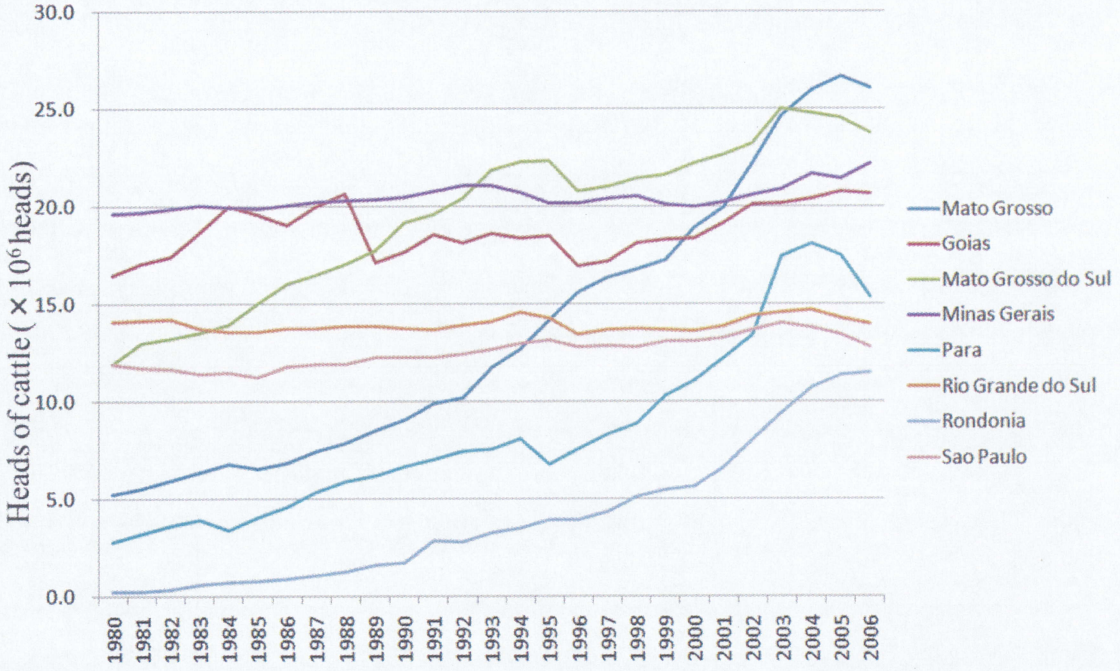

Figure 3.8. The head counts of the cattle ($\times 10^6$ heads) of the top 8 state in the Brazil.

3.5.3.2 Agricultural planted area

In Brazil, the 5 most planted areas amount to be; 14.0×10^6 ha for Soybean, 12.9×10^6 ha for Corn, 5.0×10^6 ha for Sugarcane, 3.9×10^6 ha for Kidney bean, 3.2×10^6 ha for Rice in 2001. In terms of the total production, Sugarcane accounts for 344.3×10^6 ton, Corn for 42.0×10^6 ton , Soybean for 37.9×10^6 ton, Cassava (Mandioca) for 22.6×10^6 ton and Rice for 10.2×10^6 ton in 2001 (Figure 3.9). Among the total amount of production $10{,}978.8\times10^9$ reals are for Soybean, $8{,}683.7\times10^9$ reals for Sugarcane, $6{,}317.5\times10^9$ reals for Corn, $2{,}998.6\times10^9$ reals for Rice and $2{,}393.7\times10^9$ reals for Cassava in 2001. The top three changed greatly from 1990 to 2006.

As for MT, the planted area (Figure 3.10) amounts to 312.1×10^4 ha for Soybean, 54.0×10^4 ha for Corn, 45.1×10^4 ha for Rice, 41.2×10^4 ha for Cotton, 16.7×10^4 ha for Sugarcane in 2001. The total production (Figure 3.11) for each one of them amounts to 11.1×10^6 ton for Soybean, 9.5×10^6 ton for Sugarcane, 1.7×10^6 ton for Corn, 1.5×10^6 ton for Cotton, 1.2×10^6 ton for Rice in 2001. And the total amount of production (Figure 3.12) for each one of them amounts to $2{,}261.2\times10^9$ reals for Soybean, 998.3×10^9 reals

for Cotton, 255.9×10^9 reals for Rice, 195.1×10^9 reals for Corn, 193.7×10^9 reals for Sugarcane in 2001. The top five products mentioned above make up most of the agricultural production in MT. In this chapter we focus on the role of the 3 most important products (Soybean, Sugarcane, Corn) as causes of deforestation.

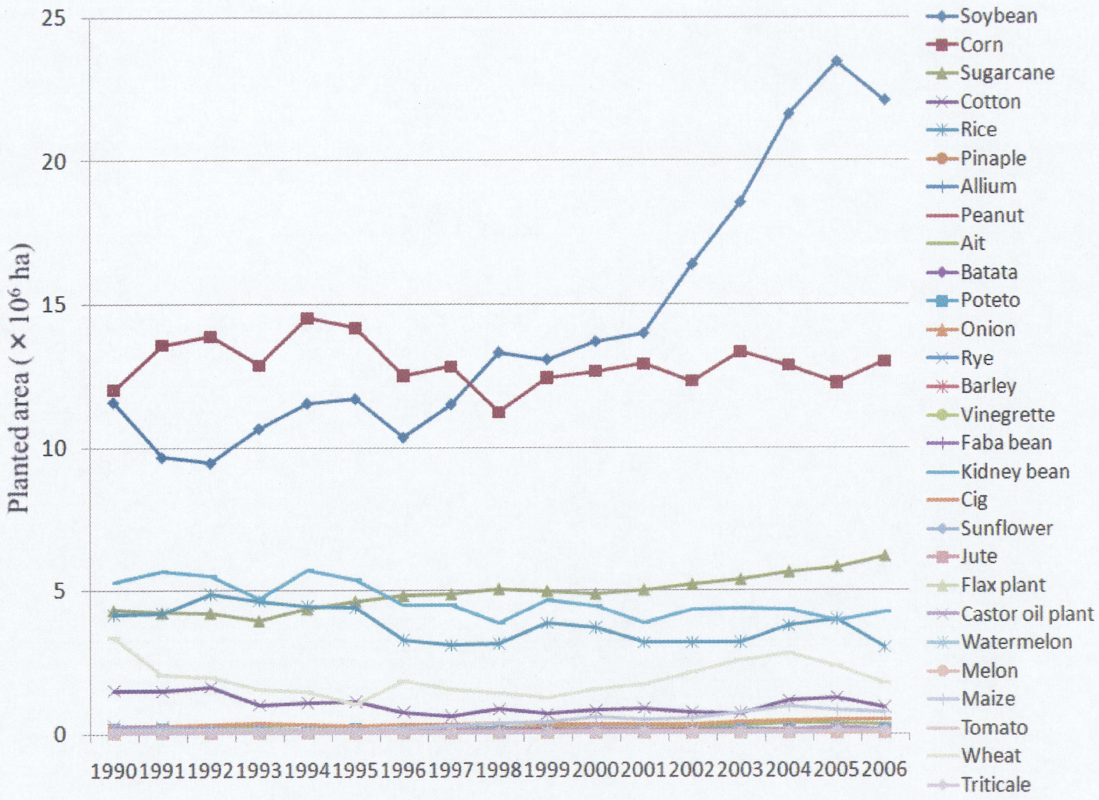

Figure 3.9. Total Planted area ($\times10^6$ ha) of all agricultural products in Brazil from 1990 to 2006.

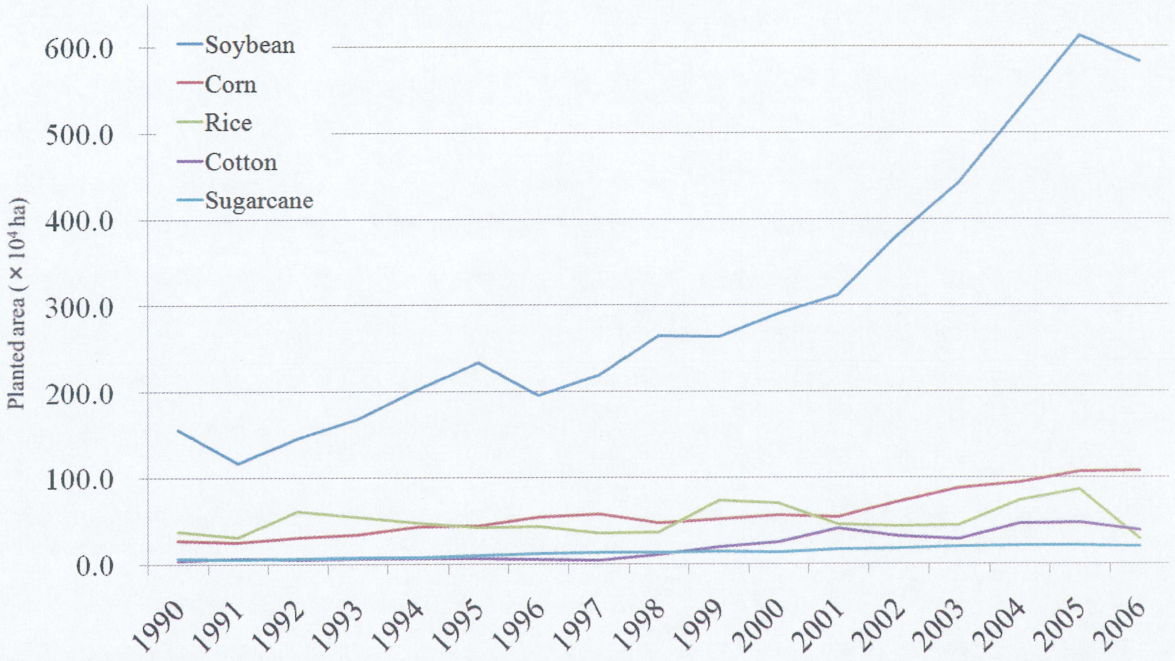

Figure 3.10. Total Planted area ($\times 10^4$ ha) of top 5 products in MT from 1990 to 2006.

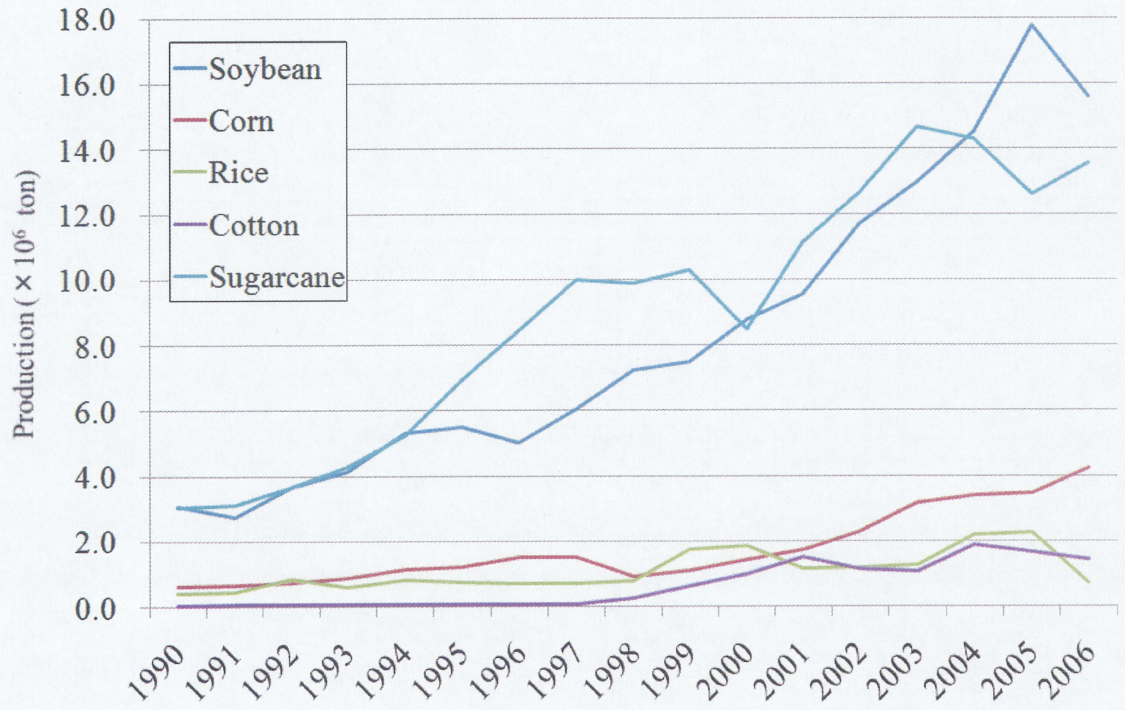

Figure 3.11. Total Production ($\times 10^6$ ton) of top 5 products in MT from 1990 to 2006.

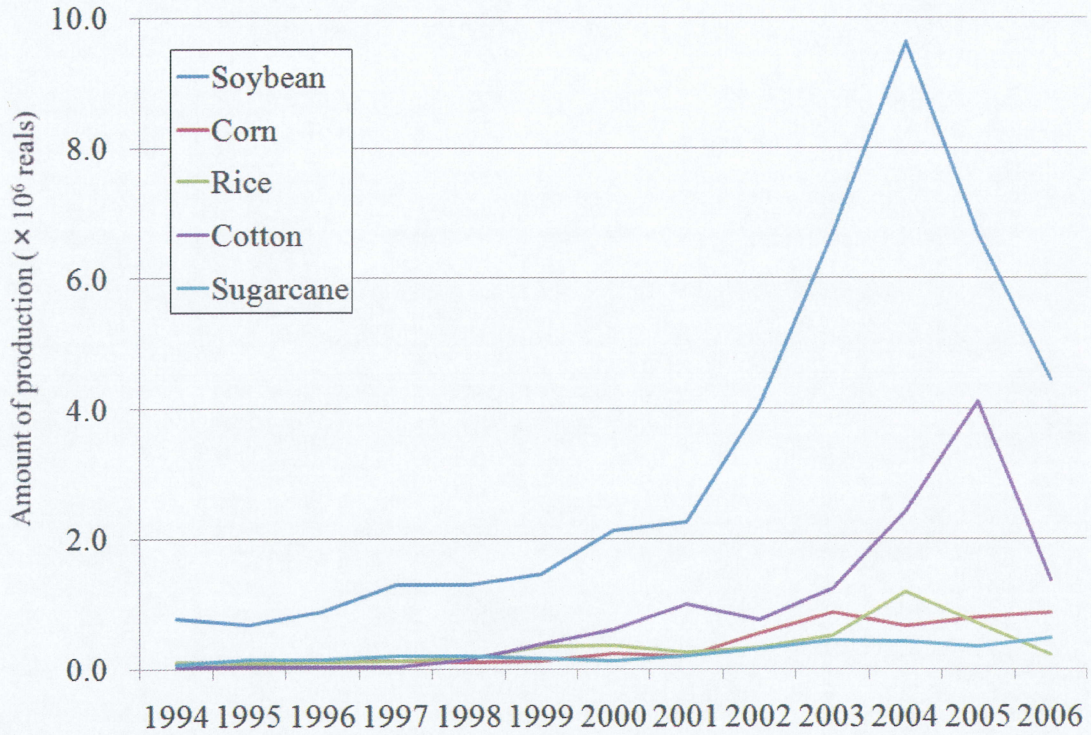

Figure 3.12. Total Amount of production ($\times 10^9$ reals) of top 5 products in MT from 1994 to 2006.

(i) Soybean

The total planted area and the amount of the Soybean production are the largest, occupying about 50 % of the total of them in MT throughout an investigated period. The total planted area in MT increased from 155.3×10^4 ha in 1990 to 612.2×10^4 ha in 2005. It decreased 582.3×10^4 ha in 2006 (Figure 3.10). The production decreased during droughts in 2004 and 2005 and contracted soybean rust disease called Phakopsora meibomiae.

Figure 2.6 mentioned in Chapter 2 show the 5-year mean soybean planted areas for each municipal district at the same periods as in the 5-year DVM maps Phases II, III and IV. With spatial distribution, there are planted areas of Phases II in the municipal district of the southeast MT, where they were sandwiched between BR-163 and BR-070 in the central and southeast MT. Such an area expanded little by little, occupying most of the planted areas of the central and southeast MT in Phase IV.

In the Campo Novo do Parecis municipal district (Figure 3.1, no.22) of the central western district along BR-364 which have many silos of André Maggi Group next to a certain Sapezal (Greenpeace, 2006), planted areas increased from 200.8×10^3 ha in Phase II (upper left of Figure 2.6) to 238.2×10^3 ha in Phase IV (lower of Figure 2.6). There is no big change. In the Sorriso municipal district (Figure 3.1, no.126) of the central district along BR-163, planted areas increased 2.0 times from 140×10^3 ha in Phase II (upper left of Figure 2.6) to 274.3×10^3 ha in Phase IV (lower of Figure 2.6). The expansions of these planted areas are particularly intense in these areas because of easy access to Cuiabá, a provincial capital, São Paulo and so on. In the Nova Ubiratã municipal district (Figure 3.1, no.80) of the central district, it was 0 ha until 1996, but increased to 39.2×10^3 ha in Phase IV (Figure 3.12c). We understood that the Soybean planted areas expand around the central MT, in particular along BR-163, and toward north MT.

Major multinational grain firms in the world and the Governor after 2002 in MT (Fearnside 2003) were concerned with soybean production (Greenpeace 2006), so the volume of production increased drastically. It is no exaggeration to say that infrastructure development is now ready for soybean production.

(ii) Sugarcane

The total planted area always holds around 15 % of the entire land in MT. The total planted area increased 3.1 times from 6.5×10^4 ha to 20.2×10^4 ha during 15 years between 1990 and 2006 (Figure 3.10).

With the spatial distribution of the 5-year mean sugarcane planted areas II, III and IV (Figure 3.13), the planted areas was expanding slightly since 1990 within limited municipal districts. The sugarcane croplands spread in the southwest of MT. In particular, cultivation is popular in the north and center of municipal districts which are sandwiched between BR–364 and BR–174. And even in Dom Aquino (Figure 3.1, no.42), Jaciara (Figure 3.1, no.55), Juscimeira (Figure 3.1, no.61) and São Pedro da

Cipa (Figure 3.1, no.112) in the southern central MT which are sandwiched between BR–070 and BR–163, Confresa (Figure 3.1 no.35) and Santa Terezinha (Figure 3.1, no.119) in the northeastern MT along BR–158, sugarcane is produced. However, the sugarcane production was becoming popular since 1990 in Pantanal of the southwestern MT, but it is hardly produced now.

In the Campo Novo do Parecis (Figure 3.1, no.22) municipal districts of the central southwestern area in MT along BR-364, the total planted area increased 2.0 times from 8.5 $\times 10^3$ ha in Phase II (upper left of Figure 3.13) to 17.3$\times 10^3$ ha in Phase IV (lower of Figure 3.13). In the Denise (Figure 3.1, no.40) municipal districts of the southwestern MT which are sandwiched between BR–364 and BR–174, it increased 4.1 times from 5.1$\times 10^3$ ha in Phase II (upper left of Figure 3.13) to 2.1$\times 10^3$ ha in Phase IV (lower of Figure 3.13). And in the Jaciara (Figure 3.1, no.55) municipal districts of the southern MT along BR–163, there is an increasing tendency from 4.0$\times 10^3$ ha to 12.4$\times 10^3$ ha between Phase II and Phase IV (Figure 3.13). Sugarcane planted area is still small.

MT always produces Sugarcane more than 40 % of the total production. It increased 4.5 times from 3.04$\times 10^6$ ton to 13.55$\times 10^6$ ton between 1990 and 2006 (Figure 3.11). Its peak was 2004. There is a tendency to increase the sugarcane production to be used as ethanol for bio-fuel of vehicles since the 1980's. In MT, the planted areas are still small, but its production is large next to the soybean. And MT always holds around 15% in the total amount of production. It increased 6.5 times from 72.7$\times 10^9$reals to 474.1$\times 10^9$ reals between 1990 and 2006 (Figure 3.12).

We clarify that although Sugarcane planted areas are still bit, the production for MT is prominent. Per unit production of sugarcane was the biggest in the planted area when compared with other crops from these results. The amount of production is still low. However, Sugarcane production may grow very high demand from international markets in the future because of the new use as bio-fuel alternative of fossil fuels. The need to follow in the future will be so high.

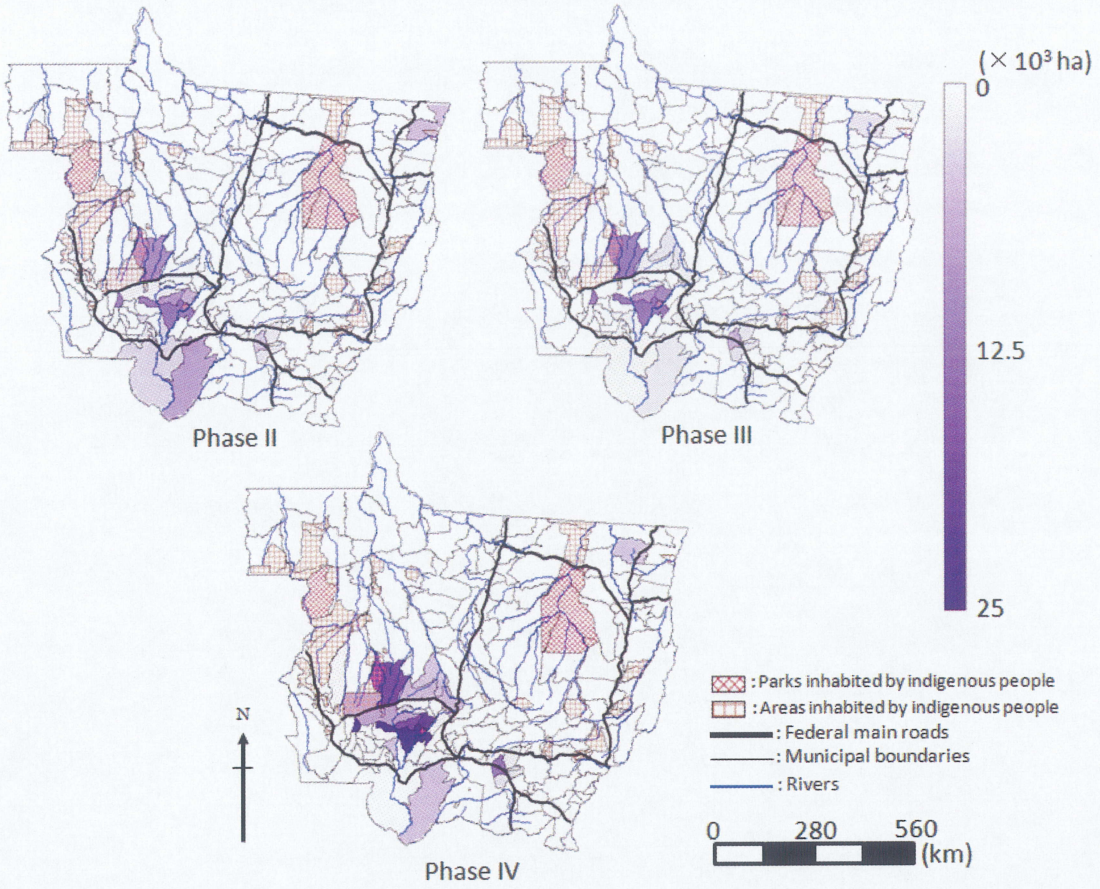

Figure 3.13. The distribution map in the 5-year mean Sugarcane planted area Phase II, III and IV of every municipal district in MT.

(iii) Corn

MT always holds around 10 % of the total planted area, amount of production and production. The total planted area doubled from 27.4×10^4 ha to 45.1×10^4 ha during ten years between 1990 and 2001. It became 107.9×10^4 ha in 2006 and doubled in five years (Figure 3.10).

The spatial distribution of 5-year mean corn planted areas Phase II, III and IV (Figure 3.14) is similar to that of cattle ranching and soybean production areas and distribution, although its numerical value is low. Corn planted areas as general trend expand in the central, central north and central south MT. These mean that corn is also the main ingredient for ethanol as well as grain feeds in the world.

Therefore, every characteristic of the municipal district which is the same as cattle and soybean speculation in the Campo Novo do Parecis (Figure 3.1, no. 22), there was a decrease by 0.81 times from 24.7×10^3 ha to 20.1×10^3 ha from Phase II to Phase IV (Figure 3.18a and c). In the Sorriso (Figure 3.1, no. 126), it continues to increase steadily by 16 times from 3.3 $\times10^3$ ha in Phase II (upper left of Figure 3.14) to 52.8×10^3 ha in Phase IV (lower of Figure 3.14). In the Nova Ubiratã (Figure 3.1, no. 80), it increased from 0 ha to 5.5×10^3 ha between Phase II, and IV (Figure 3.14).

The total production in MT increased smoothly by 6.83 times from 0.62×10^6 ton to 4.23×10^6 ton between 1990 and 2006. It shows sudden increase after 2000 (Figure 3.11). The total amount of production in MT increases smoothly by 9.35 times from 92.7×10^9 reals to 866.8×10^9 reals between 1994 and 2006 (Figure 3.12).

Our results can suggest that there is less Corn planted area compared to Soybean area in MT. Because of the higher cost of Corn production, along with a historically lower demand for Corn than for Soybeans (i.e. beef in the Center-West is grass-fed and soybeans for export are more liquid), are the main reasons why there is less corn area compared to soybean area in the Center-West of Brazil (USDA 2007). While Brazil's corn area has been quite stable over the last decade, high world prices, largely influenced by increasing U.S. ethanol demand, are creating an invigorated interest in planting corn. For the purpose of use for bio-fuel, production of not only sugarcane but also corn is promoted in recent years. If world Corn demand continues to grow, a larger Corn planted area in these newer agricultural areas is likely to be witnessed. Brazil is currently the world's third biggest corn exporter behind the United State of America and Argentina, and was exported 5.5 million tons of Corn in 2007.

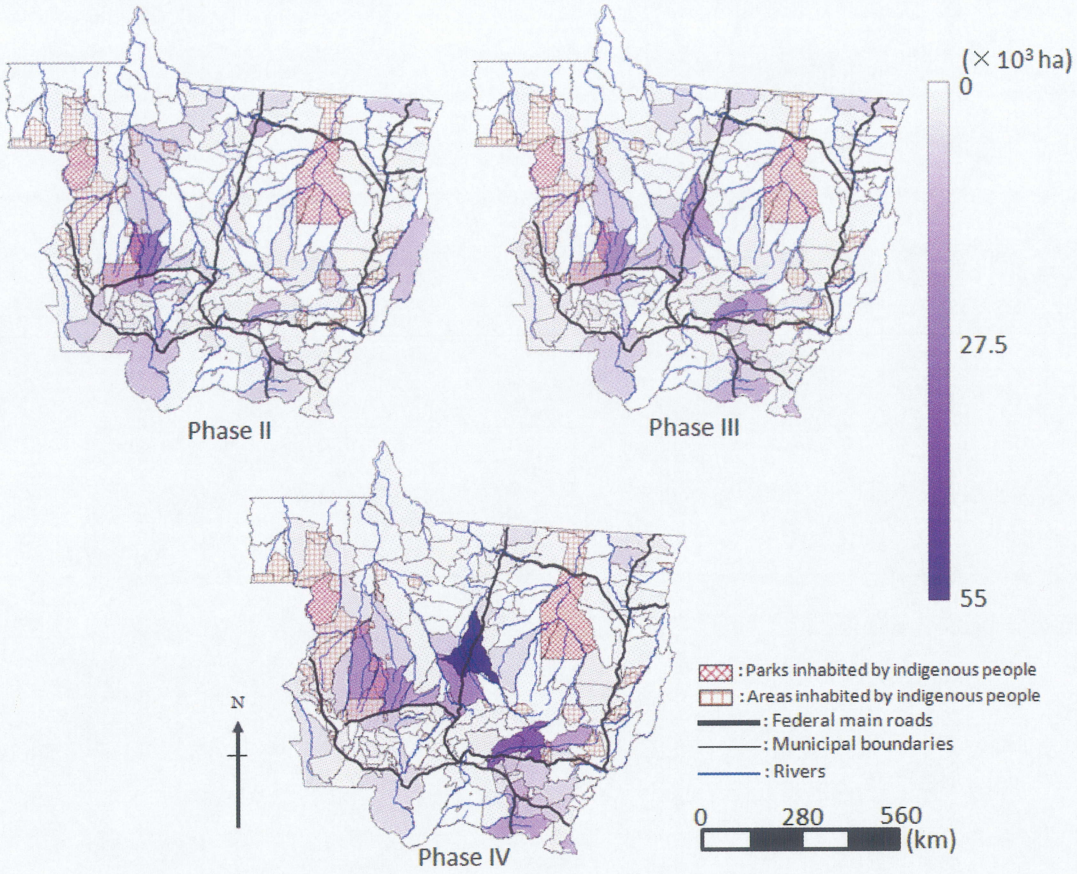

Figure 3.14. The distribution map in the 5-year mean Corn planted area Phase II, III and IV of every municipal district in MT.

3.5.4 Statistical analysis for causes of vegetation change

Figure 3.15 shows the quantity of each Reclassified 5-year DVM Map Phase I, II, III and IV of each 4 vegetation types (*f1*, *f2*, *Deeply Altered Areas* and *Savanna*) in the area ($\times 10^6$ ha) with dependent variables on the left side and change of each 5-year mean of cattle ($\times 10^7$ heads) or 5-year agricultural planted area of Soybean, Sugarcane or Corn with dependent variables on the right side. And independent variables are shown in Phase I, II, III and IV during 1981–2001. We calculated correlation coefficients (r) in vegetation and the number of cattle or the agricultural planted area (Table 3.2).

Comparison between each area of 4 vegetation types and each head count of cattle or agricultural planted area is positively and highly correlated with the number of cattle (r=

1.0), Soybean (r= 0.98), Sugarcane (r= 0.96) and Corn (r= 1.0) of P-value below 0.1 for *DAA*, in addition Soybean (r= 0.85) and Sugarcane (r= 0.89) for *Sv*. However there is negatively and highly correlated with Heads of cattle (r= -0.89) and Corn (r= -0.88) for *f1*, and Soybean (r= -0.84) and Sugarcane (r= -0.88) for *f2* (Table 3.2). The relation of the head count of cattle with *f1* is close and it can be surmised that Evergreen Broadleaf Forests are destroyed whenever cattle ranching increases. Similarly, Corn as grain feeds increases in the region of cattle ranching. Where Soybean and Sugarcane planted areas increase, *f2* decreases. This does not penetrate directly into virgin forests and suggests that SdF, BSF, and SW are opened up greatly. Such changes contribute to the vegetation change greatly. In addition, we understand that it is very likely that Soybean and Sugarcane planted area is used after cattle ranching. However, when cattle, Soybean, Sugarcane and Corn planted area increase, *DAA* increases. This is the evidence that too much conversion to cropland and pastures is performed in the area of DA. And the increase of the farm development for Soybean and Sugarcane accelerates *Sv*.

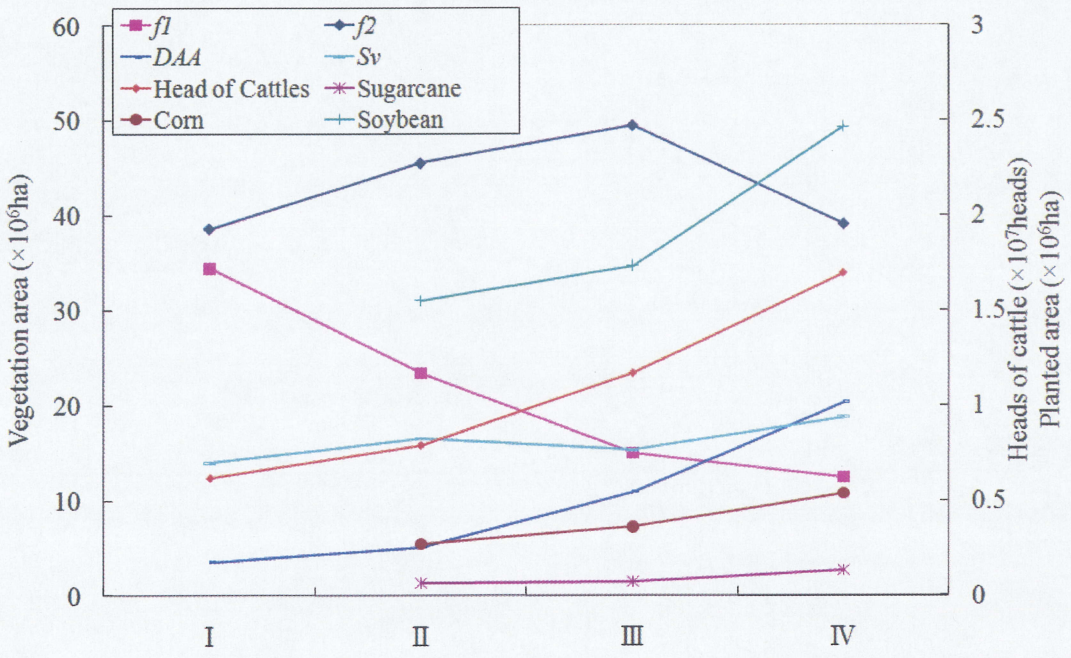

Figure 3.15. Area ($\times 10^6$ ha) of vegetation (*f1*, *f2*, *DAA* and *Sv*) and 5-year mean Heads of Cattle ($\times 10^7$ heads) and 5-year mean (Soybean, Sugarcane and Corn) Planted area ($\times 10^6$ ha) in total MT.

Table 3.2. Correlation coefficient Vegetation type and 5-year mean Head of cattle and 5-year mean Soybean, Sugarcane or Corn planted area. Red character denote correlation coefficients of P-value below 0.1.

	Cattles	Soybean	Sugarcane	Corn
f1	-0.89	-0.80	-0.76	-0.88
f2	-0.07	-0.84	-0.88	-0.76
DAA	1.00	0.98	0.96	1.00
Sv	0.83	0.85	0.89	0.77

At municipal districts, then, we derived correlation coefficients between changes of the 5-year mean head count of cattle (Soybean, Sugarcane, or Corn planted areas) and each 4 category changes of the Reclassified 5-year DVM vegetation Map from Phase I to IV. Test of significance using the correlation coefficients were obtained by t-test. The correlation coefficients of P-value below 0.05 from the test results were adopted as significant correlation coefficients.

In consequence, Figure 3.16 shows significant correlation coefficients between changes of cattle ranching and 4 vegetation types. When we focus on each municipal district, in the Apiacas (Figure 3.1, no.9) and Juìna (Figure 3.1, no.59) districts, cattle ranching are negatively and highly correlated with *f1* (r= -0.992 and -0.993) in the opposite positively and highly correlated with *f2* (r= 0.992 and 0.989).

This is the increase in the head count of cattle, indicating that the decrease in tropical forests. It is the true evidence that the construction progress of the ranchers is gone up northwards destruct tropical forests directly. As for this, it is thought that the head count of cattle will further increase through the construction of the transportation system from the Juruena River basin and the unpaved road, BR–174, stepping forward from the east

Rondônia state. At the same time in the Denise (Figure 3.1, no.40) and Pedro preta (Figure 3.1, no. 88) districts, these are negatively and highly correlated with *f2* (r= -0.980 and -0.988) in the opposite positively and highly correlated with *DAA* (r= 0.980 and 0.997).

Figure 3.17 shows significant correlation coefficients between changes of Soybean planted areas and 4 vegetation types. There are no significant correlations in *f1*. At the Sorriso (Figure 3.1, no.126) and Colíer (Figure 3.1, no.32) in the central MT, Soybean are negatively and highly correlated with *f2* (r= -0.993 and -0.995) in the opposite positively and highly correlated with *DAA* (r= 0.993 and 0.999). In particular it indicates that forest development by Soybean products is performed in the municipal district, which is next to roads such as BR–163. And in the Sapezal (Figure 3.1, no.123) and Campos de Julio (Figure 3.1, no.24) in the west MT, Soybean are negatively and highly correlated with *f2* (r= -0.991and -0.999) in the opposite positively and highly correlated with *DAA* (r= 0.987 and 0.997) as well as *Sv* (r= 1.0 and 1.0). In the Gaucha do Norte districts, *f2* is negative and high correlation (r= -0.995) and *Sv* is positive and high (r= 1.0). As a result, soybean production is not directly destructions of tropical forests. However, the effects derive from degenerated forests (savanna woodlands) area to savanna vegetation around BR-174 and Xingu river basin, despite Sapezal had protected areas.

Figure 3.18 shows significant correlation coefficients between changes of Sugarcane planted areas and 4 vegetation types. Like Soybean there are no significant correlations in *f1*. In the Colíer (Figure 3.1, no.32), Sorriso (Figure 3.1, no.126) and Gaucha do Norte (Figure 3.1, no.45) districts, Sugarcane are negatively and highly correlated with *f2* (r= -0.999, -0.999 and -0.995) in the opposite positively and highly correlated with *DAA* (r= 1.0 and 0.999) or *Sv* (r=1.0 at Gaucha do Norte). These results are similar as Soybean. These indicate that the sugarcanes in the same location as soybeans are planted in the central MT. However, in the south MT, at Barra do Bugres (Figure 3.1, no.16) and Cáceres (Figure 3.1, no.20) there are negatively and highly correlated with

Sv (r= -0.998 and -0.989) in the opposite positively and highly correlated with *DAA* (r= 0.997 and 0.988). We consider that *DAA* are transformed from farm land into *Sv*.

Figure 3.19 shows significant correlation coefficients between changes of Corn planted areas and 4 vegetation types. At the Cotriguaçu (Figure 3.1, no.37) and Novo Mundo (Figure 3.1, no.82) in the north MT, Corn are negatively and highly correlated with *f1* (r= -0.997 and -1.0) in the opposite positively and highly correlated with *f2* (r= 0.997 and 0.999). Area of Corn and cattle ranching are the same vegetation changes and near location. This suggests that cattle ranching which are needed so many foods can be acquired grain feeds by the presence of Corn planted areas nearby. In addition at the Porto Estrela (Figure 3.1, no.98) and Sapezal (Figure 3.1, no.123) in the south and west MT, Corn are negatively and highly correlated with *f2* (r= -0.999 and -0.998) in the opposite positively and highly correlated with *Sv* (r= 0.998 and 1.0) and *DAA* (r= 0.987 at the Sapezal). The *f2* decreases and *Sv* increases when Corn planted area increase in these areas. This designate that expansion of corn planted areas makes directly changes with savanna.

In consequence, expansion cattle ranching and Corn planted areas are converted from tropical forests to non-dense forests like savanna woodland and Soybean and Sugarcane are from non-dense forests to human activity area or savanna. The expansion of agro-industry areas has changed the vegetation. Deforestation and savannization are progressing.

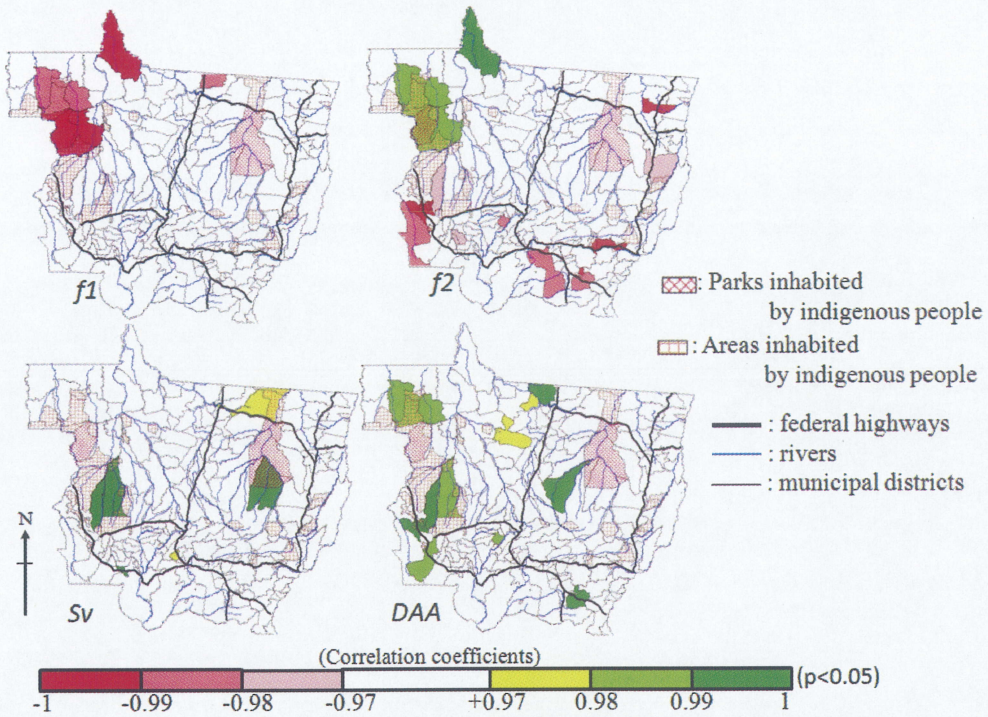

Figure 3.16. Correlation coefficient of P-value below 0.05 between 4-type Vegetation and 5-year mean head count of Cattle.

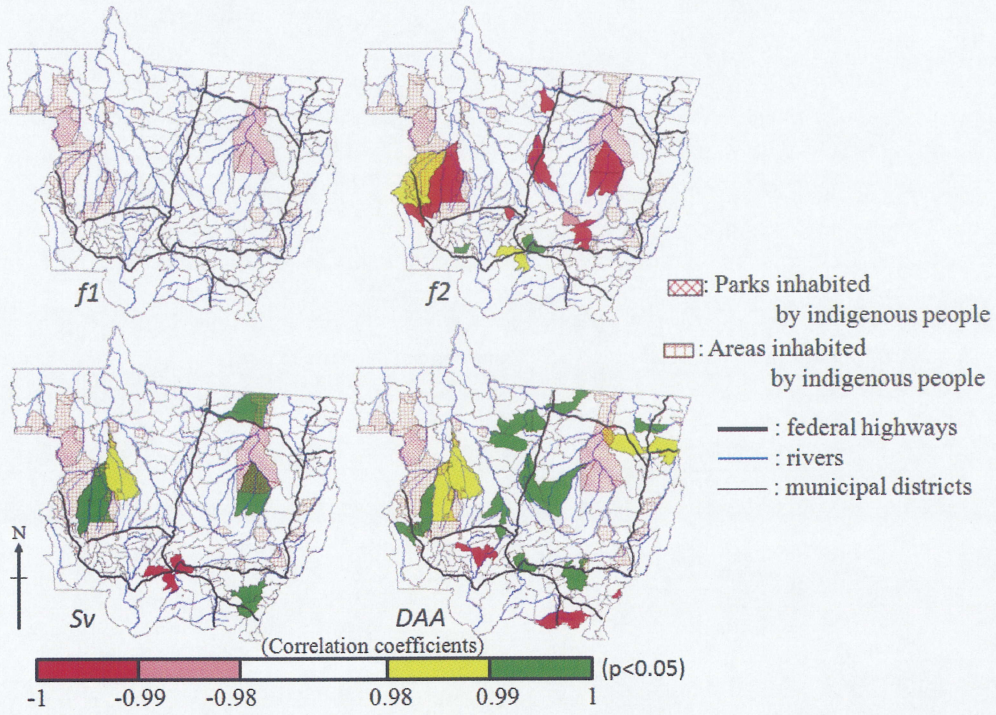

Figure 3.17. Correlation coefficient of P-value below 0.05 between 4-type Vegetation and 5-year mean Soybean planted areas.

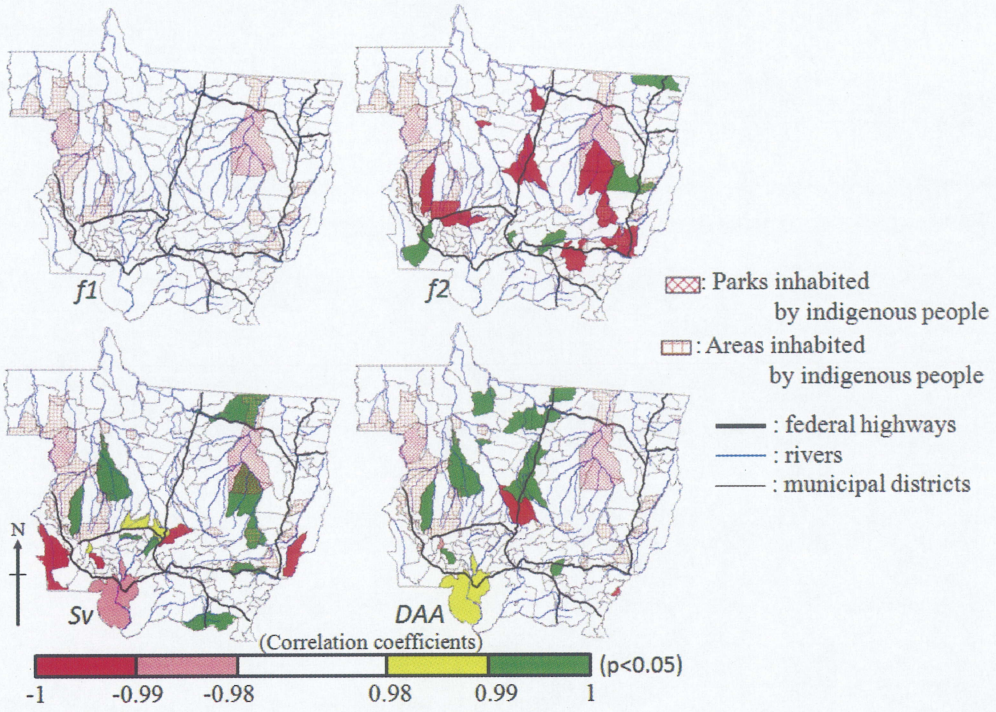

Figure 3.18. Correlation coefficient of P-value below 0.05 between 4-type Vegetation and 5-year mean Sugarcane planted areas.

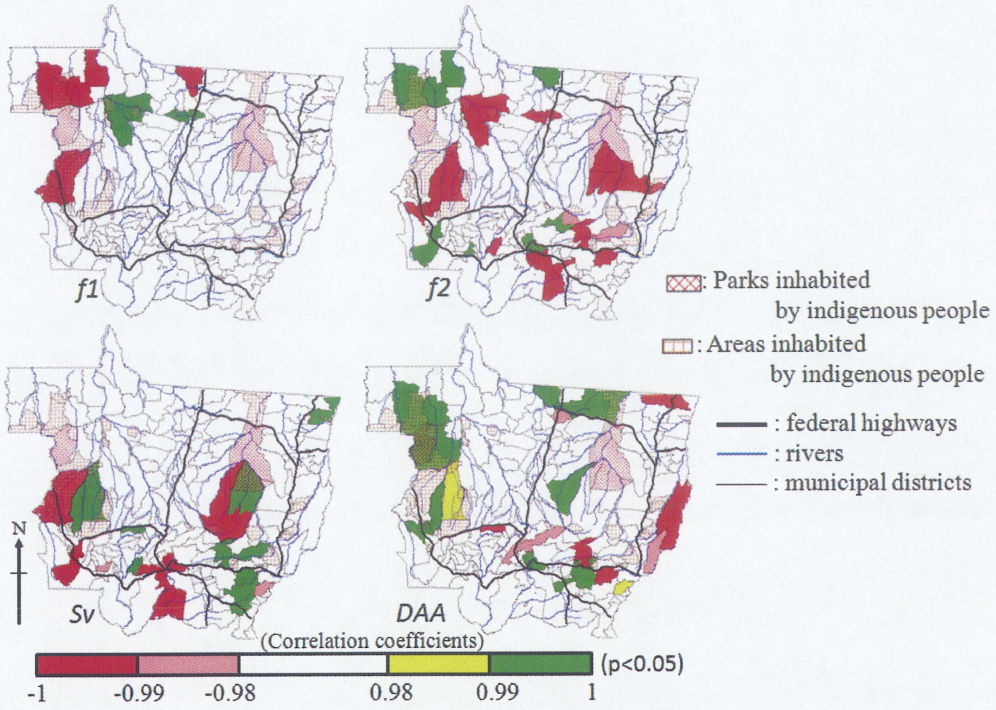

Figure 3.19. Correlation coefficient of P-value below 0.05 between 4-type Vegetation and 5-year mean Corn planted areas.

3.6 Discussion and concluding remarks

We clarified how the vegetation change occurred in 3 categories of Degradation, Recovery and Transitional area with the 5-year DVM vegetation change map Phase I–II, II–III, III–IV and I–IV (Figure 3.5a-c and 3.6) provided by Yoshikawa and Sanga-Ngoie (2009) as follows: (*a*) Degradation from *f1*to *f2* in the central part spreads over vast areas, with intense change in the 1980's around the Juruena River. This started to spread northward since the 1990's, with large-scale development, expanding even over protected areas such as Parks and Areas inhabited by indigenous people. (*b*) Changes from *Forests* to *DAA* are found mostly over the south, from the 1980's, starting in those municipal districts where access from roads and rivers is easy. These changes deeply moved into inland since the 1990's. (*c*) In the 1980's hectic land developments occur in the southern part of Pantanal, spreading toward northeast in 1990's. *Forests* are changed into *Sv* in those areas. (*d*) Recovery from *f2* to *f1* is found over the central part of MT in the 1980's, and over the northern part in the 1990's. (*e*) The little bit of recovery from *DAA* or *Sv* to *Forests*, was observed in municipal districts along the rivers. (*f*) Transitional areas over the southern and the eastern parts of *Sv* were changed into *DAA* in the 1980's. These changes then spread toward the southern and western parts in the 1990's. (*g*) Changes from *DAA* to *Sv* are found to be increasing over the whole southern area, leading to large-scale savannization. The ratios per vegetation change areas from 1981 to 2001 are (*h*) Degradation: 85.8 % (46.4 %: the ratio per MT areas), (*i*) Recovery: 1.6 % (0.85 %: the ratio per MT areas) and (*j*) Transitional area: 12.6 % (6.82 %: the ratio per MT areas).

The 5-year mean head count of Cattle, Soybean, Sugarcane and Corn planted area increased and spread the production area drastically since the 1990's in municipal districts. In particular, cattle ranching and bit of Corn planted areas continued to invade into the northern part of MT. We summarized agro-pastoral distribution in Figure 3.20. Soybean planted area spread in the central part. Corn spread nearly as much an area as

Cattle ranchers are distributed over the area surrounded by new BR-174. Most of Sugarcane planted area spread in the southwest.

By comparing the number of cattle and the agricaltural data change with vegetation change, its relation became clear as follows: (*i*) When Cattle ranching or Corn planted areas (Soybean or Sugarcane) increases, *f1* (*f2*) decreases. The expansion of Cattle ranchers and Corn planted areas in the north MT understood that the direct participation in deforestation was big. And Soybean and Sugarcane production indirectly affected its participation in deforestation. (*ii*) They are highly related to increase in *DAA*. (*iii*) Soybean and Sugarcane planted areas in the central MT and Corn in the west MT have high equilateral correlation with savannization directly. (*iv*) We understood that ranching moved toward the north in connection with corn production. (*v*) It is understood that most of the abandoned areas were changed into Soybean and Sugarcane cultivated land.

Morton *et al.* (2006) paid attention to the expansion of the soybean production and only compared relations with deforestation and clarified that deforestation for large-scale cropland accounted for 17 % of forest loss during 2001–2004 in MT. And Soares-Filho *et al.* (2006) suggest that by 2050, current trends in agricultural expansion will eliminate a total of 40 % of Amazon forests. However, as a result of this study, about 46.4 % of MT area was degraded through deforestation during 1981–2001, and was developed that Cattle ranchers and Corn planted areas (in north and south MT) around Soybean and Sugarcane in the central MT (Figure 3.20). And Jasinski *et al.* (2005) analyzed probability of conversion to mechanized agriculture based on logistic regression models using physical data (elevation, precipitation, soil types and distance to a paved road). The prediction of development in the northwest was not reflected in the result. In this study, approaches of cattle ranching in the northwest are obvious; we suggest that this progress will be continued in connection with corn farm lands.

As a cause of deforestation, Margulis (2004) discusses the occupation of the Brazilian Amazon was largely induced by government policies in the 1970s and 1980s, but recent

deforestation is basically caused by medium and large scale cattle ranching. Figure 3.21 and 3.22 show clearly cause of deforestation and savannization in each municipal districts. Following Figure 3.21, Most of deforestation in tropical rainforests is caused by cattle ranchers or corn farm land in northwest MT and soybean or sugarcane farm land in central MT. On Figure 3.22, savannization by soybean and sugarcane farm land spread mainly in the west MT and by corn in the southwest. Corn productions have more savannization impacts than the soybean crop production. Thus, if corn production as bio-ethanol or feed for cattle for growing world's demand will be continued to increase, they push ahead with the destruction of the Amazon tropical forest and made it more unrecoverable forests and savanna. In addition, in comparison with sustainable forest management, ranching is more economically viable from the point of view about municipal districts, although we must be cautious with definite conclusion.

Since the1980's, studies on the environmental assessment of the Amazon area flourished (Fearnside 1986, 1993, 2005, Skole and Tucker 1993, Gash and Nobre 1997, Greenpeace 2006, Guild *et al.* 2004, Morn *et al.* 2005, 2006, Sanga-Ngoie and Yoshikawa 2004, 2006, 2007, 2008 (a), 2008 (b), 2008 (c), 2009 (a), 2009 (b), 2009 (c), 2009 (d), 2009 (e), 2009 (f), Yoshikawa 2002, Yoshikawa and Sanga-Ngoie 2009, 2010). However, the development which seems to promote vegetation dilapidation does not stop to date, either. We clarified that Yoshikawa and Sanga-Ngoie (2009) made more detailed vegetation maps using GIS and remote sensing data and made impact statement to the vegetation change the road construction and navigable rivers as a physical factor. In this chapter, we showed relations with the change of the vegetation and cattle ranching and agriculture as economic activities. We would like to try to use the DVM Map technique during recent years or predictions in the future.

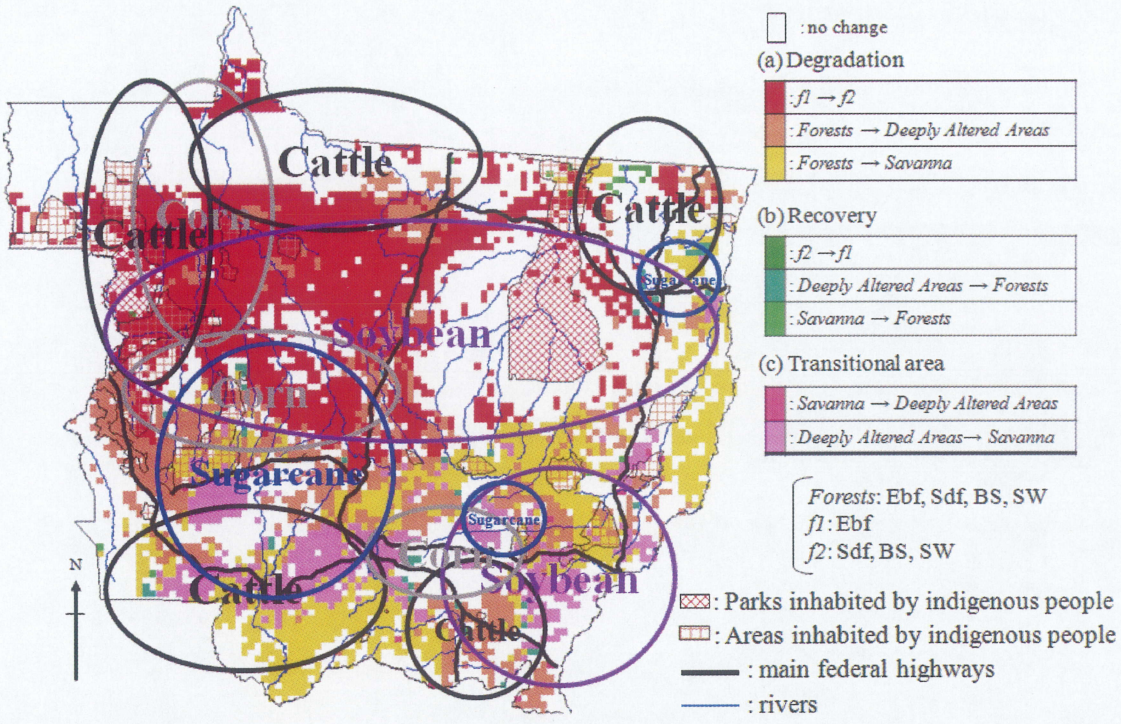

Figure 3.20. Summary of agro-pastoral distribution on the 5-year DVM vegetation change Map Phase I–IV (Figure 3.5).

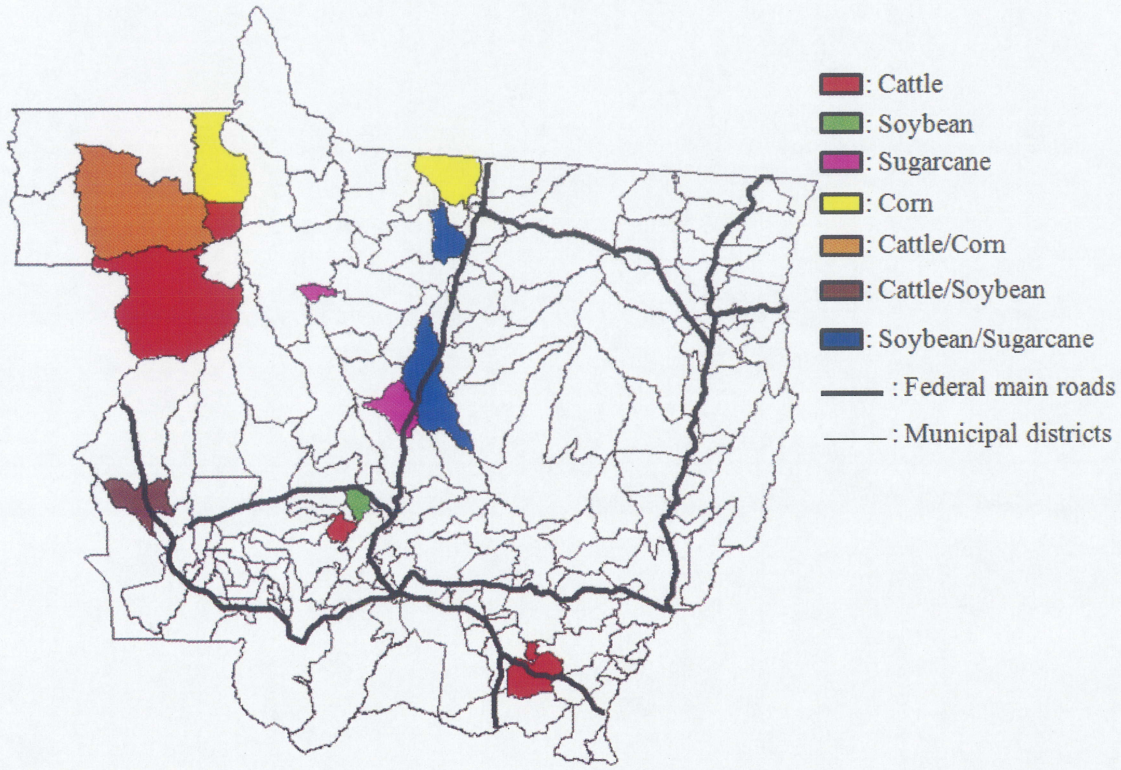

Figure 3.21. Cause of deforestation.

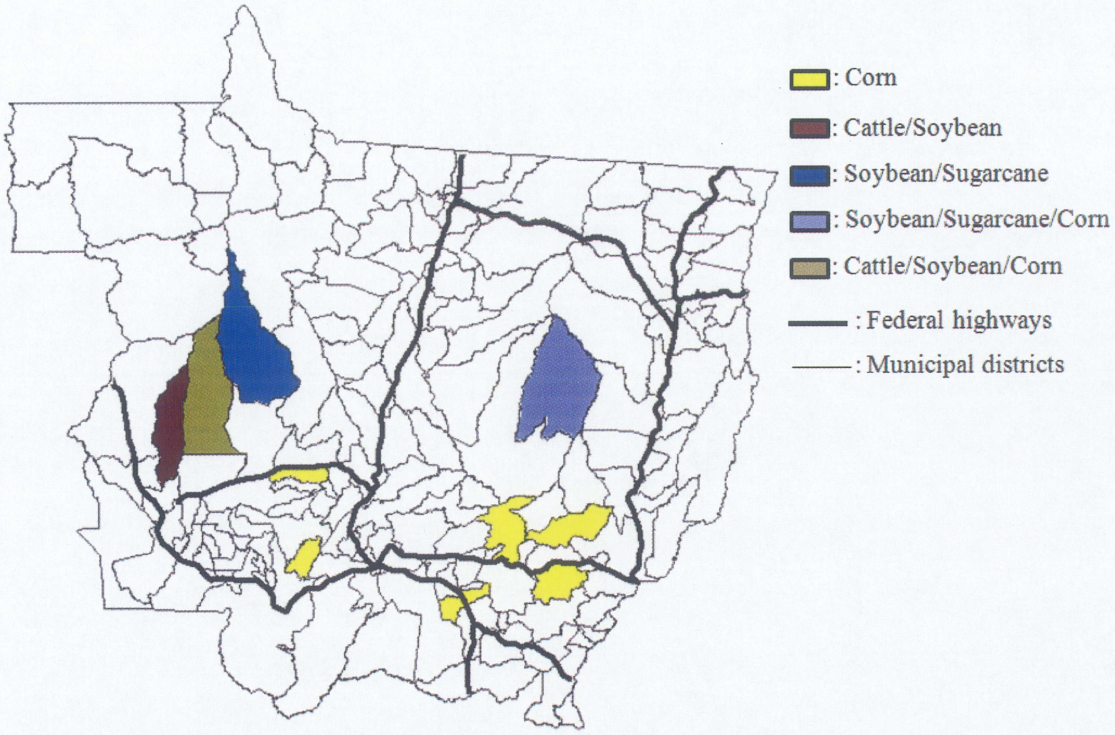

Figure 3.22. Cause of savannization

Chapter 4

Population Dynamics

Chapter 4

Population Dynamics

4.1 Introduction

Following the intensive research by Fearnside (1986, 1993, 2005, 2006) and many other works on the Amazon, and based on our findings in the previous chapter (2 and 3), we postulate that the main causes to the high rate of deforestation have to be related to life-sustaining activities by humans, as well as to infrastructure building in relation with these human activities. We therefore chose to focus our investigation on the role of population pressure, as one of the most important causes to these changes among others.

This chapter is motivated and its main objectives are: to shed new light on the causes of the deforestation, especially on causal relationships between vegetation change and population pressure. The Mato Grosso State (Figure 2.1) will be our study area for the reasons mentioned above. Geographic Information System (GIS) and remote sensing technology will be used for fast, comprehensive, multi-criteria and broad-based inquiry and analysis.

Hereafter, the data materials and the methods are presented in section 4.2 and 4.3, respectively. Our analysis results (Population and vegetation change) are given in section 4.5. Discussion and concluding remarks are highlighted in section 4.6.

4.2 Data materials

Through our previous work (Yoshikawa and Sanga-Ngoie 2009, 2010), we could obtain new vegetation maps (and change maps) as the 5-year DVM Map Phase I, II, III and IV (Figure 2.4a-d) and the 5-year vegetation change map Phase I-II, II-III, III-IV and I-IV (Figure 3.4a-c and 3.5). In this chapter, we use these vegetation maps and

population data outlined below.

The United Nations Environment Program (UNEP/GRID, Sioux Falls) provides on-line population estimates for 1960, 1970, 1980, 1990 and 2000. As data sources vary by country, population data from each census are carried out at the geographical level for which boundary data are available.

In order to provide an indication of population dynamics and maximize comparability across national boundaries, population estimates were produced for 1960, 1970, 1980, 1990 and 2000. Since population censuses are not synchronized and taking census is irregular in many countries, time interpolation was used to provide these estimates.

Province or district specific intercensal growth rates were computed from published census figures. These growth rates were then used to compute estimates for the standard years, and population predicted from these growth rates (UNEP/GRID 2000). In this research, we calculated the population of each year by the same technique using 1980, 1990, and 2000 population data, and the average value for each one of the five-year period was used.

4.3 Methods

Firstly, in order to provide an indication of population dynamics, population estimates were produced for 1970, 1980, 1990 and 2000. Since population censuses are not synchronized and census taking has been irregular in many developing countries, figures needed to be interpolated to provide these estimates. For this purpose, province or district specific intercensal growth rates were computed from published figures. These growth rates were then used to compute estimates for the standard years. The intercensal growth rate is calculated as:

$$r = \frac{\ln(\frac{P_2}{P_1})}{t} \qquad (6)$$

where r is the average annual rate of growth, P_1 and P_2 are the population totals for

two different time periods, and t is the number of years between two enumerations (Rogers 1981, 1985). The resulting growth rates were then used to derive estimates for the standard years. For example, based on enumerations in 1980 and 1990 and a corresponding rate r, the 1985 population would be calculated as:

$$P_{1985} = P_{1980} \cdot e^{3r} \qquad (6)$$

Therefore these are provided by each year's population distribution maps. The population density each year was made five years' average same as Phase in 5-year DVM maps. We can get 5-year mean population density (inhabitants/km^2) maps Phase I, II, III and IV (Figure 4.1a-d) using UNEP/GRID data.

Second, based on the 5-year mean population density maps (Figure 4.1a-d), patterns of vegetation change over the past 20 years were devised as the 5-year mean population density change map Phases I–IV.

Third, the 5-year mean population density maps Phase I, II, III and IV are compared with the 5-year DVM maps Phase I, II, III and IV. In addition similar work is done between the 5-year mean population density change map Phases I–IV and the 5-year DVM vegetation change Map Phase I–IV. Using the obtained 5-year DVM Maps, causes of deforestation are investigated by analysis of the relationship between the changes in the DVM maps and the related 5-year mean population density for each region.

4.4 Results

4.4.1 Population density and the changes

First of all, population density maps for each one of the 4 phase of analysis are obtained, and them reclassified into the following 12 categories: (1) non-inhabited areas with density x=0 inhabitants/km^2; (2) $0<x\leqq1$; (3) $1<x\leqq1.5$; (4) $1.5<x\leqq2$; (5) $2<x\leqq2.5$; (6) $2.5<x\leqq5$; (7) $5<x\leqq20$; (8) $20<x\leqq50$; (9) $50<x\leqq100$; (10) $100<x\leqq200$; (11) $200<x\leqq300$ and (12) areas with x>300 inhabitants/km^2 which was named 5-year mean population density map Phase I, II, III and IV (Figure 4.1a-d). Overall, the southern MT is distributed with much population density, as fewer to the north (Figure 4.1a-d). In addition, densely populated areas in the northern MT are along roads and rivers. Furthermore, with the increase of population, population density has increased from Phase I to Phase IV.

Population density changes between Phases I and IV which is named as the 5-year mean population density change map Phases I–IV are calculated and reclassified into 11 categories: (1) non-inhabited area; (2) no change area; (3) $x=0 \rightarrow x\leqq1$; (4) $x=0 \rightarrow x\leqq2.5$; (5) $1<x\leqq2.5 \rightarrow x\leqq5$; (6) $1<x\leqq2.5 \rightarrow x\leqq20$; (7) $x=5 \rightarrow x\leqq50$; (8) $5<x\leqq20 \rightarrow x\leqq100$; (9) $20<x\leqq50 \rightarrow x\leqq200$; (10) $50<x\leqq100 \rightarrow x\leqq300$ and (11) $100<x\leqq200 \rightarrow 300<x$ as given in Figure 4.2. In 20 years, population density increased in the deeply populated areas, but non-habitant areas are not changed at all.

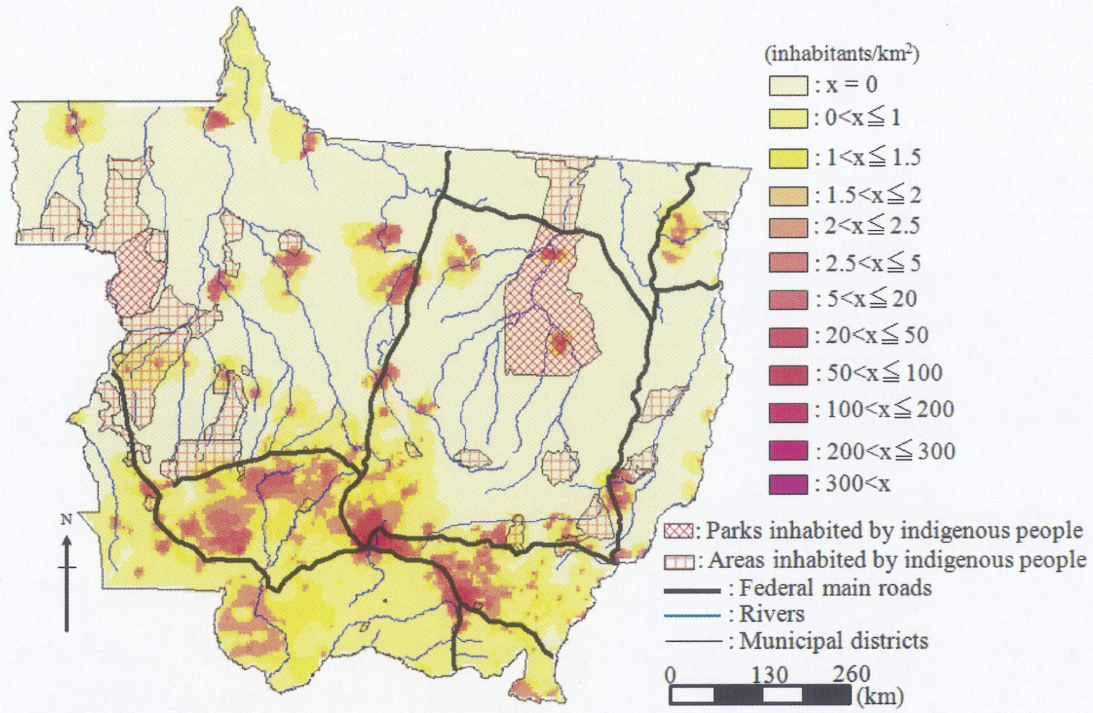

Figure 4.1a. The 5-year mean population density (inhabitants/km^2) map Phase I from the 1981 to 1986 period in MT.

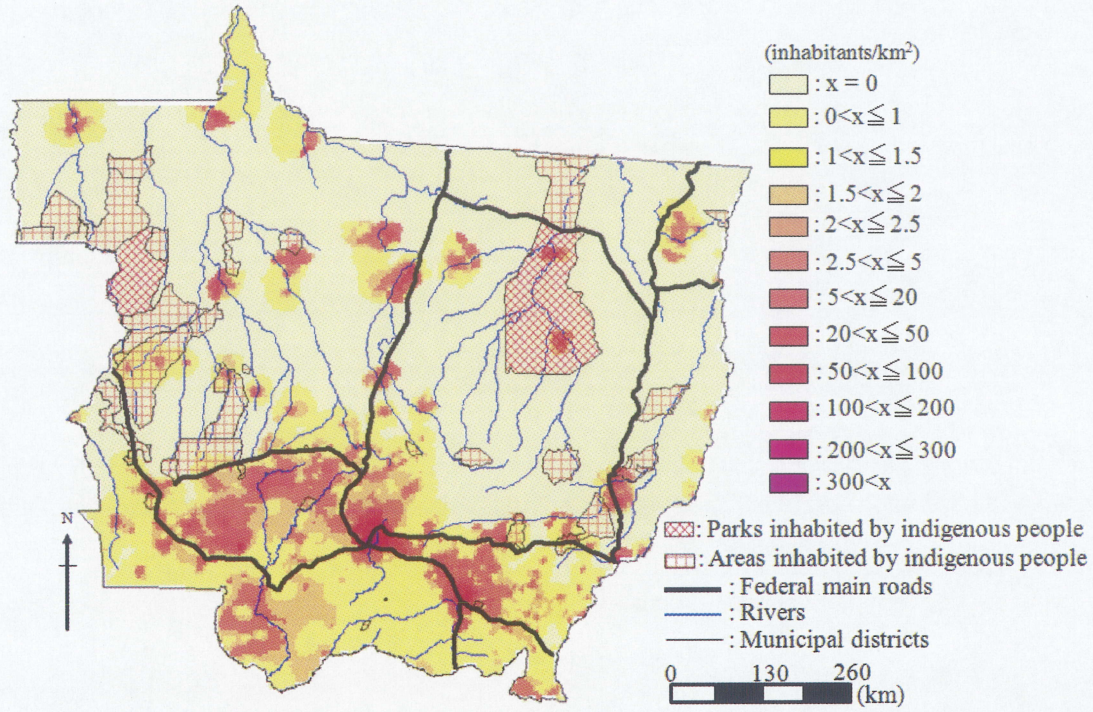

Figure 4.1b. Same as in Figure 4.1a, but for the 5-year mean population density map Phase II.

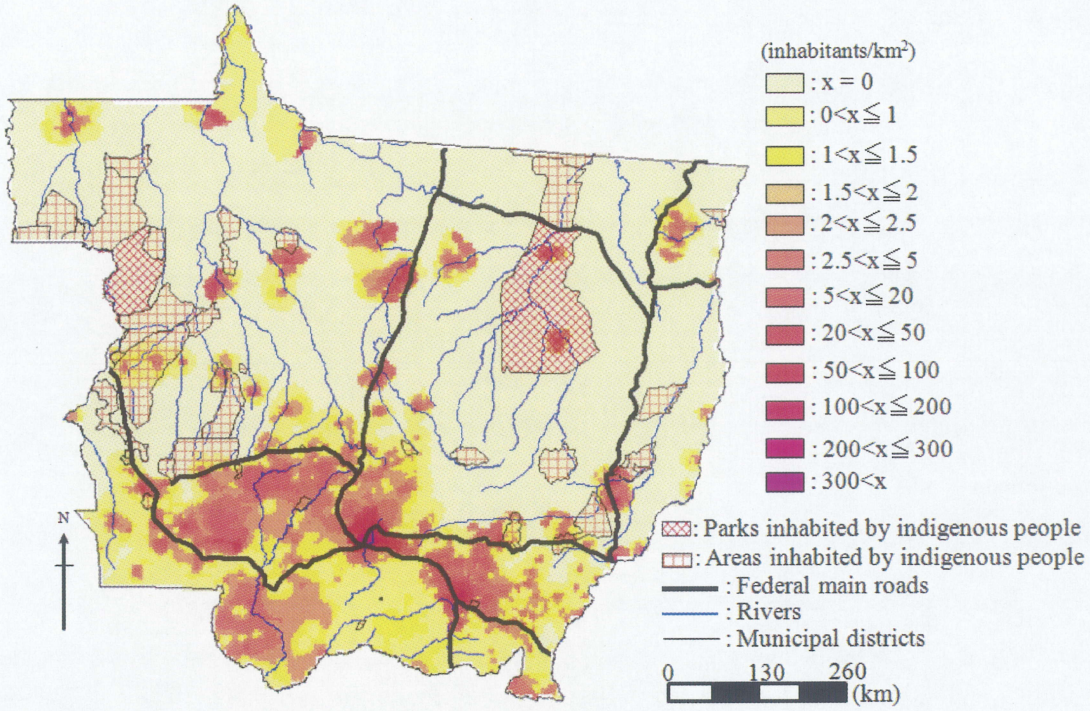

Figure 4.1c. Same as in Figure 4.1a, but for the 5-year mean population density map Phase III.

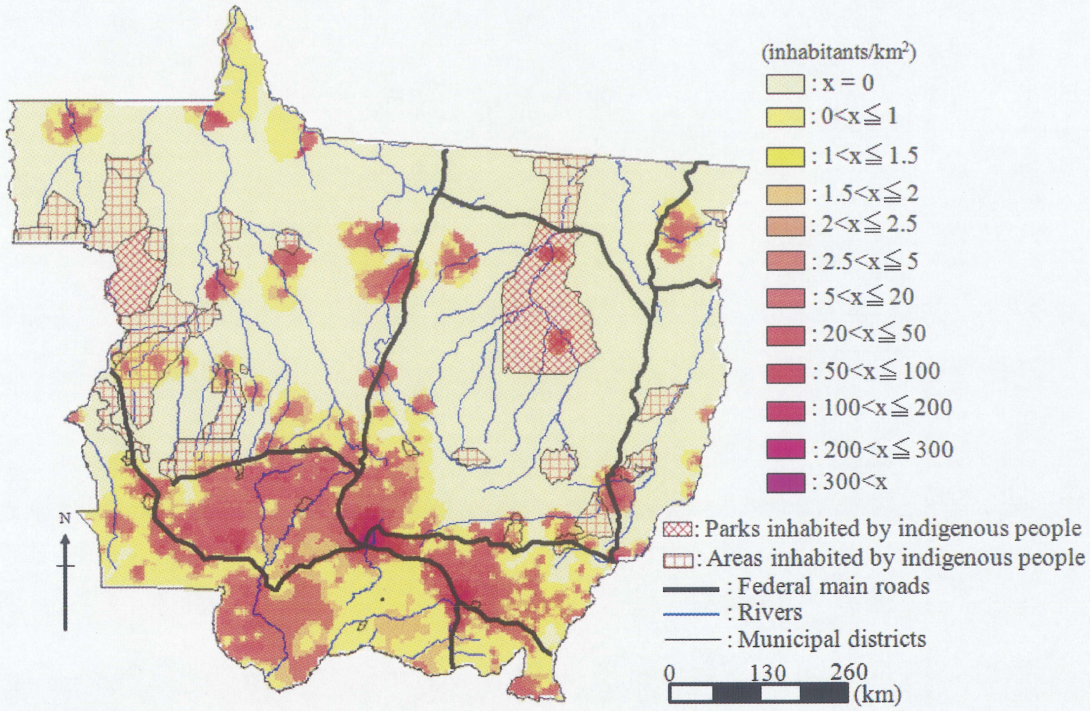

Figure 4.1d. Same as in Figure 4.1a, but for the 5-year mean population density map Phase IV.

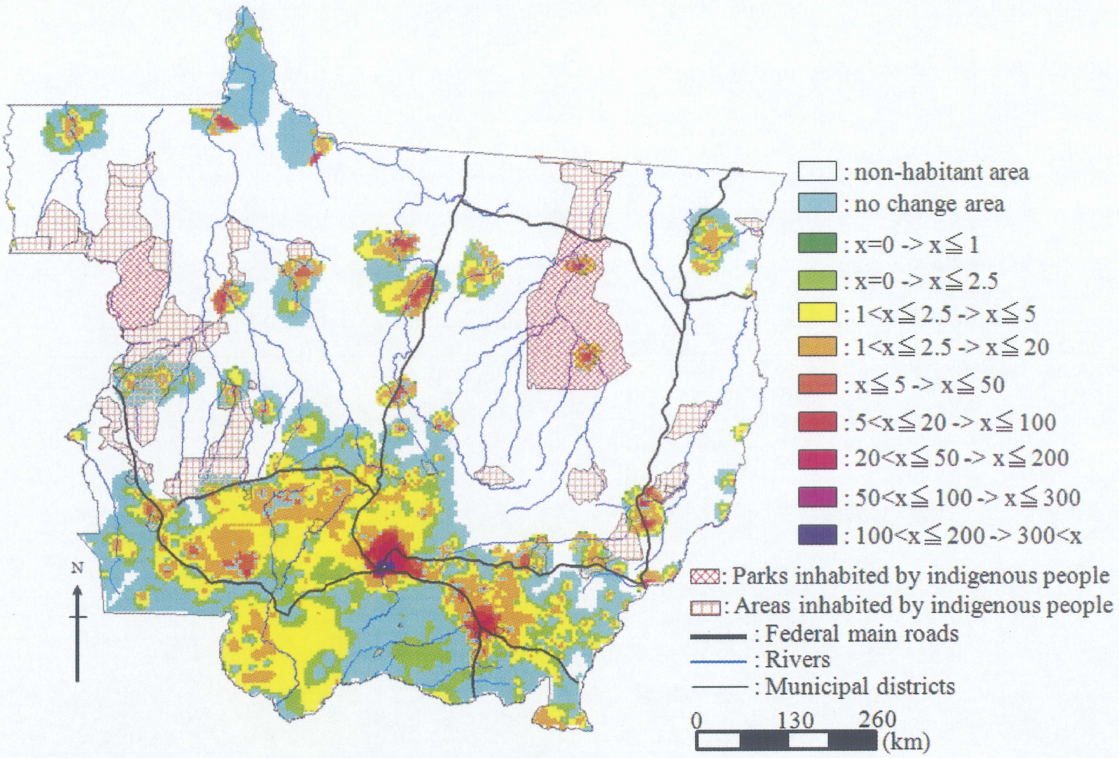

Figure 4.2. 5-year mean population density (inhabitants/km^2) change map Phases I–IV in MT.

4.4.2 Population and vegetation changes

Comparison between each vegetation type area from our 5-year DVM Maps Phases I–IV and the corresponding 5-year mean population density yields high negative correlation coefficients (r) for both Evergreen Broadleaf Forests (r= -0.8) and Savanna Woodlands (r= -0.68). On the other hand, the corresponding correlation for the Savanna and the Deeply Altered Areas are highly positive: r= 0.98 and 0.84, respectively. These findings clearly show the strong relationship between the changes in areas of these 4 land cover types and the change in population density and pressure: strong decrease in forests and Savanna Woodlands covers, and remarkable increase in non-forests covers in relation with human population invasion in the area.

Moreover, comparatively lower correlationship between change in vegetation covers and population change is obtained for Semi-deciduous Seasonal Forests (r= -0.57),

Broadleaf and Seasonal Forests (r= -0.59). Savanna Grasslands show only very low correlationship (r= -0.2). Considering that all these correlations are highly significant (p<0.1), these findings clearly denote and emphasize the strong impact on land cover changes by the population advance into Mato Grosso State.

Cross-tabulation statistics between vegetation (5-year DVM) maps (Figures 2.4a–d) and reclassified population density distribution (Figure 4.2) for each analysis period are given in Table 4.1, respectively. Table 4.2 summarizes the cross-tabulation of the overall changes (vegetation and population densities) between Phases I and IV. From these statistics, it becomes very clear that: (1) Areas of population category 1 (x=0) are almost all located within the Evergreen Broadleaf Forests cover type, throughout all the analysis period; (2) Savanna Woodlands and Deeply Altered Areas covers are distributed over those areas with population density within $0<x\leqq20$ inhabitants/km^2; (3) Highly populated areas ($20<x\leqq300$ or higher) prevail over Deeply Altered Areas lands cops, and only marginally over Savanna areas.

It is shown from Tables 4.1 that, in the population density category 1 (x=0), the EBF area decreases more than half, from 27.6 to 10.4×10^6 ha, from Phases I to IV, while the BSF increase from 12.6 to 19.6 $\times10^6$ ha between Phases I and II, and SW from 9.5 to 14.7×10^6 ha between Phases II and III. The S and DA cover types are shown to suddenly increase from 1.3 and 3.7 to 7.5 and 8.4×10^6 ha, respectively, between Phase III and IV. Non-inhabited areas in Table 4e show overall changes of 81.1×10^3 km^2 (ratio of the total vegetation changes: 15.9 %) of EBF and SW into BSF, while a total of 81.0×10^3 km^2 (ratio of the total vegetation changes: 15.9 %) of EBF, SdF and BSF into SW. Moreover, vast tracks of EBF, SdF, BSF, SW, SG and DA vegetation covers change either into S (62.6 $\times10^3$ km^2; 12.3 % of the overall changes) or into DA (61.1 $\times10^3$ km^2; 12.0 % of the overall changes). These features are also seen in areas remote from paved roads in the central and northern MT. The vegetation changes in the non-inhabited areas suggest that logged areas in the 1980's eventually changed into croplands or pastures. The overall spatial distribution of DA is shown to spread relatively fast along paved roads

and main rivers between Phases I and IV.

The $0<x\leqq1$ population density category (Tables 4.1), denotes those areas where few people live. In these areas, the EBF and the SW are shown to have sharply decreased from 4.8×10^6 ha and 6.6×10^6 ha to 1.4×10^6 ha and 2.8×10^6 ha, respectively, between Phases I and IV. On the other hand, the S cover type is shown to have increased from 0.7×10^6 ha, to 3.9×10^6 ha in the same phases. DA cover types increased from 4.7×10^6 ha to 5.6×10^6 ha between I and II and decrease from 5.6×10^6 ha to 2.9×10^6 ha between Phases II and IV. Similar land cover changes are observed to take place in the population density category with $1<x\leqq20$ inhabitants/km^2.

In the $1<x\leqq2.5$->$x\leqq20$ category (Figure 4.2, Table 4.2) where population density has increased about 10 times, changes of EBF, SdF and BSF into SW spread over 5.0×10^3 km^2 (1.0 %) while EBF, SdF, BSF, SW and S to DA changes cover 12.2×10^3 km^2 (2.4 %) throughout all phases. In general, there is a tendency of land cover change from SW (latter half of 1980's) into DA from the early 1990's, spreading from the main roads and navigable rivers, followed by changes from DA (first half of 1990's) to the S covers in the latter half of 1990's, starting from the southern part. These change patterns suggest the following scenario: most of the forested land covers, including SW, were first changed into croplands (DA) and then later on into pastures, or eventually abandoned to savannization since the early 1990s.

In the $20<x\leqq50$ population density category (Tables 4.1), changes in DA and the S covers are particularly large: these cover types increase from 0.2×10^6 ha and 0.03×10^6 ha to 0.4×10^6 ha and 0.1×10^6 ha, respectively. The population density categories with $50<x\leqq300$ inhabitants/km^2 or more show a tendency similar to that of the population density $20<x\leqq50$ category as discussed above. Zones with changes from $20<x\leqq50$ to $x\leqq200$ (Figure 4.2, Table 4.2) show 1.6×10^3 km^2 (0.3 %) of EBF, SdF, BSF, SW, SG and DA were converted to S. Most of these areas are distributed along the paved roads around major cities (Cuiabá and Rondónpolis, etc.) in the southern part. This suggests that these changes occur with the urbanization subsequent to the inflow of population

from big cities, such as São Paulo and Rio de Janeiro, advancing from the southeastern part.

The rate of human activity alterations in the low-density zone ($0<x\leqq20$ categories) is high. As these changes occur without population change, we can postulate that they are caused by commercial timber harvest or slash-and-burn cultivation by invading transient people, or in relation with the expansion of large-scale farms and cattle ranching. In the densely populated area ($50<x\leqq300$ and $300<x$ categories), changes are remarkable from the SW to DA in the 1980s, and from DA to S in the 1990s. These are zones marked by intensive urbanization with spreading permanent lifelines (paved roads, railroads, ports and dam etc...) and built up structures.

Table 4.1. Coverage ($\times 10^6$ ha) of the 7-vegetation types of the classified 5-year DVM Map Phase I, II, III and IV as related to the 5year mean population density (x: inhabitants/km^2) categories.

5-year DVM Maps (Phase I – Phase IV)	Area ($\times 10^6$ ha) per category of population density (x: km)											
	X=0	0<x≤ 1	1<x≤ 1.5	1.5<x≤ 2	2<x≤ 2.5	2.5<x≤ 5	5<x≤ 20	20<x≤ 50	50<x≤ 100	100<x≤ 200	200<x≤ 300	300<x
Evergreen Broadleaf Forests Phase I	27.61	4.57	0.81	0.01	0.47	0.44	0.42	0.08	0.01	0.00	0.00	0.00
EBF Phase II	19.20	2.90	0.00	0.37	0.06	0.32	0.28	0.13	0.01	0.00	0.00	0.00
EBF Phase III	12.52	1.52	0.30	0.00	0.14	0.14	0.13	0.06	0.01	0.01	0.00	0.00
EBF Phase IV	10.36	1.38	0.00	0.27	0.01	0.16	0.17	0.04	0.03	0.01	0.00	0.00
Semi-deciduous seasonal Forests Phase I	1.94	0.92	0.16	0.00	0.08	0.07	0.04	0.00	0.00	0.00	0.00	0.00
SdF Phase II	1.59	0.92	0.00	0.18	0.03	0.12	0.05	0.01	0.00	0.00	0.00	0.00
SdF Phase III	2.11	0.82	0.28	0.00	0.18	0.18	0.10	0.01	0.00	0.00	0.00	0.00
SdF Phase IV	0.96	0.70	0.00	0.18	0.03	0.16	0.14	0.02	0.00	0.00	0.00	0.00
Broadleaf and Seasonal Forests Phase I	12.62	0.43	0.25	0.00	0.14	0.09	0.10	0.03	0.00	0.00	0.00	0.00
BSF Phase II	19.60	1.53	0.00	0.37	0.09	0.37	0.38	0.06	0.01	0.00	0.00	0.00
BSF Phase III	18.91	0.85	0.49	0.00	0.37	0.41	0.44	0.13	0.03	0.00	0.00	0.00
BSF Phase IV	19.29	0.61	0.00	0.40	0.05	0.45	0.41	0.07	0.04	0.01	0.00	0.00
Savanna Woodlands Phase I	9.56	6.64	2.72	0.08	1.76	0.54	0.32	0.12	0.01	0.00	0.00	0.00
SW Phase II	9.45	6.15	0.00	2.14	0.20	1.63	0.53	0.08	0.07	0.04	0.01	0.01
SW Phase III	14.67	3.77	1.79	0.04	1.42	1.34	0.82	0.19	0.06	0.00	0.00	0.00
SW Phase IV	10.03	2.75	0.00	0.80	0.09	0.80	0.78	0.19	0.06	0.00	0.00	0.00
Savanna Grasslands Phase I	0.08	0.58	0.13	0.01	0.14	0.01	0.00	0.00	0.00	0.00	0.00	0.00
SG Phase II	0.05	0.38	0.00	0.12	0.02	0.11	0.00	0.00	0.00	0.00	0.00	0.00
SG Phase III	0.11	0.46	0.15	0.01	0.22	0.17	0.00	0.00	0.00	0.00	0.00	0.00
SG Phase IV	0.04	0.34	0.00	0.09	0.02	0.14	0.08	0.00	0.00	0.00	0.00	0.00
Savanna Phase I	1.34	0.68	0.17	0.00	0.24	0.07	0.04	0.03	0.00	0.00	0.00	0.00
S Phase II	2.52	1.02	0.00	0.40	0.05	0.32	0.12	0.05	0.02	0.00	0.00	0.00
S Phase III	3.11	2.21	1.36	0.03	1.63	0.99	0.26	0.06	0.11	0.04	0.02	0.00
S Phase IV	7.54	3.92	0.00	2.33	0.29	3.61	1.44	0.13	0.12	0.17	0.03	0.05
Deeply Altered Areas Phase I	3.71	4.66	2.34	0.05	1.52	0.85	0.62	0.23	0.07	0.04	0.01	0.00
DA Phase II	4.45	5.59	0.00	2.57	0.30	2.21	1.11	0.23	0.12	0.01	0.00	0.00
DA Phase III	5.22	3.01	1.67	0.03	1.85	1.84	1.39	0.24	0.13	0.03	0.02	0.02
DA Phase IV	8.44	2.96	0.00	1.46	0.23	2.33	2.82	0.43	0.14	0.03	0.00	0.00

Table 4.2. Coverage changes ($\times 10^6$ ha) and rates of change (%) as rated to the changes in population density (x) and vegetation types between Phases I and IV.

5-year DVM maps (Phases I–IV)		Area (%)										
		Non-inhabited areas	No change	x=0 -> x≦1	x=0 -> x≦2.5	1<x≦2.5 -> x≦5	1<x≦2.5 -> x≦20	x=5 -> x≦50	5<x≦20 -> x≦100	20<x≦50 -> x≦200	50<x≦100 -> x≦300	100<x≦200 -> 300<x
Recovery Type 1	BSF・SW・S →EBF	1.39 (0.27)	0.00 (0.00)	0.00 (0.00)	0.00 (0.00)	0.00 (0.00)	0.00 (0.00)	0.00 (0.00)	0.00 (0.00)	0.00 (0.00)	0.00 (0.00)	0.00 (0.00)
Recovery Type 2	SW・SG・DA →SdF	0.96 (0.19)	1.57 (0.31)	0.00 (0.00)	0.39 (0.08)	0.29 (0.06)	0.42 (0.08)	0.00 (0.00)	0.00 (0.00)	0.00 (0.00)	0.00 (0.00)	0.00 (0.00)
Recovery Type 3	S・DA→BSF	0.69 (0.14)	0.00 (0.00)	0.00 (0.00)	0.00 (0.00)	0.00 (0.00)	0.00 (0.00)	0.00 (0.00)	0.00 (0.00)	0.00 (0.00)	0.00 (0.00)	0.00 (0.00)
Recovery Type 4	SG・S・DA →SW	2.51 (0.49)	1.29 (0.25)	0.02 (0.00)	0.58 (0.11)	0.63 (0.12)	0.41 (0.08)	0.12 (0.02)	0.02 (0.00)	0.00 (0.00)	0.00 (0.00)	0.00 (0.00)
Degradation Type 1	EBF・BSF→SdF	1.35 (0.27)	0.54 (0.11)	0.00 (0.00)	0.37 (0.07)	0.17 (0.03)	0.02 (0.00)	0.00 (0.00)	0.00 (0.00)	0.00 (0.00)	0.00 (0.00)	0.00 (0.00)
Degradation Type 2	EBF・SW→BSF	81.07 (15.94)	4.81 (0.95)	0.07 (0.01)	2.91 (0.57)	2.74 (0.54)	1.95 (0.38)	0.05 (0.15)	0.03 (0.05)	0.01 (0.00)	0.00 (0.00)	0.00 (0.00)
Degradation Types 3	EBF・SdF・BSF →SW	81.00 (15.92)	17.52 (3.44)	0.15 (0.03)	4.85 (0.95)	4.26 (0.84)	4.96 (0.98)	1.63 (0.32)	0.49 (0.10)	0.05 (0.01)	0.00 (0.00)	0.00 (0.00)
Degradation Types 4	SdF・SW・S →SG	0.19 (0.04)	0.78 (0.15)	0.00 (0.00)	0.15 (0.03)	0.14 (0.03)	0.48 (0.10)	0.00 (0.00)	0.00 (0.00)	0.00 (0.00)	0.00 (0.00)	0.00 (0.00)
Transitional area Types 1	EBF・SdF・BSF ・SW・S→DA	61.08 (12.01)	16.44 (3.23)	0.12 (0.02)	8.92 (1.75)	11.22 (2.21)	12.19 (2.40)	1.73 (0.34)	0.97 (0.19)	0.12 (0.02)	0.00 (0.00)	0.00 (0.00)
Transitional area Types 2	EBF・SdF・BSF ・SW・SG・DA→S	62.57 (12.30)	36.07 (7.09)	0.10 (0.02)	22.86 (4.49)	33.81 (6.65)	11.55 (2.27)	1.07 (0.21)	1.05 (0.21)	1.63 (0.32)	0.29 (0.06)	0.46 (0.09)

4.5 Discussion and concluding remarks

Park (1992) noted a 10-time increase of non-indigenous population in the Brazilian Amazon since the 1960s, from about 2 million to 20 million people, as a result of transmigration from other areas in Brazil, especially from highly populated southern urban areas. He postulated this to be the biggest impetus to deforestation in this region. Moreover, Margulis (2004) and Fearnside (2006) suggest that expanding road networks strongly increases the access to remote forests by ranchers and colonists, bringing in tremendous industrial logging, mining, large-scale mechanized agriculture, and cattle ranching, as well as negative ecological impacts, which is not accounted for so far.

Taking the population density into consideration, we could shed new light on their important role as multiplicand factors to the deforestation rates. Population patterns show human inflows from the southeast in settlements of up to 20 inhabitants/km^2 in density, almost entirely within SW and DA, during all the analysis period. Our results made clear the following features of the relationships between these settlements and deforestation (Tables 4.1 and 4.2): 56 % of the land cover degradation (deforestation, savannization, and Deeply Altered Areas) occur in non-inhabited places, while only

42% of the changes occur where humans live.

Deforestation in areas without population (Tables 4.1), is to be understood as a consequence to commercial timber harvesting and selective logging which started in the 1980's, just to give place to commercial pastures and croplands since the early 1990's, as also noted by Asner *et al.* (2005). In low density areas (Tables 4.1), croplands in the late 1980's are changed into pastures or simply abandoned to savannization since the early 1990's. Urbanization is intense in high density areas, with massive inflow from southern big cities in Brazil (São Paulo and Rio de Janeiro, etc.). Pressure from lifeline and settlement infrastructure building (roads paved or unpaved, railroads, housings, etc.) brings up to 42 % of the total vegetation changes (Table 4.2), as shown in the vast DA and over-spreading savannization, especially from SW cover types. All these changes almost follow the same pattern as noted by Moran (1993) in the 1970's, but smaller in scale.

Chapter 5

General Conclusion

Chapter 5

General Conclusion

5.1 Overall discussion on this dissertation

This research focused on making the new vegetation maps and clarifying causes of vegetation change which are compared with affecters such as roads and access networks, agro-industrial data and population density. To achieve these main objectives we did as follows:

(a) To quantitatively assess the extent of vegetation change for more accurate eco-climatic impact analysis over the past two decades (1981-2001)

(b) To clarify the relation between vegetation change and roads construction or agro-industry or population pressure in Mato Grosso.

At the start of this dissertation, the introductory Chapter 1 consists of the introduction to various characteristics of the Amazon, the background knowledge of environmental problems and these policies on the Brazilian Amazon were discussed.

In the first part of study, in Chapter 2, Mato Grosso has emerged as the Brazilian state with the highest deforestation rate, and with the most dynamic changes in vegetation and land covers. A set of four 5-year Digital Vegetation Model (DVM) maps was created for every five years during the 1981-2001 period, using the first components of the principal components analysis (PCA) of NOAA/AVHRR multi-spectral data (Channels 1, 2 and 4). Vegetation and land cover changes are characterized by destruction of tropical rainforests in the north and large-scale savannization expanding from the south. Large-scale soybean production spreading over the central areas and vast cattle ranching in the north can be pointed out as the main causes of vegetation change in these areas. It is shown that 76.1 % (89.5 %) of the changes in land cover

types occur within 30 km from paved and unpaved roads as roads networks (roads and navigable rivers as access networks). This emphasizes not only the role of road building, but also that of navigable rivers, in accelerating deforestation, especially over the road-less north.

In the second part of study, in Chapter 3, we have the following specific objectives to do more detailed analysis on the cause of deforestation and savanization in particular areas using agriculture and cattle ranching industry data at municipal districts levels. We clarified how the vegetation change occurred in 3 categories of Degradation, Recovery and Transitional area with 5-year DVM vegetation change maps provided by Yoshikawa and Sanga-Ngoie (2009). About 46 % of MT was degraded through deforestation during 1981-2001, and we developed that cattle ranching and Corn production spread in the northwest and southeast of MT, Soybean and Sugarcane production in the central and west MT by using GIS. Additionally most of deforestation in tropical rainforests is caused by cattle ranchers or corn farm land in northwest MT and soybean or sugarcane farm land in central MT. savannization by soybean and sugarcane farm land spread mainly in the west MT and by corn in the southwest. Corn productions have more savannization impacts than the soybean crop production.

In the third part of study, in Chapter 4, we compared vegetation change with population density. The change rates are shown to be larger over non-inhabited areas (56 %), than over the populated zones in the south (42 %). This emphasizes not only the role of access network as roads and rivers in accelerating deforestation, but also the importance of population density, especially over the road less areas in the north.

5.2 Conclusion

To analysis the distributed widely vegetation on the same period using only field survey data is difficult and need high cost. But we can solve this problem by using the satellite data. However, previous studies have problems in the respect that errors due to climatic effects of atmospheric conditions and cloud activity were not considered. In

this study, 5-year DVM map Phase I, II, III and IV was created using NOAA/AVHRR satellite data from 1981-2001 in Brazil Mato Grosso. We understand the characteristics which exists tropical rainforests in the north, have found human activities in the south and central MT and lead the region of Degradation, Recovery and Transitional area from 5-year DVM maps. We clarify that Degradation area is 46.4 % and Transitional area is 6.8 % in the total area of MT during 2 decades. The region has recovered only 0.9 % rarely, and is also in the range of analytical error. Whereas the forests loss of the Amazon in 2050 to 40 % is expected by Soares-Filho *et al.* (2006), MT was clarified that the ongoing deforestation is deeper-than- expected.

The Degradation of forests occurred mainly in the 1980s, continued to develop toward north, in the 1990s, the northern border of MT. Recovery is very small, Transitional area increased dramatically since 1990. From the 1980s, region where was logging of natural forests, has been converted to cattle ranching and agricultural farming since 1990. Spatial trends of changes in vegetation are cleared the expansion along the roads and rivers toward the west and north from the south and east.

We compare roads or access network as causal affectors of deforestation with vegetation change and suggest that 76.1 % or 89.5 % of deforestation occur within 30 km from roads or roads and navigable rivers. Nepstad *et al.* (2001) studies out that 67 % of deforestation occur in the area less than 50 km from only main roads, in this study we could be updated to use the new vegetation map by satellite data and geographical data. In comparison with past-agricultural data, cattle ranching are expanding to the north (Margulis 2004) as well as significant expansion including Corn planted areas to north and northwest. Soybean and Sugarcane areas spread in the central and west of MT. And we clarify cause of vegetation change at each municipal district. In comparison with population density, population migration has devastated 42 % of negative vegetation change, and the remaining 56 % exists in the non-populated area.

We also indicate that the destruction of tropical forests to build cattle ranching and corn, soybean and sugarcane planted area have been found to increase the use of derelict

land. This is the expansion of cattle ranching including corn planted areas as long as soybean area can be expanded. This indirectly spurs to deforestation. In particular, expansion of soybean planted area after 2000 is intense. Greenpeace (2006) propounded Grupo André Maggi, which is the largest individual soybean producer in the world, borrowed totaling more than US$ 600 million from public and private banks in Europe, Japan and World Bank and performed massive soybean cultivation and have helped suppliers and infrastructure developers for the storage and transport of soybean. And Cargill, which is the largest private farm company in the USA, produces soybean in Rondonia and Mato Grosso to export to Europe by building new ports in Santarém and Porto Velho (Figure 5.1). When BR–163 (especially from Cuiabá to Santarém), is to be used for soybean transportation when the construction is inaugurated, deforestation will further progress. These soybeans are used as bait to breed a cock of the Fist Food chain. People in developed countries should know how and where food supply comes from more clearly.

To fulfill the stomach and life in developed countries, most of the treasured and valuable vegetation is changed and destroyed. Mass production or mass consumption of the cattle ranching for fast food, and the sugarcane and corn for bio-fuel will never last long. It is necessary to think before it is too late to recover original vegetation and the influence is reflected in climatic change in the world. Suggestion on the global, premeditated, strategic, and judicious government plan is necessary now in each country. We expect the policy is drawn up for the long-term profit (sustainable development and Climate change of Global warming etc.) not for the short-term profit (logging, cattle ranching, Soybean, Sugarcane and Corn production) and pray that these and conventional studies will be reflected in decision making about the future of Mato Grosso or the Amazon and eventually of our earth.

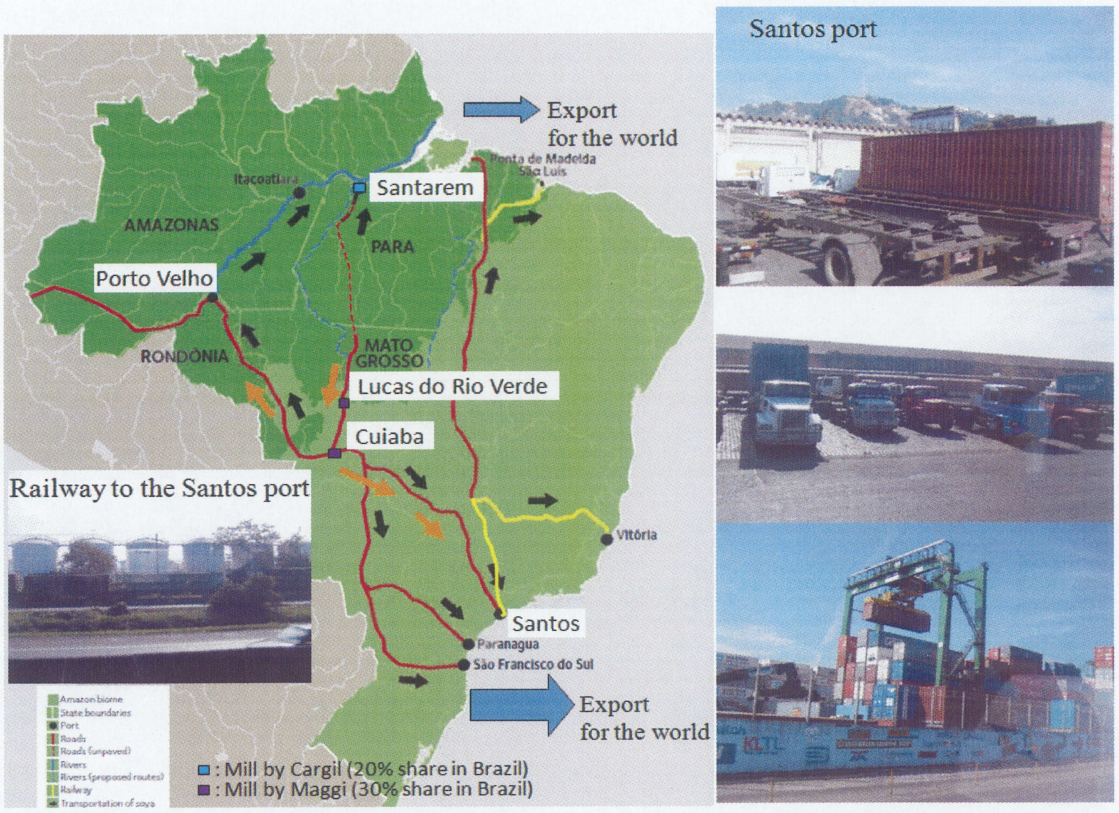

Figure 5.1 Transportation routes of soybean from Mato Grosso to the world. We modified portions of Greenpeace (2006). Red bold lines denote road using the transportation. Yellow is railroad and blue or purple squares are soybean's mill by major grain companies. The photographs were taken by Yoshikawa in the ground observation from 20th to 29th June 2008 at Santos port.

Reference

1 AGBU, P.A. and JAMES, M.E., 1994, NOAA/NASA Pathfinder AVHRR Land Data Set User's Manual. Goddard Distributed Active Archive Center, NASA Goddard Space Flight Center, Greenbelts, Technical Report, 1–105.

2 AGÊNCIA NACIONAL DE ÀGUAS, ANA, 2002, The Evolution of Water Resources Management in Brazil (Setor Policial Sul, Brazil: ANA).

3 AGÊNCIA NACIONAL DE ÀGUAS, ANA, 2002, Overview of the Amazon hydrographic Region (Setor Policial Sul, Brazil: ANA).

4 ALVES, D.S. 2002. An analysis of the geographic patterns of deforestation in the Brazilian Amazon in the period 1991-1996. *Deforestation and Land Use in the Amazon*, Wood, C. H. and Porro, R. (eds), 95–106 (Gainesville, FL: University Press of Florida).

5 ANYAMBA, A. and EASTMAN, J.R., 1996, Interannual variability of NDVI over Africa and its relation to El Niño/Southern Oscillation. *International Journal of Remote Sensing*, **17**, 2533–2548.

6 ASNER, G.P., KNAPP, D.E., BROADBENT, E.N. and OLIVEIRA, P.J.C., 2005, Selective Logging in the Brazil Amazon. *Science*, **310**, 21.

7 BARRETO, P., SOUZA C.J., ANDERSON, A., SALOMÃO, R., WILES, J., 2006, Human Pressure on the Brazilian Amazon Forests (Belém, Brazil: World Resources Institute).

8 BATISTA, G.T., SIMABUKURO, Y.E. and LAWRENCE, W.T., 1997, The long-term monitoring of vegetation cover in Amazonian region of north Brazil using NOAA-AVHRR data. *International Journal of Remote Sensing*, **18**, 3195–3210.

9 BRUIJNZEEL, L. A., 1996, Predicting the hydrological impacts of land covers transformation in the humid tropics: the need for integrated research. *Amazonian Deforestation and Climate*, Gash, J. H. C., Nobre, C. A., Roberts, J. M., and Victoria, R. L., (eds), 15–55 (Chichester, UK: John Wiley & Sons).

10 CENTRO DE PREVISÃO DE TEMPO E ESTUDOS CLIMÀTICOS, CPTEC, 2007, Plataformas de Coleta de Dados, Dados meteorológicos, hidrológicos e amientais de PCDs. Available online at: http://satelite.cptec.inpe.br/PCD/ (accessed 08 November 2007).

11 CONGALTON, R. G., 1991, A Reveiew of Assessing the Accuracy of Classification of Remotely Sensed Data. *Remote Sensing of Environment*, **37**, 35–46.

12 DALE, V.H., 1994, Terrestrial CO_2 Flux: The Challenge of Interdiscipilinary Research. Effects of Land-Use Change on Atmospheric CO_2 Concentrations, Dale, V. H., (eds), 1–14 (New York, USA: Springer–Verlag)

13 DEFRIES, R., ACHARD, F., BROWN, S., HEROLD, M., MURDIYARSO, D., SCHLAMADINGER, B., and SOUZA JR, C., 2007 Earth obsevation for estimating greenhouse gas emissions from deforestation in developing countries. *Environmental Science & Policy*, **10**, 385–394

14 DEPARTAMENTO NACIONAL DE TRÂNSITO, DENATRAN, 2009, DENATRAN Frota por tipo/UF 2008. Available online at: http://www2.cidades.gov.br/renaest/detalheNoticia.do?noticia.codigo=120. (accessed 08 April 2009)

15 EASTMAN, J.R. and FULK, M., 1993, Long sequence time series evaluation using standardized principal components. *Photogrammetric Engineering and Remote Sensing*, **59**, 991–996.

16 EASTMAN, J.R., 2001, Guide to GIS and Image Processing. **1** (Massachusetts, Clark University).

17 EASTMAN, J.R., 2001, Guide to GIS and Image Processing. **2** (Massachusetts, Clark University).

18 FAIZ A., CHRISTOPHER S.W. and MICHAEL P. W., 1996, Air pollution from motor vehicles. (Washington, D. C.: World Bank).

19 FEARNSIDE, P.M., 1986, Spatial Concentration of Deforestation in the Brazilian Amazon. *Ambio*, **15**, 74–81.

20 FEARNSIDE, P.M., 1990, The rate and extent of deforestation in the Brazilian Amazon. *Environment Consevation*, **17**, 213–226.

21 FEARNSIDE, P.M., 1993, Deforestation in Brazilian Amazonia: The Effect of Population and Land Tenure. *Ambio*, **22**, 537–545.

22 FEARNSIDE, P.M., 2002, Greenhouse Gas Emissions from a Hydroelectric Reservoir (Brazil's Tucuruí Dam) and the Energy Policy Implications. *Water, Air, & Soil Pollution*, 133, 69-96.

23 FEARNSIDE, P.M., 2003, Deforestation Control in Mato Grasso: A New Model for Slowing the Loss of Brazil's Amazon Forest. *Ambio*, **32**, 343–345.

24 FEARNSIDE, P.M., 2005, Deforestation in Brazilian Amazonia: History, Rates, and Consequences. *Conservation Biology*, **19**, 680–688.

25 FEARNSIDE, P.M., 2006, BR-319: Brazil's Manaus-Porto Velho Highway and the Potential Impact of Linking the Arc of deforestation to Central Amazonia. *Environ Manage*, **38**, 705–716.

26 GASH, J.H.C. and NOBRE, C.A., 1997, Climatic Effects of Amazonian Deforestation: Some Results from ABRACOS. *Bulletin of the American Meteorological Society*, **78**, 823–830.

27 GENTRY, A.H. and LOPEZ-PARODO, J., 1980, Deforestation and increased flooding of the upper Amazon. *Science*, **210**, 19.

28 GLOBAL PRECIPITATION CLIMATOLOGY CENTRE, GPCC, 2005, Variability Analysis of Surface Climate Observations 50-year precipitation climatology 1951–2000. Available online at: http://www.dwd.de/en/FundE/Klima/KLIS/int/GPCC/Projects/VASClimO/ (accessed 08 November 2007).

29 GUILD, L.S., COHEN, W.B. and KAUFFMAN, J.B., 2004, Detection of deforestation and land conversion in Rondônia, Brazil using change detection techniques. *International Journal of Remote Sensing*, **20**, 731–750.

30 GURGEL, H.C. and FERREIRA, N.J., 2003, Annual and interannual variability of NDVI in Brazil and its connections with climate. *International Journal of Remote Sensing*, **24**, 3595–3609.

31 GREENPEACE, 2006, Eating Up The Amazon. (Netherlands: Greenpeace International).

32 HALL, A.L., 1991, Developing Amazonia: deforestation and social conflict in Brazil's Carajàs programme. (Manchester, UK: Manchester University Press).

33 HENDERSON-SELLERS, A., ZHANG, H. and HOWE, W., 1996, Human and Physical Aspects of Tropical Deforestation. *Climate Change*, A. Henderson-Sellers and M. M. Verstraete (eds), 259–292 (Chichester, UK: John Wiley & Sons).

34 INSTITUTO BRASILIEIRO DE GEOGRAFIA E ESTATÌSTICA, IBGE, 2005, Mapas Interativos IBGE. Available online at: http://mapas.ibge.gov.br/ (accessed 08 November 2007).

35 INSTITUTO NACIONAL DE PESQUISAS ESPACIAIS, INPE, 1999, Monitoramento da Floresta amazônica brasileira por satélite 1997-1998. Available online at: http://sputnik.dpi.inpe.br:1910/col/dpi.inpe.br/vagner/2000/04.28.17.40/doc/Index.htm (accessed 02 June 2008).

36 INSTITUTO NACIONAL DE PESQUISAS ESPACIAIS, INPE, 2000, Monitoramento da Floresta amazônica brasileira por satélite 1998-1999. Available online at: http://sputnik.dpi.inpe.br:1910/col/dpi.inpe.br/banon/2000/09.12.17.24/doc/amz1998_1999/index_amz.html (accessed 02 June 2008).

37 INSTITUTO NACIONAL DE PESQUISAS ESPACIAIS, INPE, 2001, Monitoramento da Floresta amazônica brasileira por satélite 1999-2000, Available online at: http://sputnik.dpi.inpe.br:1910/col/dpi.inpe.br/lise/2001/05.16.09.55/doc/html/capa.htm (accessed 02 June 2008).

38 INSTITUTO NACIONAL DE PESQUISAS ESPACIAIS, INPE, 2002, Monitoramento da Floresta amazônica brasileira por satélite 2000–2001, Available online at: http://sputni.dpi.inpe.br:1910/col/dpi.inpe.br/lise/2001/05.16.09.55/doc/html/capa.htm (accessed 02 June 2008).

39 INSTITUTO NACIONAL DE PESQUISAS ESPACIAIS, INPE, 2006, PROJETO PRODES Monitoramento da Floresta amazônica brasileira por satélite. Available online at: http://www.obt.inpe.br/prodes/index.html (accessed 23 November 2007).

40 INSTITUTO NACIONAL DE PESQUISAS ESPACIAIS, INPE, 2009, PROJETO PRODES Monitoramento da Floresta amazônica brasileira por satélite. Available online at: http://www.obt.inpe.br/prodes/index.html (accessed 13 February 2009).

41 INTERNATIONAL WATER MANAGEMENT INSTITUTE, IWMI, 2004, Land 8km AVHRR Data Set, IWMI Remote Sensing and Geographic Information System Data Store house Pathway. Available online at: http://www.iwmidsp.org/iwmi/info/main.asp (accessed 08 November 2007)

42 JASINSKI, E., MORTON, D., DEFRIES, R., SHIMABUKURO, Y., ANDERSON, L. AND HANSEN, M., 2005, Physical Landscape Correlates of the Expansion of Mechanized Agriculture in Mato Grosso, Brazil. *Earth Interactions*, **9**, 1–18.

43 KAIMOWITZ. D., MERTENS. B., WUNDER. S. and PACHECO P., 2004, Hamburger Connection Fuels Amazon Destruction, Center for International Forestry Research (CIFOR) research report. (Bogor, Indonesia)

44 LAURANCE, W.F., MARK, A.C., SCOTT, B., FEARNSIDE, P.M., DELAMÔNICA, P., BARBER, C., D'ANGELO, S. and FERNANDES, T., 2001, Policy Forum Environment: The Future of the Brazilian Amazon. *Science*, **291**, 438–439.

45 LINDENMAYER, D. and FRANKLIN, J. F., 2002, Conserving forest biodiversity: a comprehensive multiscaled approach. (Washington, DC.: Island Press)

46 LOVELAND, T.R., REED, B.C., BROWN, J.F., OHLEN, D.O., ZHU, Z., YANG, L. and MERCHANT, J.W., 2000, Development of a global land cover characteristics

database and IGBP DISCover from 1km AVHRR data. *International Journal of Remote Sensing*, **21**, 1303–1330.

47 MARGULIS, S., 2004, Causes of Deforestation of the Brazilian Amazon, World Bank Working Paper No.22, 77 (Washington, D. C.: World Bank).

48 MARK, C., 1990, The Last Rain Forests (London, UK: Mitchell Beazley)

49 MORAN, E.F., 1981, Developing the Amazon. (Bloomington: Indiana University Press).

50 MORAN, E.F., 1993, Through the Amazonian eyes (Iowa, USA: University of Iowa Press).

51 MORTON, D.C., DEFRIES, R.S., SHIMABUKURO, Y.E., ANDERSON, L.O., DEL, B.E.S., SANTO, F., HANSEN, M.C. and CARROLL, M., 2005, Rapid Assessment of Annual Deforestation in the Brazilian Amazon Using MODIS Data. *Earth Interactions*, **9**, 1–22.

52 MORTON, D.C., DEFRIES, R.S., SHIMABUKURO, Y.E., ANDERSON, L.O., ARAI, E., DEL, B.E.S., FREITAS, R. and MORISETTE, J., 2006, Cropland expansion changes deforestation dynamics in the southern Brazilian Amazon. *PNAS*, **103**, 14637–14641.

53 MURAI, S. and HONDA, Y., 1991, World vegetation map from NOAA GVI data –How much of forest area does remain?–, In Application of Remote sensing in Asia and oceania, S. Murai (eds), 3–8 (Asian Association of Remote Sensing).

54 MYERS. N., 1981, The hamburger Connection: How Central America's Forests Became North America's Hamburgers, *Ambio*, **10**, 3–8

55 NEPSTAD, D., CARVALHO, G., BARROS, A.C., ALENCAR, A., CAPOBIANCO, J.P., BISHOP, J., MOUTINHO, P., LEFEBVRE, P., SILVA JR., U.L. and PRINS, E., 2001, Road paving, fire regime feedbacks, and the future of Amazon forests. *Forest Ecology and Management*, **154**, 395–407

56 NISHIDA, K., MASTUDA, S. and KANAE S., 2005, Response of Land Surface in Indian China Peninsula to Rainfall, El Nino, and DME. *Journal of the Remote Sensing Society of Japan*, **25**, 473–481.

57 Nobre, C. A., Sellers, P.J and Shukla, J., 1991, Amazonian Deforestation and Regional Climate Change. *Journal of Climate*, **4**, 957-988.

58 NONOMURA, A., SANGA-NGOIE, K. and FUKUYAMA, K., 2003, Devising a new digital vegetation model for eco-climatic analysis in Africa using GIS and NOAA AVHRR data, *International Journal of Remote Sensing*, **24**, 3611–3633.

59 PARK, C. C., 1992, Tropical Rainforests (New York: Rutledge).

60 RICHARD, Y. and POCCARD, I., 1998, A statistical study of NDVI sensitivity to seasonal and interannual rainfall variations in Southern Africa, *International journal of Remote Sensing*, **19**, 2907–2920.

61 Rogers, A., and Castro, L.J., 1981, *Model Migration Schedules.* Research Report 81-30 (Laxenburg, Austria: International Institute for Applied Systems Analysis).

62 Rogers, A., 1985, *Regional Population Projection Models.* Scientific Geography Series, vol. 4 (Beverly Hills, California: Sage Publications).

63 ROUSE, J.W., HAAS, R.H., SCHELL, J.A. and DEERING, D.W., 1973, Monitoring Vegetation Systems in the Great Plains with ERTS. Earth Resources Technology Satellite-1 Third Symposium, pp. 309–317 (Washington D. C.: NASA).

64 SACHS, I., WILHEIM, J., PINHEIRO, P.S. and DAVILA, J., 2009, Brazil: A Century of Change. (North Carolina: UNC Press).

65 SALATI, E. and VOSE, P.B., 1984, Amazon Basin: A System in Equibrium. *Science*, **225**, 4658.

66 SAMPAIO, G., NOBRE, C., COSTA, M.H., SATYAMURTY, P., SOARES-FILHO, B.S. and CARDOSO, M., 2007, Regional climate change over eastern Amazonia caused by pasture and soybean cropland expansion. *Geophysical Research Letters*, **34**, L17709, doi: 10.1029/ 2007GL030612

67 SANGA-NGOIE, K. and FUKUYAMA, K., 1996, Interannual and long-term climate variability over the Zaire River Basin during the last 30years. *Journal of Geophysical Research*, **101**, 21351–21360.

68 SANGA-NGOIE, K. and YOSHIKAWA, S., 2004, Digital Vegetation Map of South America using GIS and NOAA/AVHRR satellite data, *The 13th Annual Conference of Geographycal Information System Association of Japan*, p403-406, (Tokyo, Japan: GISA).

69 SANGA-NGOIE, K. and YOSHIKAWA, S., 2006, Spatial and temporal analysis of climatic environmental variability over the tropical area in Latin America, *The 41th Conference of the Remote Sensing Society of Japan*, p77-78, (Okinawa, Japan: RSSJ).

70 SANGA-NGOIE, K. and YOSHIKAWA, S., 2007, Spatial and temporal vegetation change in Southern Brazilian Amazon using GIS and NOAA/AVHRR data. *Poster Presentation in American Geophysical Union 2007 Joint Assembly*, NS31B-03, (Acapulco, Mexico: AGU).

71 SANGA-NGOIE, K. and YOSHIKAWA, S., 2008 (a), Deforestation dynamics in Mato Grosso, central-west Brazil, using GIS and NOAA/AVHRR data, The 45th Conference of the Remote Sensing Society of Japan, p81-82, (Hokaido, Japan: RSSJ).

72 SANGA-NGOIE, K. and YOSHIKAWA, S., 2008 (b), Causes of deforestation in Mato Grosso, central-west Brazil, using GIS, *The 45th Conference of the Remote Sensing Society of Japan*, p83-84, (Hokaido, Japan: RSSJ).

73 SANGA-NGOIE, K. and YOSHIKAWA, S., 2008 (c), Trends in land use and land cover changes in the Southern Brazilian Amazon using GIS and satellite data, *Asia Collaborative Forum for Women Researchers in Science and Technology*, No. 2, p12, (Mie, Japan).

74 SANGA-NGOIE, K. and YOSHIKAWA, S., 2009 (a), DEFORESTATION DYNAMICS IN MATO GROSSO, CENTRAL-WEST BRAZIL USING GIS

AND NOAA/AVHRR DATA, *American Society for Photogrammetry and Remote Sensing 2009 Annual Conference*, CD-ROM , (Baltimore, MD: ASPRS).

75 SANGA-NGOIE, K. and YOSHIKAWA, S., 2009 (b), Impact analysis of deforestation and access networks in Mato Grosso, Brazil, *The 46th Conference of the Remote Sensing Society of Japan*, p.17-18, (Tokyo, Japan: RSSJ).

76 SANGA-NGOIE, K. and YOSHIKAWA, S., 2009 (c), Changes and causes of the changes in vegetation cover in the southern Amazon, *The 18th Annual Conference of Geographycal Information System Association of Japan*, p119-122, (Niigata, Japan: GISA).

77 SANGA-NGOIE, K. and YOSHIKAWA, S., 2009 (d), Deforestation and expansion of the agro-pastoral frontier in the southern Amazon, *The 47th Conference of the Remote Sensing Society of Japan*, p.143-144, (Nagoya, Japan: RSSJ).

78 SANGA-NGOIE, K. and YOSHIKAWA, S., 2009 (e), Deforestation and Savannization in tropical areas -Case study in southern Amazon-, *Central Japan Workshop in Meteorological Society of Japan*, p.21-24, (Mie, Japan).

79 SANGA-NGOIE, K. and YOSHIKAWA, S., 2009 (f), Causes of the Deforestation and Savannization in Mato Grosso, Brazil, APU 10th Anniversary, AY 2009 Asia Pacific Conference "Reflections on the Asia Pacific -Past, Present and Future-", accepted, (Beppu, Japan: APU).

80 SANTILLI, M., MOUTINHO, P., SCHWARTZMAN S., NEPSTAD, D., CURRAN, L. and NOBRE, C., 2005, Tropical deforestation and the Kyoto Protocol. *Climate Change*, **71**, 267-276.

81 SCHWARTZMAN S. and ZIMMERMAN B., 2005, Conservation Alliances with indigenous peoples of Amazon. *Conservation Biology*, **19**, 721-727.

82 SISTEM IBGE DE RECUPERAÇÃO AUTOMÁTICA, SIDRA, 2008, Heads of cattle data IBGE. Available online at: http://www.sidra.ibge.gov.br/bda/tabela/listabl.asp?z=t&c=Tabela+73 (accessed 29 July 2008)

83 SISTEM IBGE DE RECUPERAÇÃO AUTOMÁTICA, SIDRA, 2008, Agricultural prodcution data, IBGE. Available online at: http://www.sidra.ibge.gov.br/bda/tabela/listabl.asp?c=1612&z=p&o=21 (accessed 29 July 2008).

84 SKOLE, D. and TUCKER, C., 1993, Tropical deforestation and Habitat Fragmentation in the Amazon: Satellite Data from 1978 to 1988. *Science*, **260**, 1905–1910.

85 SOARES-FILHO, B.S., NEPSTAD, D.C., CURRAN, L.M., CERQUEIRA G.C., GARCIA, R.A., ROMAS, C.A., VOLL, E., MCDONALD, A., LEFEBVRE, P. and SCHLESINGER, P., 2006, Modelling coservation in the Amazon basin, *Nature*, **440**, 520–523, doi:10.1038/nature04389

86 TORRES H. and COSTA, H., 1999, População e meio ambiente: debates e desafios. (São Paulo, Brazil: Senac).

87 TOWNSHEND, J.R.G., JUSTICE, C.O. and KALB, V., 1987, Chracterization and classification of South America land cover types using satellite data. *International Journal of Remote Sensing*, **8**, 1189–1207.

88 TSURUMI, T. and SANGA-NGOIE, K., 2000, Characteristics of a new World Vegetation map obtained from NOAA/AVHRR satellite data, *Papers and Proceedings of Journal of The Remote Sensing Society of Japan*, **29**, November 2000 (Tokyo, RSSJ), 165–166.

89 TUCKER, C., TOWNSHEND, J.R.G. and GOFF, T., 1985, African Land-Cover Classification Using Satelite Data. *Science*, **277**, 369–375.

90 UNITED NATIONS ENVIRONMENT PROGRAM, UNEP/GRID, 2000, Latin America And Caribbean Population Distribution Database, United Nations Environment Programme Environment for Development, Global Resource Information Database - Sioux Falls. Available online at: http://na.unep.net/datasets/datalist.php (accessed 08 March 2007).

91 UNITED STATES DEPARTMENT OF AGRICULTURE, USDA, 1994, Major World Crop Areas and Climatic Profiles. Agricultural Handbook No. 664, pp.279

92 UNITED STATES GEOLOGICAL SURVEY, USGS, 1997, HYDRO1K Elevation Derivative Database, United States Geological Survey, Earth Resources Observation & Science (EROS), Available online at: http://edc.usgs.gov/products/elevation/gtopo30/hydro/samerica.html (accessed 08 November 2007).

93 YOSHIKAWA S., 2002, The Destruction of Tropical Rain Forests in Brazil, 9th Tri-University International Joint Seminar & Symposium-Role of Asia in the World, p226-228, Jiangsu, China.

94 YOSHIKAWA, S. and SANGA-NGOIE, K., 2010, Deforestation Dynamics in Mato Grosso in the Southern Brazilian Amazon using GIS and NOAA/AVHRR data, *International Journal of Remote Sensing*, accepted on 03 November 2009.

95 YOSHIKAWA, S. and SANGA-NGOIE, K., 2009, Vegetation change and cause of changes in Mato Grosso, central-western Brazil, using NOAA/AVHRR and GIS during the 1981-2001, Theory and Application of GIS, Vol.17, No.2, p.11-20.

96 WORLD WILDLIFE FUND, WWF, 2001, Ecoregions map Bio Science Report WWF Conservation Science Program. Available online at: http://www.worldwildlife.org/wildworld/profiles/terrestrial_nt.html#moistbroad (accessed 14 February 2009).